

# Accepted Manuscript

*N*-(1'-naphthyl)-3,4,5-trimethoxybenzohydrazide as microtubule destabilizer: synthesis, cytotoxicity, inhibition of cell migration and *in vivo* activity against acute lymphoblastic leukemia

Livia B. Salum, Alessandra Mascarello, Rafael R. Canevarolo, Wanessa F. Altei, Angelo B.A. Laranjeira, Patrícia D. Neuenfeldt, Taisa R. Stumpf, Louise D. Chiaradia-Delatorre, Laura L. Vollmer, Hikmat N. Daghestani, Carolina P. de Souza Melo, André B. Silveira, Paulo C. Leal, Marisa J.S. Frederico, Leandro F. do Nascimento, Adair R.S. Santos, Adriano D. Andricopulo, Billy W. Day, Rosendo A. Yunes, Andreas Vogt, José A. Yunes, Ricardo J. Nunes

PII: S0223-5234(15)00137-3

DOI: [10.1016/j.ejmech.2015.02.041](https://doi.org/10.1016/j.ejmech.2015.02.041)

Reference: EJMECH 7723

To appear in: *European Journal of Medicinal Chemistry*

Received Date: 18 November 2014

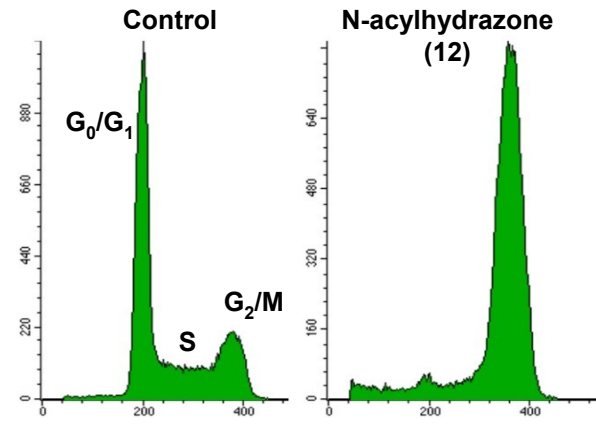
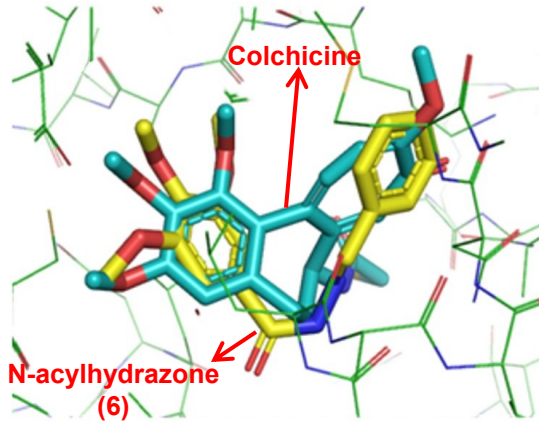
Revised Date: 20 February 2015

Accepted Date: 21 February 2015

Please cite this article as: L.B. Salum, A. Mascarello, R.R. Canevarolo, W.F. Altei, A.B.A. Laranjeira, P.D. Neuenfeldt, T.R. Stumpf, L.D. Chiaradia-Delatorre, L.L. Vollmer, H.N. Daghestani, C.P. de Souza Melo, A.B. Silveira, P.C. Leal, M.J.S. Frederico, L.F. do Nascimento, A.R.S. Santos, A.D. Andricopulo, B.W. Day, R.A. Yunes, A. Vogt, J.A. Yunes, R.J. Nunes, *N*-(1'-naphthyl)-3,4,5-trimethoxybenzohydrazide as microtubule destabilizer: synthesis, cytotoxicity, inhibition of cell migration and *in vivo* activity against acute lymphoblastic leukemia, *European Journal of Medicinal Chemistry* (2015), doi: 10.1016/j.ejmech.2015.02.041.

This is a PDF file of an unedited manuscript that has been accepted for publication. As a service to our customers we are providing this early version of the manuscript. The manuscript will undergo copyediting, typesetting, and review of the resulting proof before it is published in its final form. Please note that during the production process errors may be discovered which could affect the content, and all legal disclaimers that apply to the journal pertain.





**destabilizer: synthesis, cytotoxicity, inhibition of cell migration and *in vivo* activity  
against acute lymphoblastic leukemia**

Lívia B. Salum<sup>1#</sup>, Alessandra Mascarello<sup>2#</sup>, Rafael R. Canevarolo<sup>3</sup>, Wanessa F. Altei<sup>1</sup>, Angelo B. A. Laranjeira<sup>3</sup>, Patrícia D. Neuenfeldt<sup>2</sup>, Taisa R. Stumpf<sup>2</sup>, Louise D. Chiaradia-Delatorre<sup>2</sup>, Laura L. Vollmer<sup>4</sup>, Hikmat N. Daghestani<sup>5</sup>, Carolina P. de Souza Melo<sup>3</sup>, André B. Silveira<sup>3</sup>, Paulo C. Leal<sup>2</sup>, Marisa J. S. Frederico<sup>6</sup>, Leandro F. do Nascimento<sup>6</sup>, Adair R. S. Santos<sup>6</sup>, Adriano D. Andricopulo<sup>1</sup>, Billy W. Day<sup>7</sup>, Rosendo A. Yunes<sup>2</sup>, Andreas Vogt<sup>4,8</sup>, José A. Yunes<sup>3,\*</sup>, Ricardo J. Nunes<sup>2,\*</sup>

<sup>1</sup>Laboratório de Química Medicinal e Computacional, Universidade de São Paulo, São Carlos, SP 13560-590, Brasil;

<sup>2</sup>Laboratório Estrutura e Atividade, Universidade Federal de Santa Catarina, Florianópolis, SC 88040-900, Brasil;

<sup>3</sup>Centro Infantil Boldrini, Campinas, SP 13083-210, Brasil;

<sup>4</sup>Drug Discovery Institute, University of Pittsburgh, Pittsburgh, PA 15260, USA;

<sup>5</sup>Department of Structural Biology, University of Pittsburgh, Pittsburgh, PA 15260, USA;

<sup>6</sup>Laboratório de Neurobiologia da Dor e Inflamação, Universidade Federal de Santa Catarina, Florianópolis, SC 88040-900, Brasil;

<sup>7</sup>Department of Pharmaceutical Sciences, University of Pittsburgh, Pittsburgh, PA 15261, USA;

<sup>8</sup>Department of Computational and Systems Biology, University of Pittsburgh, Pittsburgh, PA 15260, USA.

# These authors contributed equally to this work

\*Corresponding authors:

Ricardo José Nunes: [nunesricardoj@gmail.com](mailto:nunesricardoj@gmail.com), phone number: +55 48 3721-9853.

José Andres Yunes: [andres@boldrini.org.br](mailto:andres@boldrini.org.br), phone number: +55 19 3787-5070.

**Keywords:** *acylhydrazones; colchicine; tubulin; microtubule assembly; cell migration; leukemia; cancer.*

ABT-751, *N*-(2-(4-hydroxyphenylamino)pyridin-3-yl)-4-methoxybenzenesulfonamide; CHNS, elemental analysis; DAMA-colchicine, *N*-deacetyl-*N*-(2-mercaptoacetyl)-colchicine; DMEM, Dulbecco's Modified Eagle Medium; DMSO, dimethylsulfoxide; DNA, deoxyribonucleic acid; FBS, Fetal Bovine Serum; FITC, Fluorescein Isothiocyanate; HeLa, human cervical carcinoma cell line; HL60, human promyelocytic leukemia cell line; IC<sub>50</sub>, half maximal inhibitory concentration; i.p., intraperitoneal injection; IR, Infrared; Jurkat, human T-cell acute lymphoblastic leukemia cell line; MDA-MB-231, breast cancer cell line; MDEC, Minimum Detectable Effective Concentration; mRNA, messenger RNA; MT, Microtubules; MTT, (3-(4,5-dimethylthiazol-2-yl)-2,5-diphenyltetrazolium bromide; NMR, Nuclear Magnetic Resonance; PDB, Protein Data Bank; PBMC, peripheral blood mononuclear cells; REH, human precursor B-cell acute lymphoblastic leukemia cell line; RPMI, Roswell Park Memorial Institute Medium; SD, Standard Deviation; TBAI; tetrabutylammonium iodide.

Tubulin-interacting agents, like vinca alkaloid and taxanes, play a fundamental role in cancer chemotherapy, making cellular microtubules (MT), one of the few validated anticancer targets. Cancer resistance to classical MT inhibitors has motivated the development of novel molecules with increased efficacy and lower toxicity. Aiming at designing structurally-simple inhibitors of MT assembly, we synthesized a series of thirty-one 3,4,5-trimethoxy-hydrazones and twenty-five derivatives or analogs. Docking simulations suggested that a representative *N*-acylhydrazone could adopt an appropriate stereochemistry inside the colchicine-binding domain of tubulin. Several of these compounds showed anti-leukemia effects in the nanomolar concentration range. Interference with MT polymerization was validated by the compounds' ability to inhibit MT assembly at the biochemical and cellular level. Selective toxicity investigations done with the most potent compound, a 3,4,5-trimethoxy-hydrazone with a 1-naphthyl group, showed remarkably selective toxicity against leukemia cells in comparison with stimulated normal lymphocytes, and no acute toxicity *in vivo*. Finally, this molecule was as active as vincristine in a murine model of human acute lymphoblastic leukemia at a weekly dose of 1 mg/kg.

Tubulin-interacting agents have played a fundamental role in cancer chemotherapy over the past decades, making cellular microtubules (MT) a well validated anticancer target [1, 2]. Despite the clinical success with taxoids (paclitaxel and docetaxel) and vinca alkaloids (vinblastine and vincristine), the search for novel and structurally more simple modulators of the microtubule/tubulin system has been strongly encouraged through the last several years due to drug resistance, adverse side effects, synthetic complexity, scarceness and limited bioavailability [3, 4].

Colchicine (here compound **1**) (**Figure 1A**) is a naturally occurring MT depolymerizing and cytotoxic agent that, in spite of its central role in elucidating physical properties and biological functions of microtubules, has not been used as a therapeutic alternative for the treatment of cancer due to its high toxicity [5]. Recently, however, compounds targeting the colchicine-binding site have attracted particular attention as anticancer agents [6]. The enormous interest in such molecules is reflected in the fact that combretastatin A-4 (compound **2**) analogs and *N*-(2-(4-hydroxyphenylamino)pyridin-3-yl)-4-methoxybenzenesulfonamide (ABT-751, compound **3**), both structurally simple tubulin inhibitors with potent cytotoxic and antimitotic activities, are currently under clinical investigation as potential new chemotherapeutic drugs [3, 4, 7, 8, 9]. In this context, our group has previously synthesized a series of cytotoxic 3,4,5-trimethoxychalcones (e.g., compounds **4** and **5**) capable of modulating MT assembly (**Figure 1A**) [10]. The significance of the 3,4,5-trimethoxyphenyl motif for inhibition of tubulin assembly and antimitotic activity has been discussed for this series of chalcone analogs [3, 10, 11, 12].

In this work, as a continuation of our research focused on finding novel structurally-simple mitotic arresters that inhibit MT assembly, we have designed and synthesized a series of thirty-one 3,4,5-trimethoxy-hydrazones (compounds **6-36**) (**Figure 1B**) and assessed their cytotoxic properties against leukemia cells. Like chalcones, *N*-acylhydrazones (**6-36**) and their derivatives/analogues (compounds **37-61**) (**Figure 2**) proved to be attractive chemical scaffolds for the design of novel MT inhibitors due to their chemical versatility, simplicity and efficient synthesis.

### 2.1. Synthesis

Thirty-one 3,4,5-trimethoxy-acylhydrazones (**6-36**) were prepared as shown in **Figure 1B**, with yields varying between 25 and 95%. The *N*-acylhydrazones were obtained by condensation of the suitable benzohydrazide and the appropriate aldehyde under reflux [11].

Subsequently, twenty five novel analogs or derivatives of compound **12** were synthesized (**Figure 2**). The six acylhydrazones (**37-42**) and the analog **48** were obtained as described above [11].

Some derivatives of compound **12** were synthesized by direct cyclization of the 3,4,5-trimethoxyhydrazones. The three 1,3,4-oxadiazoles (**43-45**) were prepared by cyclization of hydrazones with acetic anhydride under reflux [14], with yields varying between 25-35%. The thiazolidinones (**53, 54** and **56-61**) were obtained with yields from 60 to 92%, using mercaptoacetic acid in toluene and the appropriate 3,4,5-trimethoxyphenyl-substrate, under reflux in Dean-Stark apparatus [15].

Pyrazoline **55** was synthesized by the cyclization of chalcone A23 (previously prepared according procedure described [16]) and phenylhydrazine in acetic acid [17], with yield of 83%. Hydrazone **49** was synthesized using 3,4,5-trimethoxyhydrazide and naphthoyl chloride in the presence of pyridine in toluene, under reflux [11], yielding 91%. Imides **46** and **47** were obtained from 3,4,5-trimethoxyhydrazide and the corresponding anhydride in toluene, under reflux [18], with yields of 76 and 78%, respectively. Urea **50** was obtained from 3,4,5-trimethoxyhydrazide and 1-isocyanatophthalene in acetone, under magnetic stirring, at room temperature [19], with a yield of 84%. Sulfonamides **51** was synthesized by the reaction of 3,4,5-trimethoxyaniline with *N*-acetylbenzenesulfonyl chloride [20] with a yield of 95%. The *N*-acetyl group in compound **51** was hydrolyzed to give sulfonamide **52**, in 81% yield.

Reagents used were commercially available (Sigma-Aldrich), except the 3,4,5-trimethoxybenzohydrazide, which was prepared as previously described [21], with yield of 80%. Among the synthesized compounds, twenty-six (**6, 8, 13-19, 21, 23-25, 27-33** and **37-42**) have been

previously published by other authors [22, 23] and five (7, 9, 11, 12 and 20) by us [24]. Seven novel compounds (10, 22, 26, 34 and 43-45) were recently patented by us [25] and thirteen are unpublished until now (35, 36, 46-61).

All compounds were characterized by melting points,  $^1\text{H}$  and  $^{13}\text{C}$  NMR, including the already published compounds (Supporting Information). Detailed spectral characterization ( $^1\text{H}$  NMR,  $^{13}\text{C}$  NMR, IR and elemental analysis or mass spectrometry) for novel compounds is presented in the Material and Methods section.

## 2.2. Molecular modeling

Docking simulations were performed to explore possible binding modes of the proposed *N*-acylhydrazones in the colchicine-binding domain. Previous molecular dynamic simulations on *N*-acylhydrazone derivatives suggested that different conformational states might coexist in solution [13]. For this reason, four *N*-acylhydrazone conformers were modeled and investigated (Figure 3A). The results suggested that one of the probable conformational states (Figure 3A, conformation “b”) could adopt an appropriate stereochemistry inside the  $\alpha/\beta$  intradimer interface, resembling the conformation previously proposed for chalcone 4 [10].

As shown in Figure 3B, both *N*-acylhydrazone 6 and chalcone 4 overlapped well with DAMA-colchicine in the tubulin cavity, with their 3,4,5-trimethoxyphenyl groups sharing the same hydrophobic sub pocket. In addition, the carbonyl oxygen of compounds 4 and 6 similarly established hydrogen bonds with Asp  $\beta$ 251 and Leu  $\beta$ 255 whereas van der Waals interactions were important for the interaction of the aromatic B-rings, positioned at the opposite side of the binding cavity, in the same region as the tropone ring of colchicine.

Compounds were synthesized to explore the relation with the activity of: *i*) the presence of the 3,4,5-trimethoxyphenyl substituent on the A-ring, *ii*) the influence of the number and position of substituents on the B-ring, and the replacement of the B-phenyl ring by different fused or heterocyclic rings (compounds 6-36), *iii*) the importance of 3,4,5-trimethoxy moiety compared with acylhydrazones non-substituted on A ring (compounds 37-42), *iv*) the modifications in the skeleton of

3,4,5-trimethoxyacylhydrazones (compounds **46-52**), v) the effect of the direct cyclization of the studied acylhydrazones, forming 1,3,4-oxadiazoles **43-45** and thiazolidinones **53-54**, and vi) the influence of other cyclic conformationally-restricted analogs on the biological activity (pyrazoline **55** and thiazolidinones **56-61**).

## 2.3. Biological Evaluation

### 2.3.1. *In vitro* cell growth inhibitory activity

The 3,4,5-trimethoxyacylhydrazones synthesized were initially evaluated at three concentrations (1, 0.1, and 0.01  $\mu\text{M}$ ) for their cytotoxic effects against REH and Jurkat human acute lymphoblastic leukemia cell lines of B- and T-cell origins, respectively. As shown in **Table 1** and **Supplementary Table 1**, in this 3,4,5-trimethoxybenzohydrazone series (**6-36**), replacement of the substituent on the B-ring significantly affected anti leukemic activity. Compound **6**, which represents a general backbone for this series of compounds (except for compounds **22** and **27**, in which the phenyl B-rings were replaced by the aromatic bioisosteres imidazole and thiophene), did not show significant cytotoxic activity. In general, compounds having tri-substituted B-rings were not active (compounds **9**, **10**, **18** and **19**). Interestingly, several 3,4,5-trimethoxyhydrazones were more potent than the best 3,4,5-trimethoxychalcones previously developed by our group [10].

Compounds presenting activity at the nanomolar concentration range (<40% survival at 0.1  $\mu\text{M}$ ) were selected for the determination of their half maximal inhibitory concentration ( $\text{IC}_{50}$ ) against leukemia cells (**Table 2**). The 1-naphthalene derivative **12** was as potent as colchicine, showing  $\text{IC}_{50}$  values around 15 nM. Except for compounds **5**, **35** and **36**, all other derivatives also inhibited cell proliferation in both cell lines at nanomolar concentrations, especially compounds **7** and **21**, which showed  $\text{IC}_{50}$  around 40 nM and 70 nM, respectively.

Based on the most active compound **12**, we designed and synthesized twenty five additional derivatives and analogs (**37-61**, **Figure 2**), which were assayed under the same conditions (**Table 3**). While compounds containing the general backbone (*E*)-*N'*-benzylidene-benzohydrazide (phenyl group

as A-ring) substituted at B-ring (**37-42**) did not show activity, the presence of the 3,4,5-trimethoxy group as A-ring in the (*E*)-*N'*-benzylidene-benzohydrazide scaffold led to some very active compounds (**7**, **12**, **13-16** and **21**), confirming the importance of the 3,4,5-trimethoxyphenyl motif for the cytotoxic activity of the proposed analogs [10, 26, 27, 28]. The 1,3,4-oxadiazole derivatives (**43-45**) were also not active against leukemia cells, presumably (by docking analysis) because they were locked in a conformation that is not conducive for the interaction within the colchicine-binding site.

With respect to compounds resulting from direct modifications in the prototype **12**, structures **46**, **47**, **48**, **49** and **50** did not show antiproliferative activity. Only compound **51** was active against REH and Jurkat cell lines, with IC<sub>50</sub> values around 7 and 2 μM, respectively, being the best non-hydrazide analog obtained in this work. Compound **51** differs from analogue **52** (non active) by the presence of an acetyl group, which seems to contribute to the activity of this molecule.

Regarding analogues obtained by direct cyclization of acyl-hydrazones **12** and **13**, both thiazolidinones (compounds **54** and **53**, respectively) showed activity against leukemia cells. The IC<sub>50</sub> values obtained for **54** and **53**, although ~500-fold higher than their synthetic precursors (**12** and **13**), follow the same pattern, wherein the 1-naphthyl-substituted derivative (**12** and **54**) are more active than the 2-naphthyl substituted (**13** and **53**).

Analogs obtained by cyclization of 3,4,5-trimethoxy-derivatives (compounds **55-61**) showed variable anti-leukemia activities, but at concentrations significantly higher (~1,000-fold) than prototype **12**. Among thiazolidinones with a methylene group between the 3,4,5-trimethoxyphenyl and thiazo rings, compound **56** (which has a 1-naphthyl substituent) showed higher activity than **57** (which has one hydrogen from the 1-naphthyl group of **56** substituted by the 4-dimethylamino group). When the methylene group was deleted from **56** and **57**, a reverse pattern was observed, wherein compound **59** (correspondent to **57**) had higher activity than **58** (correspondent to **56**). The same profile was observed for compounds **60** and **61**. The pyrazoline **55** was not active in the tests.

The analysis of the relation structure activity showed that the 3,4,5-trimethoxyphenyl group, which is present also in colchicine and was found important for docking in a hydrophobic sub pocket of the colchicine-cavity in tubulin (see above). The relationship between the other part of the molecule

ACCEPTED MANUSCRIPT  
and its biological activity seems more complex and may depend on the polarity, distance and conformation of the groups as exemplified by differences observed with the naphthyl group and same substituent, as 4-dimethylamino and acetyl.

### 2.3.2. Inhibition of tubulin assembly

To address whether *N*-acylhydrazones directly interact with tubulin, representative *N*-acylhydrazones bearing the 3,4,5-trimethoxyphenyl substituent with high, low or no activity against leukemia cell lines were tested for inhibition of MT assembly. As shown in **Table 4**, in agreement with their nanomolar cytotoxic potencies, compounds **7**, **12**, **13**, and **21** were also nanomolar inhibitors of MT polymerization *in vitro*, exceeding the activity of colchicine **1** and of the most potent previously described chalcone **4**. In agreement with their lack of cytotoxic effects, compounds **18** (a 3,4,5-trisubstituted analog), **20** (an extended non-branched side chain analog), and **22** (phenyl B-ring replaced by a heterocyclic aromatic ring) did not inhibit MT polymerization at concentrations up to 10  $\mu$ M. In general, in agreement with our docking studies, some B-mono-substituted analogs presented increased activity against tubulin assembly (as for compounds **7**, **8**, **16** and **21**), while tri-substituted analogs had reduced potency (as for compounds **10** and **18**), probably due to steric hindrance [14]. Steric factors may also explain the somewhat decreased activity of the binuclear compounds **13** and **15** (both with *beta* orientation) when compared to **12** (*alpha* orientation).

### 2.3.3. Cellular microtubule perturbation, cell cycle arrest, and apoptosis induction

Microtubule-interacting agents characteristically provoke cell cycle arrest and cellular microtubule perturbation [1, 10, 33]. To examine the phenotypic alterations in cells caused by the selected *N*-acylhydrazones, multi-parameter high-content analyses were performed in HeLa cells. We evaluated the effects of the 12 representative derivatives (**6-8**, **10**, **12**, **13**, **15**, **16**, **18**, **20-22**) and colchicine **1** on microtubule perturbation, apoptotic morphology, cell cycle arrest and histone H3 phosphorylation. Fluorescence micrographs of representative images of nuclei (blue), tubulin (green), and phosphohistone H3 (red) staining are shown in **Figure 4**. In comparison to control (vehicle),

ACCEPTED MANUSCRIPT

colchicine treatment resulted in microtubule disorganization and increased numbers of phosphohistone H3 positive cells. Similar results were obtained with equivalent concentrations of the most potent derivative **12** and with high-nanomolar concentrations of the general backbone of this series (compound **6**). The mitotic arrest phenotype was then quantified by high-content analysis as previously described [10] (**Table 4**). A representative experiment showing quantitative analysis of IC<sub>50</sub> values for cell loss and minimum detectable effective concentrations (MDEC) for mitotic arrest from ten-point, two-fold concentration gradients is presented in **Supplementary Figure 1**.

Cellular toxicity, mitotic arrest, nuclear morphology and microtubule perturbation results were all in accordance with the ability of these compounds to inhibit MT assembly *in vitro* (**Table 4**). Most of the compounds promoted cell loss in the mid- to high-nanomolar range, either through detachment or lysis. In agreement with the preliminary assessment of cytotoxicity against leukemia cells, (*E*)-*N'*-benzylidene-3,4,5-trimethoxybenzohydrazides **7**, **12**, **13**, **15**, **16** and **21** were the most potent ones in affecting cell density, and to a lesser extent compound **8** and the B-non-substituted analog **6**. Compounds **18**, **20** and **22**, which did not inhibit MT assembly, were not cytotoxic at concentrations as high as 50  $\mu$ M. Compounds having trisubstituted B-rings (**10** and **18**) were among the least active. All tested agents, except for the inactive compounds **18**, **20** and **22**, showed chromatin condensation, decreases in cellular tubulin staining, and increased numbers of phospho-histone H3 positive cells at mid- to high nanomolar concentrations, consistent with mitotic arrest (**Table 4**). The most potent agent (**12**) was equipotent to colchicine (**1**) and represented a substantial improvement over the general backbone of this series (**6**) (**Table 4**).

Measurements of nuclear morphology and DNA content (not shown) after Hoechst 33342 counterstaining revealed the presence of condensed and fragmented nuclei, suggesting that the cytotoxic effect promoted by compound **12** occurs by cell cycle arrest in G2/M and apoptosis (**Table 4 and Supplementary Figure 1**). This was confirmed by flow cytometry of DNA content and annexin V staining in Jurkat cells (**Figure 5**), which documented that compound **12** is a strong inducer of apoptosis.

The identification of compounds with nanomolar cytotoxic potencies motivated further evaluations of their ability to inhibit metastatic breast cancer cell migration. Colchicine (**1**) and compounds **12** (the most potent among the evaluated compounds), **6** (backbone similar to **12**, but activity against leukemia at micromolar concentrations, **Supplementary Table 1**) and **37** (the general backbone that did not show significant activity against leukemia cell), were selected as representative compounds for such evaluation.

The breast cancer cell line MDA-MB-231, an estrogen-independent aggressive breast cancer model, was used for the assays due to its high metastatic potential. Initially, the selected compounds were evaluated in a wound healing assay [29, 30], which involves a migratory response of confluent monolayer cells after mechanical injury. As expected, compound **37** demonstrated no ability to inhibit the migration of MDA-MB-231 cells even at high concentrations (data not shown). In contrast, representative *N*-acylhydrazones bearing the 3,4,5-trimethoxyphenyl group (**6** and **12**), efficiently inhibited MDA-MB-231 migration at 1  $\mu$ M (**Table 5**) and even lower concentrations (**Figure 6**). Compound **12** showed inhibitory activity as strong as colchicine (**1**) in the scratch-wound assay.

The antimigratory activities of compounds **6** and **12** were confirmed in transwell cell culture chambers [31, 32]. Again, data obtained from this assay indicated that compound **12** represented an improvement over compound **6**, with potency similar to colchicine (**Table 5** and **Supplementary Figure 2**).

#### 2.3.5. Selective cytotoxicity and *in vivo* acute toxicity

Selective targeting and low toxicity for normal host tissues are important requisites for novel anticancer agents. Peripheral blood mononuclear cells from healthy donors and the leukemia cell lines Jurkat and REH were treated with increasing doses of compound **12** in order to investigate the selective cytotoxicity of compound **12** against cancer cells. As shown in **Figure 7**, compound **12** was at least three orders of magnitude more toxic to leukemia cells than to normal lymphocytes, documenting exquisite selectivity for malignant over nonmalignant cells.

We have previously shown that acylhydrazones (compounds **7**, **12**, **13** and **24**) are rapidly absorbed after oral administration, as judged by their remarkable effect on glucose tolerance tests in Wistar rats, at 10 mg/kg. Importantly, no tissue damage was recorded after 180 min of acylhydrazone administration, as evaluated by serum lactate dehydrogenase levels (Frederico *et al.*, 2012). In this work, we extended the *in vivo* toxicity evaluation of acylhydrazones by performing acute toxicity tests on mice. Groups of twelve mice (six of each gender) received a single oral dose of compound **12** (0.1 to 1,000 mg/kg). Mortality, behavioral changes, clinical signs, body weight (**Supplementary Figure 3**), intake of food and drink (**Supplementary Table 2**) and macroscopic organ appearance at sacrifice were measured for 14 days. No obvious acute toxic symptoms were observed, suggesting that the estimated p.o. LD50 for compound **12** is higher than 1,000 mg/kg. Moreover, macroscopic examination (general appearance of the organ, consistency, shape, color and weight) of heart, lung, liver, kidney, spleen, stomach, salivary gland, adrenal gland, thymus, mesenteric lymph nodes and brain revealed no pathological changes after compound **12** treatment (**Supplementary Table 3 and 4**).

### 2.3.6. *In vivo* sensitivity of ALL xenografts to compound **12**

To test the *in vivo* efficacy of compound **12** against leukemia, NOD/SCID mice were transplanted with a patient-derived xenograft B-cell precursor ALL cells. Animals were weekly monitored for the presence of ALL cells. Mice were randomized and treatment began when the ALL percentage in the peripheral blood of half of the animals reached  $\geq 0.5\%$ . Compound **12** was well tolerated by mice during the whole experiment. As shown in **Figure 8A**, weekly i.p. doses of 1 mg/kg of compound **12** were able to significantly slow the progression of primary human ALL in NOD/SCID mice, the effect being comparable to that obtained with vincristine (0.15 mg/kg/1x week). At the end of four weeks, animals were sacrificed and the infiltration of ALL in different organs was evaluated. Animals treated with compound **12** had lower infiltration of leukemic cells in both bone marrow, spleen and liver compared to control. In general the results obtained with compound **12** were similar to those with vincristine (**Figure 8B**).

### 3. CONCLUSIONS

We have designed and synthesized a series of *N*-acylhydrazones and analogs, and assessed their potential as anti-leukemia agents. Some compounds showed activity at nanomolar concentrations against acute lymphoblastic leukemia cell lines, a human cervical cancer cell line (HeLa), and inhibited mobility of a breast cancer cell line (MDA-MB-231). The compounds induced mitotic arrest in G2/M and cell death through apoptosis. The most potent agent (**12**) displayed only modest toxicity toward normal T lymphocytes and *in vivo* model of acute toxicity. Importantly, compound **12** was as active as vincristine in a murine model of human acute lymphoblastic leukemia. The proposed mechanism of action of these compounds is interference with MT polymerization, as demonstrated by their ability to inhibit *in vitro* MT assembly at concentrations similar to colchicine. An attractive feature of these molecules is that they bind to tubulin at the colchicine binding site, distinct from the binding sites of the vinca alkaloids and taxanes, but the same site as an antitumor molecule (combretastatin A4 phosphate) in Phase 2 clinical studies for solid tumors. In sum, some of the *N*-acylhydrazones described here are attractive lead compound for the design of novel microtubule modulators that complement existing MT-targeted therapies.

### 4. EXPERIMENTAL SECTION

#### 4.1. Synthesis

##### 4.1.1. General procedure for the synthesis and purification of 3,4,5-trimethoxybenzohydrazide [21]

The 3,4,5-trimethoxybenzohydrazide was obtained from a mixture of gallic acid (6 mmol), dimethyl sulphate (28 mmol), anhydrous K<sub>2</sub>CO<sub>3</sub> (26 mmol) and tetrabutylammonium iodide (TBAI) (0.1 g) in acetone (30 mL) [21]. The mixture was refluxed for 12 h, after the precipitate was filtered and washed with acetone. The ester obtained (6 mmol) was treated with a solution of 99% N<sub>2</sub>H<sub>4</sub> (4.4 mmol) in methanol (20 mL) and refluxed for 5 h, and then kept at room temperature overnight. The

ACCEPTED MANUSCRIPT  
solid obtained was filtered and recrystallized from hot methanol to afford the 3,4,5-trimethoxybenzohydrazide (80%).

#### 4.1.2. General procedure for the synthesis and purification of (*E*)-*N'*-benzylidene-benzohydrazide (**6-42**)

The hydrazones were synthesized from the 3,4,5-trimethoxybenzohydrazide (2 mmol) or benzohydrazide (2 mmol) and the appropriate aldehydes (2 mmol) in methanol (15 mL) and refluxed for 2 h. After cooling, the crude product was collected by filtration, washed and recrystallized from hot ethanol to give white solids [11]. Hydrazones **10**, **22**, **26** and **34** are novel compounds, which were recently patented by our group [25].

#### 4.1.3. General procedure for the synthesis and purification of oxadiazoles derivatives (**43-45**)

The 1,3,4-oxadiazoles were prepared by cyclization of the previously obtained (*E*)-*N'*-benzylidene-benzohydrazide with acetic anhydride under reflux for 3 h. After cooling, the crude product was collected by filtration, washed and recrystallized from acetone/water to give white solids [14]. All 1,3,4-oxadiazoles synthesized in this work (**43**, **44** and **45**) are novel compounds, which were recently patented by our group [25].

#### 4.1.4. General procedure for the synthesis and purification of thiazolidinones (**53**, **54**, **56-61**)

The thiazolidinones **53** and **54** were synthesized by adding of 3,4,5-trimethoxyhydrazone (1 mmol) and mercaptoacetic acid (0.5 mL) in toluene (35 mL), under reflux with a Dean-Stark apparatus for 16 h until complete removal of water from the system. The mixture was washed with saturated solution of NaHCO<sub>3</sub> (3 x 10 mL), the organic phase was dried with MgSO<sub>4</sub> and the solvent evaporated. The product was recrystallized from hexane [15]. The methods to obtain the compounds **56-61** were by *one pot* cycloaddition with respective 3,4,5-trimethoxyamine (1 mmol), 1-naphthaldehyde or 4-dimethylamine-1-naphthaldehyde (1 mmol) and mercaptoacetic acid (3 mmol) in

toluene (35 mL), following the same methods described above. These thiazolidinones were then recrystallized from ethanol. All of them are novel compounds.

#### 4.1.5. General procedure for the synthesis and purification of pyrazoline (**55**)

The 1,3,5-triaryl-2-pyrazoline **55** were prepared by the reaction of the chalcone (*E*)-3-(naphthalen-1-yl)-1-(3,4,5-trimethoxyphenyl)prop-2-en-1-one (1 mmol) previously synthesized [16] with phenylhydrazine (3 mmol), under reflux in acetic acid (10 mL) for 3 hours [17]. The crude product was poured in an ice bath, being the precipitate filtered and recrystallized from ethanol to form pyrazoline **55**, a novel compound.

#### 4.1.6. General procedure for the synthesis and purification of imides (**46-47**)

The imides **46** and **47** were synthesized using the methodology proposed by Brosse *et al.* [18]. The reaction from 3,4,5-trimethoxyhydrazide (1 mmol) and the corresponding anhydride (1 mmol) in 50 mL of toluene was kept under reflux for 3 h. Further, the solution was cooled to 0 °C to precipitate the product, which was recrystallized from hexane/ethyl acetate. The imides **46** and **47** are novel compounds.

#### 4.1.7. General procedure for the synthesis and purification of compounds **48** and **49**

The compound **48** was synthesized with the same methodology described for the *N'*-benzylidene-benzohydrazide [11]. Compound **49** was synthesized using 3,4,5-trimethoxyhydrazide (1 mmol) and naphthoyl chloride (1 mmol) in the presence of pyridine (1 mmol) in toluene (50 mL), under reflux for 2.5 h. The solution was cooled to 0 °C to precipitate the product, which was recrystallized from hexane. Both compounds are original.

#### 4.1.8. General procedure for the synthesis and purification of a urea derivative (**50**)

The urea **50** was synthesized using 3,4,5-trimethoxyhydrazide (1 mmol) and 1-isocyanatonaphthalene (1 mmol) in acetone (10 mL) at room temperature for 3 hours [19]. The crude

product was poured in an ice bath, being the precipitate filtered and recrystallized in ethanol. The urea derivative **50** is a novel compound.

#### 4.1.9. General procedure for the synthesis and purification of sulfonamides (**51-52**)

The sulfonamide **51** was synthesized by reaction of the 3,4,5-trimethoxyaniline (1 mmol) with *N*-acetylbenzenesulfonyl chloride (1 mmol) in dichlorometane (10 mL) and presence of pyridine (1mmol) [20]. Subsequently, the solvent was evaporated and the crude product was washed with water to give *N*-(4-(*N*-(3,4,5-trimethoxyphenyl)sulfamoyl)phenyl)acetamide **51**. The compound **52** was obtained by controlled hydrolysis of acetyl group with hydrochloric acid 6M. Thereafter, the solution was treated with charcoal to remove colored impurities. The last step was the reaction neutralization with sodium bicarbonate solution, resulting in the precipitation of compound **52**. The sulfonamides **51** and **52** are novel compounds.

#### 4.1.10. Physicochemical data on synthesized compounds

The purified compounds were obtained with yields ranging from 25% to 95%. Melting points were determined with a Microquímica MGAPF-301 apparatus and are uncorrected. IR spectra were recorded with an AbbBomen FTLA 2000 spectrometer on KBr disks. NMR (<sup>1</sup>H and <sup>13</sup>C NMR) were recorded on a Varian Oxford AS-400 (400 MHz) spectrometer, using tetramethylsilane as an internal standard. Elemental analysis was carried out with a CHNS EA 1110. Percentages of C and H were in agreement with the product formula (within + 0.4% of theoretical values to C). High resolution mass data was collected on a micrOTOF-QII (Bruker Daltonics) electrospray/ion trap instrument in positive and negative ion modes.

*(E)*-*N'*-(4-hydroxy-3-iodo-5-methoxybenzylidene)-3,4,5-trimethoxybenzohydrazide (**10**). White solid, mp 247-248 °C; yield 69%; <sup>1</sup>H NMR (DMSO-d<sub>6</sub>) δ 3.71 (s, 3H, *p*-OCH<sub>3</sub>), 3.85 (s, 6H, *m*-OCH<sub>3</sub>), 3.86 (s, 3H, *m*-OCH<sub>3</sub>), 7.20 (s, 2H, H<sub>2</sub>, H<sub>6</sub>), 7.32 (s, 1H, H<sub>6'</sub>), 7.59 (s, 1H, H<sub>2'</sub>), 8.29 (s, 1H, HC=N), 10.07 (1H, OH), 11.65 (s, 1H, NH). <sup>13</sup>C NMR (DMSO-d<sub>6</sub>) δ 56.78 (*m*-OCH<sub>3</sub>), 60.81 (*p*-OCH<sub>3</sub>), 85.17

(C3'), 105.84 (C2, C6), 109.72 (C6'), 128.28 (C1), 129.31 (C1'), 130.75 (C2'), 141.03 (C4), 147.35 (C=N), 147.97 (C5'), 149.00 (C4'), 153.36 (C3, C5), 163.16 (C=O). IR  $\lambda_{\max}/\text{cm}^{-1}$  3382 (N-H), 1636, 1228 (C=O), 1565 (C=N), 1290, 1045 (C-O), 2999, 2839, 1585, 1490, 1334, 1137, 997 (Ar) (KBr). Anal. Calcd for C<sub>18</sub>H<sub>19</sub>IN<sub>2</sub>O<sub>6</sub>: C 44.46, H 3.94, N 5.76. Found: C 44.64, H 3.99, N 5.88.

(*E*)-*N'*-((1*H*-imidazol-5-yl)methylene)-3,4,5-trimethoxybenzohydrazide (**22**). White solid, mp 230-231 °C; yield 75%; <sup>1</sup>H NMR (DMSO-*d*<sub>6</sub>)  $\delta$  3.74 (s, 3H, *p*-OCH<sub>3</sub>), 3.88 (s, 6H, *m*-OCH<sub>3</sub>), 7.23 (s, 2H, H<sub>2</sub>, H<sub>6</sub>), 7.53 (s, 1H, H<sub>2</sub>'), 7.66 (m, 1H, H<sub>4</sub>'), 8.02 (s, 1H, NH<sub>5</sub>'), 8.43 (s, 1H, HC=N), 11.37 (s, 1H, NH). <sup>13</sup>C NMR (DMSO-*d*<sub>6</sub>)  $\delta$  56.76 (*m*-OCH<sub>3</sub>), 60.81 (*p*-OCH<sub>3</sub>), 105.71 (C2, C6), 129.51 (C1), 131.94 (C1'), 132.16 (C2'), 135.37 (C4'), 145.45 (C=N), 153.35 (C3, C5), 162.29 (C=O). IR  $\lambda_{\max}/\text{cm}^{-1}$  3212 (N-H), 1623, 1234 (C=O), 1580 (C=N), 1280, 1054 (C-O), 2994, 2941, 2838, 1503, 1456, 1411, 1344, 1125, 1006, 844 (Ar) (KBr). Anal. Calcd for C<sub>14</sub>H<sub>16</sub>N<sub>4</sub>O<sub>4</sub>: C 55.26, H 5.33, N 18.41. Found: C 55.35, H 5.53, N 18.23.

(*E*)-*N'*-(2,6-dimethoxybenzylidene)-3,4,5-trimethoxybenzohydrazide (**26**). White solid, mp 245-246 °C; yield 93%; <sup>1</sup>H NMR (DMSO-*d*<sub>6</sub>)  $\delta$  3.71 (s, 3H, *p*-OCH<sub>3</sub>), 3.79 (s, 6H, *o*-OCH<sub>3</sub>), 3.85 (s, 6H, *m*-OCH<sub>3</sub>), 6.72 (d, *J* = 8.0 Hz, 2H, H<sub>3</sub>', H<sub>5</sub>'), 7.23 (s, 2H, H<sub>2</sub>, H<sub>6</sub>), 7.34 (t, *J* = 8.0 Hz, 1H, H<sub>4</sub>'), 8.60 (s, 1H, HC=N), 11.52 (s, 1H, NH). <sup>13</sup>C NMR (DMSO-*d*<sub>6</sub>)  $\delta$  56.72 (*m*-OCH<sub>3</sub>), 56.78 (*o*-OCH<sub>3</sub>), 60.76 (*p*-OCH<sub>3</sub>), 105.08 (C3', C5'), 105.76 (C2, C6), 111.75 (C1'), 129.37 (C1), 131.87 (C4'), 140.88 (C4), 143.92 (C=N), 153.31 (C3, C5), 159.38 (C2', C6'), 162.81 (C=O). IR  $\lambda_{\max}/\text{cm}^{-1}$  3186 (N-H), 1644, 1240 (C=O), 1586 (C=N), 1258, 1068 (C-O), 3002, 2928, 2838, 1502, 1473, 1417, 1378, 1342, 1121, 1007, 783 (Ar) (KBr). Anal. Calcd for C<sub>19</sub>H<sub>22</sub>N<sub>2</sub>O<sub>6</sub>: C 60.95, H 5.92, N 7.48. Found: C 60.56, H 6.10, N 7.55.

(*E*)-*N'*-(4-chloro-3-(trifluoromethyl)benzylidene)-3,4,5-trimethoxybenzohydrazide (**34**). White solid, mp 203-204 °C; yield 83%; <sup>1</sup>H NMR (DMSO-*d*<sub>6</sub>)  $\delta$  3.72 (s, 3H, *p*-OCH<sub>3</sub>), 3.85 (s, 6H, *m*-OCH<sub>3</sub>), 7.23 (s, 2H, H<sub>2</sub>, H<sub>6</sub>), 7.82 (d, *J* = 8.6 Hz, 1H, H<sub>5</sub>'), 8.02 (d, *J* = 8.6 Hz, 1H, H<sub>6</sub>'), 8.15 (s, 1H, H<sub>2</sub>'), 8.52

(s, 1H, HC=N), 11.96 (s, 1H, NH). <sup>13</sup>C NMR (DMSO-d<sub>6</sub>) δ 56.65 (*m*-OCH<sub>3</sub>), 60.73 (*p*-OCH<sub>3</sub>), 105.96 (C<sub>2</sub>, C<sub>6</sub>), 126.29 (C<sub>2'</sub>), 127.98 (C<sub>1'</sub>), 128.88 (C<sub>1</sub>), 132.31 (CF<sub>3</sub>), 132.91 (C<sub>4'</sub>), 133.01 (C<sub>5'</sub>), 134.82 (C<sub>6'</sub>), 141.27 (C<sub>4</sub>), 145.61 (C=N), 153.40 (C<sub>3</sub>, C<sub>5</sub>), 163.50 (C=O). IR λ<sub>max</sub>/cm<sup>-1</sup> 3182 (N-H), 1655, 1242 (C=O), 1587 (C=N), 1269, 1039 (C-O), 3008, 2938, 2838, 1506, 1480, 1417, 1336, 1316, 1173, 1121, 1006, 958, 666 (Ar) (KBr). Anal. Calcd for C<sub>18</sub>H<sub>16</sub>ClF<sub>3</sub>N<sub>2</sub>O<sub>4</sub>: C 51.87, H 3.87, N 6.72. Found: C 51.70, H 4.05, N 6.74.

(*E*)-3,4,5-trimethoxy-*N'*-(quinoxalin-6-yl-methylene)benzohydrazide (**35**). Yellow solid, m.p. 207-208°C; yield 83%; <sup>1</sup>H NMR (DMSO-d<sub>6</sub>) δ 3.75 (s, 3H, OCH<sub>3</sub>); 3.90 (s, 6H, OCH<sub>3</sub>); 7.29 (s, 2H, H<sub>2</sub>, H<sub>6</sub>); 8.17 (d, *J*=8.0Hz, 1H, H<sub>2'</sub>); 8.34 (m, 2H, H<sub>9'</sub>, H<sub>10'</sub>); 8.70 (s, 1H, HC=N); 8.99 (d, *J*=8.0Hz, 2H, H<sub>5'</sub>, H<sub>6'</sub>); 12.02 (s, 1H, NH). <sup>13</sup>C NMR (DMSO-d<sub>6</sub>) δ 56.56 (2C, OCH<sub>3</sub>); 60.59 (1C, OCH<sub>3</sub>); 105.73 (C<sub>2</sub>, C<sub>6</sub>); 127.39 (C<sub>1</sub>); 128.70 (C<sub>10'</sub>); 129.44 (C<sub>1'</sub>); 130.29 (C<sub>2'</sub>, C<sub>9'</sub>); 136.62 (C<sub>4</sub>); 142.91 (C<sub>5'</sub>, C<sub>6'</sub>); 143.61 (C<sub>3'</sub>); 146.55 (C<sub>8'</sub>); 146.86 (C<sub>3</sub>, C<sub>5</sub>); 153.16 (CH); 163.22 (C=O). IR λ<sub>max</sub>/cm<sup>-1</sup> 3446 (NH), 1663 (C=O), 1576 (C=N), 1233 (C-O), 2941, 2832, 1008, 913, 862, 767 (Ar) (KBr). Anal. Calcd for C<sub>19</sub>H<sub>18</sub>N<sub>4</sub>O<sub>4</sub>: C 62.26; H 4.95; N 15.29. Exp.: C 62.80; H 5.16; N 15.21.

(*E*)-*N'*-[(4-(dimethylamino)naphtalen-1-yl)methylene]-3,4,5-trimethoxybenzohydrazide (**36**). Yellow solid, m.p. 214-215°C; yield 89%; <sup>1</sup>H NMR (DMSO-d<sub>6</sub>) δ 2.90 (s, 6H, CH<sub>3</sub>); 3.75 (s, 3H, OCH<sub>3</sub>); 3.90 (s, 6H, OCH<sub>3</sub>); 7.17 (d, *J*=8Hz, 1H, H<sub>3'</sub>); 7.30 (s, 2H, H<sub>2</sub>, H<sub>6</sub>); 7.58-7.67 (m, 2H, H<sub>7'</sub>, H<sub>8'</sub>); 7.83 (d, *J*=8.0Hz, H<sub>9'</sub>); 8.22 (d, *J*=8.0Hz, H<sub>6'</sub>); 8.97-9.00 (m, 2H, HC=N, H<sub>2'</sub>); 11.70 (s, 1H, NH). <sup>13</sup>C NMR (DMSO-d<sub>6</sub>) δ 45.03 (2C, CH<sub>3</sub>); 56.56 (2C, OCH<sub>3</sub>); 60.58 (1C, OCH<sub>3</sub>); 105.59 (C<sub>2</sub>, C<sub>6</sub>); 113.78 (C<sub>3'</sub>); 123.91 (C<sub>1'</sub>); 125.23 (C<sub>6'</sub>); 125.42 (C<sub>7'</sub>); 125.77 (C<sub>8'</sub>, C<sub>2'</sub>); 127.51 (C<sub>1</sub>); 128.26 (C<sub>9'</sub>); 129.17 (C<sub>5'</sub>); 129.44 (C<sub>10'</sub>); 132.09 (C<sub>4</sub>); 140.80 (CH); 148.66 (C<sub>4'</sub>); 153.17 (C<sub>3</sub>, C<sub>5</sub>); 163.22 (C=O). IR λ<sub>max</sub>/cm<sup>-1</sup> 3454 (NH), 1663 (C=O), 1576 (C=N), 1233 (C-O), 2941, 2833, 1008, 862, 767 (Ar) (KBr). Anal. Calcd for C<sub>23</sub>H<sub>25</sub>N<sub>3</sub>O<sub>4</sub>: C 67.80; H 6.18; N 10.31. Exp.: C 67.46; H 6.11; N 10.42.

*1-(2-(3-bromo-4-acethyl-5-methoxyphenyl)-5-(3,4,5-trimethoxyphenyl)-1,3,4-oxadiazol-3(2H)-*

*yl)ethanone (43)*. White solid, mp 177-179 °C; yield 30%; <sup>1</sup>H NMR (DMSO-d<sub>6</sub>) δ 2.36 (s, 3H, CH<sub>3</sub>), 2.38 (s, 3H, CH<sub>3</sub>), 3.84 (s, 3H, *p*-OCH<sub>3</sub>), 3.91 (s, 3H, *m*-OCH<sub>3</sub>), 3.92 (s, 6H, *m*-OCH<sub>3</sub>), 6.99 (s, 1H, H2'), 7.06 (s, 1H, H6'), 7.11 (s, 2H, H2, H6), 7.17 (s, 1H, HC-N). <sup>13</sup>C NMR (DMSO-d<sub>6</sub>) δ 20.68 (CH<sub>3</sub>), 21.75 (CH<sub>3</sub>), 56.56 (*m*-OCH<sub>3</sub>), 61.25 (*p*-OCH<sub>3</sub>), 91.52 (C-N), 104.44 (C2, C6), 117.93 (C5'), 119.37 (C2'), 122.52 (C6'), 136.02 (C1', C1), 139.24 (C4'), 141.49 (C4), 152.90 (C3'), 153.64 (C3, C5), 155.84 (C=N), 168.00 (C=O), 168.32 (C=O). IR λ<sub>max</sub>/cm<sup>-1</sup> 1766, 1238 (C=O), 1667, 1582 (C=N), 1254, 1047 (C-O), 1177 (C-N), 3445 (OH), 1130, 621 (C-Br), 3004, 2941, 2838, 1466, 1416, 1366, 1306, 1190, 998, 858 (Ar) (KBr). MS (ESI) *m/z* 523.07 (M + H)<sup>+</sup>.

*1-(2-(4-acethyl-3-methoxyphenyl)-5-(3,4,5-trimethoxyphenyl)-1,3,4-oxadiazol-3(2H)-yl)ethanone*

*(44)*. White solid, mp 170-172 °C; yield 25%; <sup>1</sup>H NMR (DMSO-d<sub>6</sub>) δ 2.37 (s, 3H, CH<sub>3</sub>), 2.38 (s, 3H, CH<sub>3</sub>), 3.83 (s, 3H, *p*-OCH<sub>3</sub>), 3.91 (s, 3H, *m*-OCH<sub>3</sub>), 3.93 (s, 6H, *m*-OCH<sub>3</sub>), 6.98-7.07 (m, 3H, H2', H6'), 7.11 (s, 2H, H2, H6), 7.18 (s, 1H, HC-N), 7.45 (m, 1H, H5'); <sup>13</sup>C NMR (DMSO-d<sub>6</sub>) δ 20.82 (CH<sub>3</sub>), 21.54 (CH<sub>3</sub>), 56.27 (*m*-OCH<sub>3</sub>), 56.33 (*m*-OCH<sub>3</sub>), 61.02 (*p*-OCH<sub>3</sub>), 91.14 (C-N), 92.06 (C2'), 104.22 (C2, C6), 119.16 (C5'), 128.09 (C6'), 136.402 (C1', C1), 141.24 (C4'), 141.96 (C4), 151.78 (C3'), 153.42 (C3, C5), 155.60 (C=N), 167.75 (C=O), 168.10 (C=O). IR λ<sub>max</sub>/cm<sup>-1</sup> 1767, 1243 (C=O), 1665, 1581 (C=N), 1250, 1043 (C-O), 1177 (C-N), 3445 (OH), 1129, 644 (C-Br), 2967, 2945, 2838, 1507, 1466, 1417, 1365, 1036, 1287, 1197, 1083, 997, 958, 861, 699 (Ar) (KBr). MS (ESI) *m/z* 445.14 (M + H)<sup>+</sup>.

*1-(2-(naphthalen-1-yl)-5-(3,4,5-trimethoxyphenyl)-1,3,4-oxadiazol-3(2H)-yl)ethanone (45)*. White

solid, mp 189-192 °C; yield 35%; <sup>1</sup>H NMR (DMSO-d<sub>6</sub>) δ 2.47 (s, 3H, CH<sub>3</sub>), 3.87 (s, 9H, OCH<sub>3</sub>), 7.08 (s, 2H, H2, H6), 7.48 (t, *J* = 8.0 Hz, 1H, H3'), 7.55 (t, *J* = 8.0 Hz, 1H, H7', H8'), 7.62 (t, *J* = 8.0 Hz, 1H, H7'), 7.76 (m, 1H, H4'), 7.92 (d, *J* = 8.0 Hz, 1H, H6'), 8.22 (d, *J* = 8.0 Hz, 1H, H9'). <sup>13</sup>C NMR (DMSO-d<sub>6</sub>) δ 21.57 (CH<sub>3</sub>), 56.28 (*m*-OCH<sub>3</sub>), 60.98 (*p*-OCH<sub>3</sub>), 91.17 (C-N), 104.27 (C2, C6), 119.61 (C1), 123.04 (C2'), 125.07 (C9'), 125.20 (C3'), 126.05 (C7'), 126.95 (C8'), 128.95 (C4'), 130.51

(C6'), 130.61 (C10'), 130.79 (C5'), 134.04 (C1'), 141.11 (C4), 153.29 (C3, C5), 155.83 (C=N), 168.26 (C=O). IR  $\lambda_{\max}/\text{cm}^{-1}$  1731, 1243 (C=O), 1669, 1587 (C=N), 1254, 1039 (C-O), 1124 (C-N), 2997, 2941, 2827, 1509, 1465, 1416, 1369, 1332, 1191, 1006, 980, 847, 784, 699 (Ar) (KBr). MS (ESI)  $m/z$  429.14 (M + Na)<sup>+</sup>.

*N*-(1,3-dioxisoindolin-2-yl)-3,4,5-trimethoxybenzamide (**46**). White solid, m.p. 198-199°C; yield 73%; <sup>1</sup>H NMR (DMSO-d<sub>6</sub>)  $\delta$  3.74 (s, 3H, OCH<sub>3</sub>); 3.85 (s, 6H, OCH<sub>3</sub>); 7.30 (s, 2H, H<sub>2</sub>, H<sub>6</sub>); 7.95-8.02 (m, 4H, H<sub>4</sub>', H<sub>5</sub>', H<sub>6</sub>', H<sub>7</sub>'); 11.25 (s, 1H, NH). <sup>13</sup>C NMR (DMSO-d<sub>6</sub>)  $\delta$  56.52 (2C, OCH<sub>3</sub>); 60.64 (1C, OCH<sub>3</sub>); 105.72 (C<sub>2</sub>, C<sub>6</sub>); 124.34 (C<sub>4</sub>', C<sub>7</sub>'); 126.02 (C<sub>1</sub>); 129.93 (C<sub>2</sub>', C<sub>3</sub>'); 135.88 (C<sub>5</sub>', C<sub>6</sub>'); 141.59 (C<sub>4</sub>); 153.28 (C<sub>3</sub>, C<sub>5</sub>); 165.15 (C=O); 165.89 (C=O). IR  $\lambda_{\max}/\text{cm}^{-1}$  3441 (NH), 1796 (C=O), 1746 (C=O), 1657 (C=O), 1234 (C-O), 1002, 882, 707 (Ar) (KBr). Anal. Calcd for C<sub>18</sub>H<sub>16</sub>N<sub>2</sub>O<sub>6</sub>: C 60.67; H 4.53; N 7.86. Exp.: C 60.83; H 4.79; N 7.87.

*N*-(2,5-dioxo-2,5-dihydro-1H-pyrrol-1-yl)-3,4,5-trimethoxybenzamide (**47**). White solid, m.p. 146-147°C; yield 78%; <sup>1</sup>H NMR (DMSO-d<sub>6</sub>)  $\delta$  3.71 (s, 3H, OCH<sub>3</sub>); 3.83 (s, 6H, OCH<sub>3</sub>); 6.43-6.32 (dd, 2H, H<sub>3</sub>', H<sub>4</sub>'); 7.23 (s, 2H, H<sub>2</sub>, H<sub>6</sub>); 10.57 (s, 1H, NH). <sup>13</sup>C NMR (DMSO-d<sub>6</sub>)  $\delta$  56.45 (2C, OCH<sub>3</sub>); 60.56 (1C, OCH<sub>3</sub>); 105.48 (C<sub>2</sub>, C<sub>6</sub>); 127.43 (C<sub>4</sub>'); 127.66 (C<sub>3</sub>'); 133.38 (C<sub>1</sub>); 140.91 (C<sub>4</sub>); 153.10 (C<sub>3</sub>, C<sub>5</sub>); 163.69 (C=O); 165.06 (C=O); 167.39 (C=O). IR  $\lambda_{\max}/\text{cm}^{-1}$  3437 (NH), 1704 (C=O), 1663 (C=O), 1590 (C=C), 1126 (C-O), 991, 851, 773 (Ar) (KBr). Anal. Calcd for C<sub>14</sub>H<sub>14</sub>N<sub>2</sub>O<sub>6</sub>: C 54.90; H 4.61; N 9.15. Exp.: C 54.32; H 4.22; N 9.06.

*N*-benzoyl-3,4,5-trimethoxybenzohydrazide (**48**). White solid, m.p. 188-189°C; yield 88%; <sup>1</sup>H NMR (DMSO-d<sub>6</sub>)  $\delta$  3.71 (s, 3H, OCH<sub>3</sub>); 3.83 (s, 6H, OCH<sub>3</sub>); 7.25 (s, 2H, H<sub>2</sub>, H<sub>6</sub>); 7.50-7.61 (m, 3H, H<sub>3</sub>', H<sub>4</sub>', H<sub>5</sub>'); 7.91 (d,  $J=8.0\text{Hz}$ , H<sub>2</sub>', H<sub>6</sub>'); 10.45 (s, 1H, NH); 10.49 (s, 1H, NH). <sup>13</sup>C NMR (DMSO-d<sub>6</sub>)  $\delta$  56.45 (2C, OCH<sub>3</sub>); 60.57 (1C, OCH<sub>3</sub>); 105.39 (C<sub>2</sub>, C<sub>6</sub>); 127.88 (C<sub>2</sub>', C<sub>6</sub>'); 128.92 (C<sub>3</sub>', C<sub>5</sub>'); 132.66 (C<sub>1</sub>); 140.75 (C<sub>4</sub>'); 148.92 (C<sub>1</sub>'); 149.80 (C<sub>4</sub>); 152.84 (C<sub>3</sub>); 152.84 (C<sub>3</sub>); 164.96 (C=O);

165.58 (C=O). IR  $\lambda_{\max}/\text{cm}^{-1}$  3450 (NH), 1651 (C=O), 1588 (C=O), 1239 (C-O), 1002, 863, 708 (Ar) (KBr). Anal. Calcd for  $\text{C}_{17}\text{H}_{18}\text{N}_2\text{O}_5$ : C 61.81; H 5.49; N 8.48. Found: C 61.27; H 5.78; N 8.19.

*N*-(3,4,5-trimethoxybenzoyl)-2-naphthohydrazide (**49**). White solid, m.p. 210-211°C; yield 91%;  $^1\text{H}$  NMR (DMSO- $d_6$ )  $\delta$  3.75 (s, 3H, OCH<sub>3</sub>); 3.88 (s, 6H, OCH<sub>3</sub>); 7.34 (s, 2H, H<sub>2</sub>, H<sub>6</sub>); 7.63 (m, 2H, H<sub>5'</sub>, H<sub>6'</sub>); 7.69 (d,  $J=8.0\text{Hz}$ , H<sub>10'</sub>); 8.01-8.10 (m, 3H, H<sub>4'</sub>, H<sub>7'</sub>, H<sub>9'</sub>); 8.43 (d,  $J=8.0\text{Hz}$ , H<sub>2'</sub>); 10.49 (s, 1H, NH); 10.61 (s, 1H, NH).  $^{13}\text{C}$  NMR (DMSO- $d_6$ )  $\delta$  56.47 (2C, OCH<sub>3</sub>); 60.87 (1C, OCH<sub>3</sub>); 105.40 (C<sub>2</sub>, C<sub>6</sub>); 125.47 (C<sub>10'</sub>); 125.94 (C<sub>6'</sub>, C<sub>1</sub>); 126.90 (C<sub>2'</sub>); 127.33 (C<sub>7'</sub>); 127.85 (C<sub>5'</sub>); 128.66 (C<sub>9'</sub>); 128.69 (C<sub>4'</sub>); 130.38 (C<sub>8'</sub>); 130.73 (C<sub>1'</sub>); 133.31 (C<sub>3'</sub>); 133.54 (C<sub>4</sub>); 153.23 (C<sub>3</sub>, C<sub>5</sub>); 165.59 (C=O); 168.58 (C=O). IR  $\lambda_{\max}/\text{cm}^{-1}$  3445 (NH), 1688 (C=O), 1644 (C=O), 1238 (C-O), 1008, 852, 776 (Ar) (KBr). Anal. Calcd for  $\text{C}_{21}\text{H}_{20}\text{N}_2\text{O}_5$ : C 66.31; H 5.30; N 7.36. Exp.: C 66.49; H 4.98; N 6.90.

*N*-(naphthalen-1-yl)-2-(3,4,5-trimethoxybenzoyl)hydrazinecarboxamide (**50**). White solid, m.p. 225°C. yield 84%;  $^1\text{H}$  NMR (DMSO- $d_6$ )  $\delta$  3.73 (s, 3H, 4-OCH<sub>3</sub>); 3.86 (s, 6H, 3-OCH<sub>3</sub>, 5-OCH<sub>3</sub>); 7.30 (s, 2H, H<sub>2</sub>, H<sub>6</sub>); 8.13-7.44 (m, 7H, naphthyl ring); 8.49 (s, 1H, NH); 8.95 (s, 1H, NH); 10.39 (s, 1H, NH).  $^{13}\text{C}$  NMR (DMSO- $d_6$ )  $\delta$  56.4 (3-OCH<sub>3</sub>, 5-OCH<sub>3</sub>); 60.5 (4-OCH<sub>3</sub>); 105.5 (C<sub>2</sub>, C<sub>6</sub>); 122.4-134.7 (naphthyl ring and C<sub>1</sub>); 140.8 (C<sub>4</sub>); 153.0 (C<sub>3</sub>, C<sub>5</sub>); 156.8 (C=O); 166.2 (C=O). HRMS (ESI+)  $m/z$ : calculated for  $\text{C}_{21}\text{H}_{21}\text{N}_3\text{O}_5$  [ $\text{M}^+$ ]: 396.1554; found, 396.1554.

*N*-(4-(*N*-(3,4,5-trimethoxyphenyl)sulfamoyl)phenyl)acetamide (**51**). Gray solid, m.p. 191°C; yield 95%;  $^1\text{H}$  NMR (DMSO- $d_6$ )  $\delta$  2.06 (s, 3H, COCH<sub>3</sub>); 3.55 (s, 3H, 4-OCH<sub>3</sub>); 3.64 (s, 6H, 3-OCH<sub>3</sub>, 5-OCH<sub>3</sub>); 6.37 (s, 2H, H<sub>2</sub>, H<sub>6</sub>); 7.71 (s, 4H, H<sub>2'</sub>, H<sub>3'</sub>, H<sub>5'</sub>, H<sub>6'</sub>); 10.01 (s, 1H, NH); 10.32 (s, 1H, NH).  $^{13}\text{C}$  NMR (DMSO- $d_6$ )  $\delta$  24.5 (COCH<sub>3</sub>); 56.1 (3-OCH<sub>3</sub>, 5-OCH<sub>3</sub>); 60.4 (4-OCH<sub>3</sub>); 98.2 (C<sub>2</sub>, C<sub>6</sub>); 118.9 (C<sub>2'</sub>, C<sub>6'</sub>); 128.5 (C<sub>3'</sub>, C<sub>5'</sub>); 133.3 (C<sub>1</sub>); 134.2 (C<sub>4'</sub>); 134.4 (C<sub>1'</sub>); 143.4 (C<sub>4</sub>); 153.3 (C<sub>3</sub>, C<sub>5</sub>); 169.4 (C=O). HRMS (ESI+)  $m/z$ : calculated for  $\text{C}_{17}\text{H}_{20}\text{N}_2\text{O}_6\text{S}$  [ $\text{M}^+$ ]: 381.1115; found, 381.1114

ACCEPTED MANUSCRIPT  
*4-amino-N-(3,4,5-trimethoxyphenyl)benzenesulfonamide (52)*. White solid, m.p. 173°C; yield 81%; <sup>1</sup>H NMR (DMSO-d<sub>6</sub>) δ 3.55 (s, 3H, 4-OCH<sub>3</sub>); 3.65 (s, 6H, 3-OCH<sub>3</sub>, 5-OCH<sub>3</sub>); 6.37 (s, 2H, H<sub>2</sub>, H<sub>6</sub>); 6.56 (d, 2H, H<sub>3</sub>', H<sub>5</sub>', *J* = 8.7 Hz); 7.43 (d, 2H, H<sub>2</sub>', H<sub>6</sub>', *J* = 8.7 Hz); 9.70 (s, 2H, NH). <sup>13</sup>C NMR (CDCl<sub>3</sub>) δ 56.0 (3-OCH<sub>3</sub>, 5-OCH<sub>3</sub>); 60.4 (4-OCH<sub>3</sub>); 97.6 (C<sub>2</sub>, C<sub>6</sub>), 113.0 (C<sub>2</sub>', C<sub>6</sub>') ; 124.7 (C<sub>1</sub>); 129.3 (C<sub>3</sub>', C<sub>5</sub>'); 134.0 (C<sub>4</sub>'); 134.9 (C<sub>1</sub>'); 153.2 (C<sub>3</sub>, C<sub>5</sub>). HRMS (ESI+) *m/z*: calculated for C<sub>15</sub>H<sub>18</sub>N<sub>2</sub>O<sub>5</sub>S [M<sup>+</sup>]: 339.1009; found, 339.1015.

*3,4,5-trimethoxy-N-(2-(naphthalen-2-yl)-4-oxotiazolidin-3-yl)benzamide (53)*. White solid, m.p. 107-109°C; yield 89%; <sup>1</sup>H NMR (CDCl<sub>3</sub>) δ 3.67 (s, 6H, OCH<sub>3</sub>); 3.76 (s, 3H, OCH<sub>3</sub>); 3.74-3.80 (m, 1H, CH<sub>2</sub>); 3.97-3.93 (m, 1H, CH<sub>2</sub>); 6.23 (s, 1H, CH); 6.81 (s, 2H, H<sub>2</sub>, H<sub>6</sub>); 7.95-7.18 (m, 7H, naphthyl); 9.02 (br, 1H, NH). <sup>13</sup>C NMR (CDCl<sub>3</sub>) δ 30.60 (CH<sub>2</sub>); 55.97 (OCH<sub>3</sub>); 60.69 (OCH<sub>3</sub>); 63.58 (CH); 104.55 (C<sub>2</sub>, C<sub>6</sub>); 124.25-133.94 (naphthyl); 141.30 (C<sub>4</sub>); 152.68 (C<sub>3</sub>, C<sub>5</sub>); 164.79 (C=O); 171.86 (C=O). IR λ<sub>max</sub>/cm<sup>-1</sup> 3252 (NH); 1706 (C=O thiazol.); 1670 (C=O); 1240 (C-O); 1127 (C-N); 1415, 1337, 1003, 852, 806, 747 (Ar). Anal. Calcd for C<sub>23</sub>H<sub>22</sub>N<sub>2</sub>O<sub>5</sub>S: C 63.00; H 5.06; N 6.39; S 7.31. Exp.: C 62.97; H 5.41; N 6.24; S 7.58.

*3,4,5-trimethoxy-N-(2-(naphthalen-1-yl)-4-oxotiazolidin-3-yl)benzamide (54)*. Yellow solid, m.p. 114-116°C; Yield 92%; <sup>1</sup>H NMR (CDCl<sub>3</sub>) δ 3.67 (s, 6H, OCH<sub>3</sub>); 3.76 (s, 3H, OCH<sub>3</sub>); 3.76-3.80 (m, 1H, CH<sub>2</sub>); 3.93-3.97 (m, 1H, CH<sub>2</sub>); 6.80 (s, 2H, H<sub>2</sub>, H<sub>6</sub>); 7.91-7.16 (m, 7H, naftil); 9.45 (br, 1H, NH). <sup>13</sup>C NMR (CDCl<sub>3</sub>) δ 30.47 (CH<sub>2</sub>); 56.02 (OCH<sub>3</sub>); 60.69 (OCH<sub>3</sub>); 104.79 (C<sub>2</sub>, C<sub>6</sub>); 122.42 (C<sub>2</sub>'); 125.28 (C<sub>8</sub>'); 125.38 (C<sub>7</sub>'); 125.45 (C<sub>9</sub>'); 125.47 (C<sub>4</sub>'); 126.15 (C<sub>3</sub>'); 128.20 (C<sub>1</sub>); 129.01 (C<sub>6</sub>'); 129.14 (C<sub>10</sub>'); 129.17 (C<sub>5</sub>'); 130.73 (C<sub>1</sub>'); 141.25 (C<sub>4</sub>); 152.62 (C<sub>3</sub>, C<sub>5</sub>); 165.08 (C=O). IR λ<sub>max</sub>/cm<sup>-1</sup> 3247 (NH); 1704 (C=O thiazol.); 1668 (C=O); 1235 (C-O); 1126 (C-N); 1414, 1336, 1004, 852, 776 (Ar). Anal. Calcd for C<sub>23</sub>H<sub>22</sub>N<sub>2</sub>O<sub>5</sub>S: C 63.00; H 5.06; N 6.39; S 7.31. Exp.: C 62.86; H 5.37; N 6.25; S 7.37.

*5-(naphthalen-1-yl)-3-(3,4,5-trimethoxyphenyl)-1-phenyl-4,5-dihydro-1H-pyrazole (55)*. Yellow solid, m.p: 207-208°C, yield 83%; <sup>1</sup>H NMR (acetone-d<sub>6</sub>) δ 3.18 (dd, 1H, Ha, *J* = 17.1 Hz, 6.2 Hz); 3.74

(s, 3H, *p*-OCH<sub>3</sub>); 3.87 (s, 6H, *m*-OCH<sub>3</sub>); 4.24 (dd, 1H, H<sub>b</sub>, *J* = 17.5 Hz, 12.5 Hz); 6.18 (dd, 1H, H<sub>c</sub>, *J* = 12.1 Hz, 7.0 Hz); 6.72 (m, 1H, H<sub>4''</sub>); 7.02 (d, 2H, H<sub>2''</sub>, H<sub>6''</sub>, *J* = 7.8 Hz); 7.14 (m, 4H, H<sub>2'</sub>, H<sub>6'</sub>, H<sub>3''</sub>, H<sub>5''</sub>); 7.33 (m, 1H, H<sub>2</sub>); 7.42 (dd, 1H, H<sub>3</sub>, *J* = 7.8 Hz, 7.4 Hz); 7.62 (dd, 1H, H<sub>7</sub>, *J* = 7.4 Hz, 7.0 Hz); 7.69 (dd, 1H, H<sub>6</sub>, *J* = 7.8 Hz, 7.4 Hz); 7.87 (d, 1H, H<sub>4</sub>, *J* = 8.2 Hz); 8.03 (d, 1H, H<sub>5</sub>, *J* = 8.2 Hz); 8.36 (d, 1H, H<sub>8</sub>, *J* = 7.8 Hz). <sup>13</sup>C NMR (acetone-*d*<sub>6</sub>) δ 43.2 (C<sub>ab</sub>); 56.3 (*m*-OCH<sub>3</sub>); 60.4 (*p*-OCH<sub>3</sub>); 62.8 (C<sub>c</sub>); 103.3 (C<sub>2'</sub>, C<sub>6'</sub>); 113.6 (C<sub>2''</sub>, C<sub>6''</sub>); 119.2 (C<sub>4''</sub>); 124.1 (C<sub>2</sub>, C<sub>8</sub>); 124.9 (C<sub>6</sub>); 126.3 (C<sub>7</sub>); 126.6 (C<sub>4</sub>); 127.1 (C<sub>3</sub>); 128.5 (C<sub>1'</sub>); 128.9 (C<sub>4'</sub>); 129.5 (C<sub>3''</sub>, C<sub>5''</sub>); 129.6 (C<sub>5</sub>); 129.9 (C<sub>4<sub>a</sub></sub>); 130.7 (C<sub>8<sub>a</sub></sub>); 137.9 (C<sub>1</sub>); 146.5 (C<sub>1''</sub>); 148.4 (C=N); 154.1 (C<sub>3'</sub>, C<sub>5'</sub>). HRMS (ESI+) *m/z*: calculated for C<sub>28</sub>H<sub>26</sub>N<sub>2</sub>O<sub>3</sub> [M<sup>+</sup>]: 438.1937; found, 438.1940.

*2-(naphthalen-1-yl)-3-(3,4,5-trimethoxybenzyl)thiazolidin-4-one (56)*. Beige solid, m.p. 142-143°C; yield 80%; <sup>1</sup>H NMR (CDCl<sub>3</sub>) δ 3.58 (d, 1H, CH<sub>2</sub>, *J* = 14.4 Hz); 3.72 (s, 6H, 3-OCH<sub>3</sub>, 5-OCH<sub>3</sub>); 3.81 (d, 1H, CH<sub>2</sub>-S, *J* = 15.6 Hz); 3.83 (s, 3H, 4-OCH<sub>3</sub>); 3.96 (dd, 1H, CH<sub>2</sub>-S, *J* = 15.6 Hz, *J* = 1.56 Hz); 5.06 (d, 1H, CH<sub>2</sub>, *J* = 14.4 Hz); 5.60 (d, 1H, CH, *J* = 1.56 Hz); 6.26 (s, 2H, H<sub>2</sub>, H<sub>6</sub>); 7.40-7.90 (m, 7H, naphthyl ring). <sup>13</sup>C NMR (CDCl<sub>3</sub>) δ 33.2 (CH<sub>2</sub>-S); 43.3 (CH<sub>2</sub>); 56.0 (3-OCH<sub>3</sub>, 5-OCH<sub>3</sub>); 60.8 (4-OCH<sub>3</sub>); 63.2 (CH); 105.5 (C<sub>2</sub>, C<sub>6</sub>); 124.0-139.2 (naphthyl ring and C<sub>1</sub>); 146.8 (C<sub>4</sub>); 153.5 (C<sub>3</sub>, C<sub>5</sub>); 171.2 (C=O). HRMS (ESI+) *m/z*: calculated for C<sub>23</sub>H<sub>23</sub>NO<sub>4</sub>S [M<sup>+</sup>]: 410.1421; found, 410.1423

*2-(4-(dimethylamino)naphthalen-1-yl)-3-(3,4,5-trimethoxybenzyl)thiazolidin-4-one (57)*. White solid, m.p. 161-162°C; yield 71%; <sup>1</sup>H NMR (CDCl<sub>3</sub>) δ 2.92 (s, 6H, N(CH<sub>3</sub>)<sub>2</sub>); 3.64-3.93 (m, 12H, OCH<sub>3</sub>, CH<sub>2</sub>, CH<sub>2</sub>-S); 5.19 (m, 1H, CH<sub>2</sub>); 6.22 (s, 2H, H<sub>2</sub>, H<sub>6</sub>); 7.46-8.34 (m, 6H, naphthyl ring). <sup>13</sup>C NMR (CDCl<sub>3</sub>) δ 32.9 (CH<sub>2</sub>-S); 45.0 (N(CH<sub>3</sub>)<sub>2</sub>); 47.0 (CH<sub>2</sub>); 55.9 (3-OCH<sub>3</sub>, 5-OCH<sub>3</sub>); 60.7 (4-OCH<sub>3</sub>); 105.6 (C<sub>2</sub>, C<sub>5</sub>); 125.2-137.6 (naphthyl ring and C<sub>1</sub>); 151.7 (C<sub>4</sub>) 153.3 (C<sub>2</sub>, C<sub>6</sub>); 171.8 (C=O). HRMS (ESI+) *m/z*: calculated for C<sub>25</sub>H<sub>28</sub>N<sub>2</sub>O<sub>4</sub>S [M<sup>+</sup>]: 453.1843; found, 453.1837

*2-(naphthalen-1-yl)-3-(3,4,5-trimethoxyphenyl)thiazolidin-4-one (58)*. Yellow solid, m.p. 145-146°C; yield 72%; <sup>1</sup>H NMR (CDCl<sub>3</sub>) δ 3.62 (s, 6H, 3-OCH<sub>3</sub>, 5-OCH<sub>3</sub>); 3.73 (s, 3H, 4-OCH<sub>3</sub>); 3.93 (d, 1H,

CH<sub>2</sub>,  $J = 15.6$  Hz); 4.07 (dd, 1H, CH<sub>2</sub>,  $J = 15.6$  Hz  $J = 1.95$  Hz); 6.11 (s, 1H, CH); 6.33 (s, 2H, H<sub>2</sub>, H<sub>6</sub>); 7.48-7.88 (m, 7H, naphthyl ring). <sup>13</sup>C NMR (CDCl<sub>3</sub>)  $\delta$  33.4 (CH<sub>2</sub>); 55.9 (3-OCH<sub>3</sub>, 5-OCH<sub>3</sub>); 60.7 (4-OCH<sub>3</sub>); 66.4 (CH); 103.9 (C<sub>2</sub>, C<sub>6</sub>); 124.0-136.0 (naphthyl ring and C<sub>1</sub>); 153.2 (C<sub>3</sub>, C<sub>5</sub>); 164.2 (C<sub>4</sub>); 171.1 (C=O). HRMS (ESI+)  $m/z$ : calculated for C<sub>22</sub>H<sub>21</sub>NO<sub>4</sub>S [M<sup>+</sup>]: 396.1264; found, 396.1264

*2-(4-(dimethylamino)naphthalen-1-yl)-3-(3,4,5-trimethoxyphenyl)thiazolidin-4-one* (**59**). Yellow solid, m.p. 156-157°C; yield 73%; <sup>1</sup>H NMR (DMSO-d<sub>6</sub>)  $\delta$ /ppm 2.78 (s, 6H, N-(CH<sub>3</sub>)<sub>2</sub>); 3.55 (s, 3H, 4-OCH<sub>3</sub>); 3.26 (s, 6H, 3-OCH<sub>3</sub>, 5-OCH<sub>3</sub>); 3.73 (m, 2H, CH<sub>2</sub>); 6.85 (s, 2H, H<sub>2</sub>, H<sub>6</sub>); 7.48-8.19 (m, 6H, naphthyl ring). <sup>13</sup>C NMR (DMSO-d<sub>6</sub>)  $\delta$ /ppm 30.0 (CH<sub>2</sub>); 45.1 (N-(CH<sub>3</sub>)<sub>2</sub>); 56.4 (3-OCH<sub>3</sub>, 5-OCH<sub>3</sub>); 60.3 (4-OCH<sub>3</sub>); 124.6-136.2 (naphthyl and phenyl rings); 146.4 (C<sub>4</sub>); 152.9 (C<sub>3</sub>, C<sub>5</sub>); 171.1 (C=O). HRMS (ESI+)  $m/z$ : calculated for C<sub>24</sub>H<sub>26</sub>N<sub>2</sub>O<sub>4</sub>S [M<sup>+</sup>]: 439.1686; found, 439.1685

*4-(2-(naphthalen-1-yl)-4-oxothiazolidin-3-yl)-N-(3,4,5-trimethoxyphenyl)benzenesulfonamide* (**60**). White solid, m.p. 256°C; yield 74%; <sup>1</sup>H NMR (DMSO-d<sub>6</sub>)  $\delta$ /ppm 3.45 (s, 3H, 4-OCH<sub>3</sub>); 3.49 (s, 6H, 3-OCH<sub>3</sub>, 5-OCH<sub>3</sub>); 4.00 (m, 2H, CH<sub>2</sub>); 6.20 (s, 2H, H<sub>2</sub>, H<sub>6</sub>); 6.77 (s, 1H, CH); 7.48-7.85 (m, 11H, naphthyl and phenyl rings); 9.98 (s, 1H, NH). <sup>13</sup>C NMR (DMSO-d<sub>6</sub>)  $\delta$ /ppm 33.3 (CH<sub>2</sub>); 55.9 (3-OCH<sub>3</sub>, 5-OCH<sub>3</sub>); 60.4 (4-OCH<sub>3</sub>); 63.5 (CH); 98.9 (C<sub>2</sub>, C<sub>6</sub>); 124.5-137.1 (naphthyl and phenyl rings); 141.8 (C<sub>4</sub>); 153.2 (C<sub>3</sub>, C<sub>5</sub>); 171.3 (C=O). HRMS (ESI+)  $m/z$ : calculated for C<sub>28</sub>H<sub>26</sub>N<sub>2</sub>O<sub>6</sub>S<sub>2</sub> [M<sup>+</sup>]: 551.1305; found, 551.1303.

*4-(2-(4-(dimethylamino)naphthalen-1-yl)-4-oxothiazolidin-3-yl)-N-(3,4,5-trimethoxyphenyl)benzenesulfonamide* (**61**). Yellow solid, m.p. 234°C; yield 60%; <sup>1</sup>H NMR (DMSO-d<sub>6</sub>)  $\delta$ /ppm 2.77 (s, 6H, N-(CH<sub>3</sub>)<sub>2</sub>); 3.73 (m, 11H, CH<sub>2</sub> and 3,4,5-tri-OCH<sub>3</sub>); 6.26 (s, 2H, H<sub>2</sub>, H<sub>6</sub>); 6.38 (s, 1H, CH); 7.39-8.16 (m, 10H, naphthyl and phenyl rings); 10.03 (s, 1H, NH). <sup>13</sup>C NMR (DMSO-d<sub>6</sub>)  $\delta$ /ppm 33.0 (CH<sub>2</sub>); 45.0 (N-(CH<sub>3</sub>)<sub>2</sub>); 56.1 (3-OCH<sub>3</sub>, 5-OCH<sub>3</sub>); 60.4 (4-OCH<sub>3</sub>); 98.7 (C<sub>2</sub>, C<sub>6</sub>); 119.3-134.6 (naphthyl and phenyl rings); 153.3 (C<sub>3</sub>, C<sub>5</sub>); 167.8 (C=O). HRMS (ESI+)  $m/z$ : calculated for C<sub>30</sub>H<sub>31</sub>N<sub>3</sub>O<sub>6</sub>S<sub>2</sub> [M<sup>+</sup>]: 594.1727; found, 594.1722.

## 4.2. Molecular modeling

The structures of the *N*-acylhydrazone derivatives were constructed using the standard tools available in SYBYL 8.0. Four different conformers were modeled for each derivative [13] for which the energy values were minimized employing the Tripos force field and Gasteiger-Huckel charges. Docking protocols were used as implemented in GOLD 3.1 [34]. The X-ray crystal structures of the tubulin-colchicine, tubulin-ABT751 and tubulin-T138067 complexes (PDB IDs 1SA0, 3HKC and 3HKE, respectively) were retrieved from the Protein Data Bank [35, 36]. For the docking calculations, the ligands were removed and hydrogen atoms were added using the Biopolymer module (SYBYL 8.0). Residues in the binding site were manually checked for possible flipped orientation, protonation and tautomeric states. The binding cavity was centered on the C22 atom of DAMA-colchicine and a radius sphere of 10 Å was considered for the docking procedures, which were repeated 10 times for each selected conformation of the *N*-acylhydrazone derivatives.

## 4.3. Antiproliferative assay

REH and Jurkat human acute lymphoblastic leukemia cell lines were maintained in RPMI-1640, supplemented with 10% fetal bovine serum (FBS) and penicillin/streptomycin, at 37 °C and 5% CO<sub>2</sub>. For the cytotoxic assay, compounds were dissolved in DMSO to obtain a stock solution of 20 mM. Further dilutions were made in culture medium immediately before use. Eighty microliters of a REH or Jurkat suspension ( $3.75 \times 10^5$  cells/mL) were seeded in a 96-well plate. Immediately, 20 µL of compound dilutions were added to each well, in triplicate, in final concentrations ranging from 0.01 to 1 µM. Culture plates were then kept at 37 °C and 5% CO<sub>2</sub> for 48 h, when 20 µL of MTT reagent (5 mg/mL) was added. After 4.5 h, the precipitated formazan crystals were dissolved by the addition of 100 µL of an acid sodium dodecyl sulfate solution (10% SDS, 0.01 mol/L HCl). Following overnight incubation, absorbance was measured at 570 nm. Percentage of cell survival was calculated in relation to controls, and IC<sub>50</sub> values were determined using GraphPad Prism 5 software.

4.4.1. *Cell culture.* Breast cancer cell line MDA-MB-231 was kindly provided by Prof. Heloisa Sobreiro Selistre de Araújo (Departamento de Ciências Fisiológicas, Universidade Federal de São Carlos, Brazil). The stock cells were maintained in a 75-cm<sup>2</sup> flask in DMEM (Dulbecco's Modified Eagle's Medium) supplemented with 10% FBS. Cells were incubated at 37 °C in 5% CO<sub>2</sub> humidified atmosphere. The Trypan Blue exclusion test was used to evaluate cell viability before experiments.

4.4.2. *Wound healing assay.* For cell motility determination, cells were seeded in 24-well tissue culture plate (Becton Dickinson) and grown to 80-90% confluence. After aspirating the medium, the center of the cell monolayers were scraped with a sterile micropipette tip to create a denuded zone. Subsequently, cellular debris was washed away with DMEM (without FBS supplementation) and cells were incubated at 37 °C for 22 h, in growth medium containing different concentrations of compounds. Photographs of the wounded monolayers were taken at time points 0 and 22 h, and the percentage of wound closure was calculated by Java's Image J software.

4.4.3. *Boyden chamber migration assay.* Cell migration was assayed with Boyden chambers [8.0 µm pore size, polyethylene terephthalate membrane, FALCON cell culture insert (Becton-Dickinson)]. MDA-MB-231 cells were cultured in DMEM until 80-90% confluency. For the migration assay, cells were detached with trypsin and resuspended in serum-free medium. After cell counting,  $4.0 \times 10^4$  cells (in 350 µL of serum free medium) were added in the upper chamber. In the lower chamber, 700 µL of culture medium containing 10% FBS (a chemoattractant) was added. The transwells were incubated for 6 h at 37 °C with different concentrations of the compounds in both upper and lower chambers. Controls were given the vehicle in the same way. After incubation, cells inside the inserts were removed with a cotton swab and cells on the underside of the insert were fixed with methanol and stained with toluidine blue stain (Sigma). Transmigrated cells were counted in a light microscope, using six random regions of the membrane. The NIS Elements software (NIKON) was used to count the cells. Two independent experiments were carried out in duplicate for each compound.

#### 4.5 Inhibition of MT Assembly

Electrophoretically homogeneous bovine brain tubulin (final concentration 10  $\mu$ M; 1mg/ mL) was pre-incubated with test agents dissolved in DMSO (1% v/v final concentration) and monosodium glutamate (0.8 M final concentration) at 30 °C in 96-well plates. The reaction mixtures were cooled on ice for 10 min and GTP (0.4 mM final concentration) was added. The absorbance at 350 nm was immediately followed in a spectrophotometer. Baselines were established and temperature was quickly raised to 37 °C. The turbidity value after 20 min at 30 °C for DMSO 1% was assigned as 100% assembly and for colchicine 10  $\mu$ M, as 0% assembly. The IC<sub>50</sub> were calculated by nonlinear regression from the percent assembly values at the same time-point obtained with 0.625, 1.25, 2.5, 5 and 10  $\mu$ M of the tested agents.

#### 4.6. Automated High-Content Cellular Analyses

The effects of 12 representative *N*-acylhydrazones on mitotic arrest, nuclear morphology and cellular microtubules were studied as previously described using a multiparameter, high-content imaging assay on an ArrayScan II (Thermo Fisher Cellomics, Pittsburgh, PA) [10]. Briefly, asynchronously growing HeLa cells were treated for 18 h with each compound or vehicle (DMSO 0.1% final concentration) in collagen-coated 384-well microplates, fixed, and incubated with primary antibodies for tubulin and the mitotic marker protein phosphohistone H3, followed by addition of fluorescein isothiocyanate (FITC) and Cy3-conjugated secondary antibodies, respectively. Cells were detected by nuclear counterstaining with Hoechst 33342, which also provided information about chromatin condensation and cell density as markers of cell death. Analysis of cell cycle arrest, mitotic index, nuclear morphology, and cellular toxicity was performed exactly as described [10].

#### 4.7. Flow cytometry for Cell Cycle and Apoptosis Analysis

Jurkat cells were maintained in RPMI-1640, supplemented with 10% FBS and penicillin/streptomycin, 37 °C and 5% CO<sub>2</sub>. Cells were incubated for 12 h in fresh medium before

ACCEPTED MANUSCRIPT  
experiments.  $2 \times 10^6$  cells were treated with 125 nM of compound **12** or DMSO for 18 h. For cell cycle analysis, cells were fixed in 70% ethanol for 2 h, washed in PBS and incubated for 30 min in PBS 20  $\mu\text{g}/\text{mL}$  propidium iodide, 80  $\mu\text{g}/\text{mL}$  RNase A and 0.1% Triton X-100. For apoptosis analysis, cells were incubated with Alexa Fluor® 488 Annexin V conjugate according to manufacturer protocol. Stained cells were read in a BD Biosciences FACSCalibur flow cytometer.

#### 4.8. Selective cytotoxicity

Peripheral blood mononuclear cells (PBMC) were isolated from the blood of two healthy individuals using Ficoll-Paque gradient. PMBC ( $2.5 \times 10^6$  cells/mL), REH and Jurkat cell (both at  $3.75 \times 10^5$  cells/mL) were resuspended in RPMI-1640 supplemented with 10% FBS and penicillin/streptomycin. PBMC's culture medium was supplemented with phytohemagglutinin (25  $\mu\text{L}/\text{mL}$ , Cultilab) and Interleukin 2 (50U/mL) to induce proliferation of T lymphocytes. Eighty microliters of cell suspensions were seeded in a 96-well plate and incubated for 24 h at 37 °C and 5% CO<sub>2</sub> for cell acclimation. Next, 20  $\mu\text{L}$  of culture medium with increasing concentrations of compound **12** or vehicle (DMSO) were added to each well and cytotoxicity was evaluated by the MTT reduction assay after 48 h of treatment. Survival was calculated in relation to controls.

#### 4.9. Toxicity assays *in vivo*

To investigate the safety profiles of compound **12**, we performed acute toxicity tests on mice, according to guidelines of the Organization for Economic Co-operation and Development (OECD, 2001). All experimental protocols were carried out following recommendations of the National Institutes of Health Animal Care Guidelines (NIH publications No. 80–23), and conducted in accordance to the protocol approved by the Committee of the Ethical Use of Animals of the Federal University of Santa Catarina (CEUA/UFSC). Briefly, 7- to 8-week-old Swiss mice (25 – 35 g) were acquired from the animal facility of the Federal University of Santa Catarina (UFSC, Florianópolis, SC, Brazil). Animals were housed in cages (six animals per cage), at  $22 \pm 1^\circ\text{C}$ , under a 12-hour light/12-h dark cycle (lights on at 06:00 hours), 60–80% humidity, with free access to food (Nuvital,

Curitiba, PR, Brazil) and tap water. Female and male mice (n = 6 of each sex) were orally administrated with a single bolus injection by gavage of compound **12** at dose levels of 0.1, 1, 10, 100 and 1,000 mg/kg. Control mice were administered the same volume of vehicle (2% DMSO in saline). Animals were observed 0.25; 0.5; 1; 2; 4; 8 and 24 h after treatment and everyday for 14 days. Mice death and gross behavior alterations such as piloerection, palpebral ptoses, abdominal contortions, muscular tonus, shacking, posterior paws paralysis, salivation, diarrhea and convulsions among others were considered. Body weight, intake of food and drink were also registered during the 14 days. On day 14, mice were sacrificed and glands or organs, such as heart, lung, liver, kidney, spleen, stomach, salivary gland, adrenal gland, thymus, mesenteric lymph nodes and brain were weighted and carefully examined by macroscopic observation with respect to general appearance, shape, consistency and color.

#### **4.10. Anti-leukemia *in vivo* experiments**

Patient-derived xenograft sample of acute lymphoblastic leukemia were thawed, washed with PBS and  $1 \times 10^7$  cells were injected via the tail vein in unconditioned NOD/SCID (NOD.CB17-Prkdcscid/J) mice (The Jackson Laboratory, Bar Harbor, ME) for an *in vivo* expansion step. The patient-derived xenograft was established during the course of a previous study (CAAE 0014.0.144.146-08), approved by the Research Ethics Committee of the Faculty of Medical Sciences, State University of Campinas (protocol 3624-1). Successfully engrafted mice were sacrificed, ALL cells were collected from spleen, liver and bone marrow and  $1 \times 10^7$  fresh cells were immediately injected in higher number of secondary recipient mice (n=9) for the experiments. Animals were monitored every 7 days for ALL engraftment and progression as previously described [37]. Briefly, 50  $\mu$ l of blood were collected by retro-orbital bleeding into EDTA containing tube and mononuclear cells were isolated by ficoll gradient centrifugation. The percentage of ALL cells over total CD45+ cells (human CD45 cells / human CD45 + mouse CD45 cells) was evaluated by flow cytometry in a FACSCanto II equipment (Becton Dickinson, Franklin Lakes, NJ), using anti-hCD45-PE (clone HI30, BD Pharmingen, San Diego, CA or EXBIO, Prague, Czech Republic) and anti-mCD45-FITC (clone

30F-11, BD Pharmingen). When the percentage of leukemia cells reached  $\geq 0.5\%$  (median value from 9 mice), animals were randomly distributed among three different groups of treatment: (1) control (saline solution), (2) vincristine (0.15 mg/kg) and (3) compound **12** (1 mg/kg), administered i.p. once a week for a period of 4 weeks. Every week, before the injection of the drug (saline, vincristine, compound **12**), blood was collected and the percentage of leukemic cells was measured by flow cytometry, as described above. At the end of the fourth week of treatment, animals were sacrificed in an isoflurane chamber. Bone marrow cells were obtained by flushing the femoral bones with PBS. Liver and spleen (whole organs) were mechanically homogenized and suspended with PBS. Mononuclear cells from bone marrow, spleen and liver were obtained by centrifugation on ficoll gradient and the percentage of ALL cells was analyzed as above.

## **ASSOCIATED CONTENT**

### **Supporting Information**

Figures S1-S3, Tables S1-S4. This material is available free of charge via the Internet at <http://pubs.acs.org>.

## **ACKNOWLEDGMENTS**

We would like to thank CNPq, CAPES and FAPESP for financial support and fellowships. The authors also thank the Chemistry Department and the Structural Molecular Biology Center from Universidade Federal de Santa Catarina for equipments for chemical analysis and staff for technical assistance. . This project used the University of Pittsburgh Cancer Institute Chemical Biology Facility that is supported in part by US National Institutes of Health award P30CA047904.

- [1] A. Vogt, P. A. McPherson, X. Shen, R. Balachandran, G. Zhu, B. S. Raccor, S. G. Nelson, M. Tsang, B. W. Day. High-content analysis of cancer-cell-specific apoptosis and inhibition of in vivo angiogenesis by synthetic (-)-pironetin and analogs. *Chem. Biol. Drug Des.* 74 (2009) 358-368.
- [2] R. Mikstacka, T. Stefański, J. Rózański. Tubulin-interactive stilbene derivatives as anticancer agents. *Cell. Mol. Biol. Lett.* 18 (2013) 368-397.
- [3] C. Rappl, P. Barbier, V. Bourgarel-Rey, C. Grégoire, R. Gilli, M. Carre, S. Combes, J.-P. Finet, V. Peyrot. Interaction of 4-arylcoumarin analogues of combretastatins with microtubule network of HBL100 Cells and binding to tubulin. *Biochemistry* 45 (2006) 9210-9218.
- [4] M. A. Jordan, L. Wilson. Microtubules as a target for anticancer drugs. *Nat. Rev. Cancer* 4 (2004) 253-265.
- [5] Z.-Y. Lin, C.-C. Wu, Y.-H. Chuang, W.-L. Chuang. Anti-cancer mechanisms of clinically acceptable colchicine concentrations on hepatocellular carcinoma. *Life Sci.* 93 (2013) 323-328.
- [6] A. Kamal, A. Mallareddy, P. Suresh, T. B. Shaik, V. Lakshma Nayak, C. Kishor, R. V. Shetti, N. Sankara Rao, J. R. Tamboli, S. Ramakrishna, A. Addlagatta. Synthesis of chalcone-amidobenzothiazole conjugates as antimitotic and apoptotic inducing agents. *Bioorg. Med. Chem.* 20 (2012) 3480-3492.
- [7] X. Zhai, Q. Huang, N. Jiang, D. Wu, H. Zhou, P. Gong. Discovery of Hybrid Dual N-Acylhydrazone and Diaryl Urea Derivatives as potent antitumor agents: design, synthesis and cytotoxicity evaluation. *Molecules* 18 (2013) 2904-2923.

- [8] S. S. Mohamed, A. R. Tamer, S. M. Bensaber, M. I. Jaeda, N. B. Ermeli, A. A. Allafi, I. A. Mrema, M. Erhuma, A. Hermann, A. M. Gbaj. Design, synthesis, molecular modeling, and biological evaluation of sulfanilamide-imines derivatives as potential anticancer agents. *Naunyn. Schmiedebergs. Arch. Pharmacol.* 386 (2013) 813-822.
- [9] G. S. Jedhe, D. Paul, R. G. Gonnade, M. K. Santra, E. Hamel, T. L. Nguyen, G. J. Sanjayan. Correlation of hydrogen-bonding propensity and anticancer profile of tetrazole-tethered combretastatin analogues. *Bioorg. Med. Chem. Lett.* 23 (2013) 4680-4684.
- [10] L. B. Salum, W. F. Altei, L. D. Chiaradia, M. N. S. Cordeiro, R. R. Canevarolo, C. P. S. Melo, E. Winter, B. Mattei, H. N. Daghestani, M. C. Santos-Silva, T. B. Creczynski-Pasa, R. A. Yunes, J. A. Yunes, A. D. Andricopulo, B. W. Day, R. J. Nunes, A. Vogt. Cytotoxic 3,4,5-trimethoxychalcones as mitotic arresters and cell migration inhibitors. *Eur. J. Med. Chem.* 63 (2013) 501-510.
- [11] L. Troeberg, X. Chen, T. M. Flaherty, R. E. Morty, M. Cheng, H. Hua, C. Springer, J. H. McKerrow, G. L. Kenyon, J. D. Lonsdale-Eccles, T. H. T. Coetzer, F. E. Cohen. Chalcone, acyl hydrazide, and related amides kill cultured *Trypanosoma brucei brucei*. *Mol. Med.* 6 (2000) 660-669.
- [12] D. N. Amaral, B. C. Cavalcanti, D. P. Bezerra, P. M. P. Ferreira, R. P. Castro, J. R. Sabino, C. M. L. Machado, R. Chammas, C. Pessoa, C. M. R. Sant'Anna, E. J. Barreiro, L. M. Lima. Docking, Synthesis and Antiproliferative Activity of N-Acylhydrazone Derivatives Designed as Combretastatin A4 Analogues. *Plos One*, 9 (2014) e85380.
- [13] L. Pol-Fachin, C. A. M. Fraga, E. J. Barreiro, H. Verli. Characterization of the conformational ensemble from bioactive n-acylhydrazone derivatives. *J. Mol. Graph. Model.* 28 (2010) 446-454.

[14] L. Jin, J. Chen, B. Song, Z. Chen, S. Yang, Q. Li, D. Hu, R. Xu. Synthesis, structure, and bioactivity of n'-substituted benzylidene-3,4,5-trimethoxybenzohydrazide and 3-acetyl-2-substituted phenyl-5-(3,4,5-trimethoxyphenyl)-2,3-dihydro-1,3,4-oxadiazole derivatives. *Bioorg. Med. Chem. Lett.* 16 (2006) 5036-5040.

[15] Neuenfeldt, P. D., Drawanz, B., Aguiar, A., Figueiredo Jr., F., Krettli, A., Cunico, W. Multicomponent synthesis of new primaquine thiazolidinone derivatives. *Synthesis* v.2011 (2011) 3866-3870.

[16] M. F. Maioral, P. C. Gaspar, G. R. R. Souza, A. Mascarello, L. D. Chiaradia, M. A. Licínio, A. C. R. Moraes, R. A. Yunes, R. J. Nunes, M. C. Santos-Silva. Apoptotic events induced by synthetic naphthylchalcones in human acute leukemia cell lines. *Biochimie* 95 (2013) 866-874.

[17] A. Lévai, J. Jekö. Synthesis of 1-substituted 3,5-diaryl-2-pyrazolines by the reaction of  $\alpha,\beta$ -unsaturated ketones with hydrazines. *J. Heterocyclic Chem.* 43 (2006) 111-115.

[18] N. Brosse, M. F. Pinto, B. Jamart-Grégoire. Preparation of multiply protected alkylhydrazine derivatives by Mitsunobu and PTC approaches. *Eur. J. Org. Chem.* 24 (2003) 4757-4764.

[19] Santos, L., Lima, L. A., Cechinel-Filho, V., Corrêa, R., Buzzi, F. C., Nunes, R. J. Synthesis of new 1-phenyl-3-{4-[(2E)-3-phenylprop-2-enoyl]phenyl}-thiourea and urea derivatives with anti-nociceptive activity. *Bioorg. Med. Chem.* 16 (2008) 8526-8534.

[20] Harmata, M., Zheng, P., Huang, C., Gomes, G. M., Ying, W., Ranyanil, K., Balan, G., Calkins, L. N. Expedient synthesis of sulfonamides from sulfonyl chlorides. *J. Org. Chem.* 72 (2007) 683-685.

- [21] A. S. Chida, P. V. S. N. Vani, M. Chandrasekharam, R. Srinivasan, A. K. Singh. Synthesis of 2,3-dimethoxy-5-methyl-1,4-benzoquinone: a key fragment in coenzyme-Q series. *Synth. Commun.* 31 (2001) 657-660.
- [22] G. Mazzone, F. Bonina, G. Puglisi, A. M. Panico, R. Arrigo Reina. 2,5-Diaryl-substituted 1,3,4-oxadiazoles: synthesis and preliminary pharmacological investigation. *Farmaco. Sci.* 39 (1984) 414-20.
- [23] C. Cave, H. Galons, M. Miocque, P. Rinjard, G. Tran, P. Binet. Hydrazidones à action antihypertensive: étude des dichloroarylhydrazones acylées. *Eur. J. Med. Chem.* 25 (1990) 75-79.
- [24] D. M. Borchhardt, A. Mascarello, L. D. Chiaradia, R. J. Nunes, G. Oliva, R. A. Yunes, A. D. Andricopulo. Biochemical evaluation of a series of synthetic chalcone and hydrazone derivatives as novel inhibitors of cruzain from *Trypanosoma cruzi*. *J. Braz. Chem. Soc.* 21 (2010) 142-150.
- [25] R. J. Nunes, A. Mascarello, R. A. Yunes, T. R. Stumpf, P. C. Leal, J. A. Yunes, C. P. S. Melo, R. R. Canevarolo, L. D. Chiaradia, A. B. Silveira. Compostos acil-hidrazonas e oxadiazóis, composições farmacêuticas compreendendo os mesmos e seus usos. Patent WO 2013/075199 A1 (2013).
- [26] N. J. Lawrence, R. P. Patterson, L.-L. Ooi, D. Cook, S. Ducki. Effects of alpha-substitutions on structure and biological activity of anticancer chalcones. *Bioorg. Med. Chem. Lett.* 16 (2006) 5844-5848.
- [27] S. Ducki, D. Rennison, M. Woo, A. Kendall, J. F. D. Chabert, A. T. McGown, N. J. Lawrence. Combretastatin-like chalcones as inhibitors of microtubule polymerization. Part 1: synthesis and biological evaluation of antivasular activity. *Bioorg. Med. Chem.* 17 (2009) 7698-7710.

- [28] S. Ducki. Antimitotic chalcones and related compounds as inhibitors of tubulin assembly. *Anticancer. Agents Med. Chem.* 9 (2009) 336-347.
- [29] J. C. Yarrow, Z. E. Perlman, N. J. Westwood, T. J. Mitchison. A high-throughput cell migration assay using scratch wound healing, a comparison of image-based readout methods. *BMC Biotechnol.* 4 (2004) 21.
- [30] P. Y. K. Yue, E. P. Y. Leung, N. K. Mak, R. N. S. A. Wong. A Simplified method for quantifying cell migration/wound healing in 96-well plates. *J. Biomol. Screen.* 15 (2010) 427-433.
- [31] A. Albini, Y. Iwamoto, H. K. Kleinman, G. R. Martin, S. A. Aaronson, J. M. Kozlowski, R. N. McEwan. A rapid in vitro assay for quantitating the invasive potential of tumor cells. *Cancer Res.* 47 (1987) 3239-3245.
- [32] D. D. Shan, L. Chen, J. T. Njardarson, C. Gaul, X. J. Ma, S. J. Danishefsky, X. Y. Huang. Synthetic analogues of migrastatin that inhibit mammary tumor metastasis in mice. *Proc. Natl. Acad. Sci. U. S. A.* 102 (2005) 3772-3776.
- [33] Z. Wang, P. A. McPherson, B. S. Raccor, R. Balachandran, G. Zhu, B. W. Day, A. Vogt, P. Wipf. Structure-activity and high-content imaging analyses of novel tubulysins. *Chem. Biol. Drug Des.* 70 (2007) 75-86.
- [34] G. Jones, P. Willett, R. C. Glen, A. R. Leach, R. Taylor. Development and validation of a genetic algorithm for flexible docking. *J. Mol. Biol.* 267 (1997) 727-748.

[35] A. Dorléans, B. Gigant, R. B. G. Ravelli, P. Mailliet, V. Mikol, M. Knossow. Variations in the colchicine-binding domain provide insight into the structural switch of tubulin. *Proc. Natl. Acad. Sci. U. S. A.* 106 (2009) 13775-13779.

[36] R. B. G. Ravelli, B. Gigant, P. A. Curmi, I. Jourdain, S. Lachkar, A. Sobel, M. Knossow. Insight into tubulin regulation from a complex with colchicine and a stathmin-like domain. *Nature* 428 (2004), 198-202.

[37] R. B. Lock, N. Liem, M. L. Farnsworth, C. G. Milross, C. Xue, M. Tajbakhsh. The nonobese diabetic/severe combined immunodeficient (NOD/SCID) mouse model of childhood acute lymphoblastic leukemia reveals intrinsic differences in biologic characteristics at diagnosis and relapse. *Blood* 99 (2002), 4100-4108.

**Figure 1.** (A) Representative microtubule-interacting agents that binds to the colchicine site on tubulin. Ph, phenyl (B) Synthesized 3,4,5-trimethoxy-acylhydrazones (**6-36**). Reagents and conditions: (a)  $(\text{CH}_3)_2\text{SO}_4$ ,  $\text{K}_2\text{CO}_3$ , TBAI, acetone, reflux, 12 h; (b)  $\text{N}_2\text{H}_4 \cdot \text{H}_2\text{O}$ , methanol, reflux, 5 h; (c) methanol, reflux, 2 h.

**Figure 2.** Derivatives and analogs from compound **12** designed and synthesized in this work.

**Figure 3.** (A) Conformational states of *N*-acylhydrazone backbone (a-d). (B) Crystallographic position of DAMA-colchicine (dark gray) into the tubulin binding cavity (a); Docking pose of chalcone **4** (light gray) into the tubulin binding cavity (b); Docking pose of B-conformation of *N*-acylhydrazone **6** (violet) into the tubulin binding cavity (c). Tubulin PDB file 1SA0.

**Figure 4.** Immunofluorescence staining for markers of mitotic arrest in HeLa cells. HeLa cells were treated with (A) vehicle (dimethyl sulfoxide, DMSO 0.1%), (B) colchicine **1** (62 nM), (C) the general backbone of the series **6** (312 nM), or (D) the most potent derivative **12** (62 nM), followed by simultaneous immunostaining of  $\alpha$ -tubulin (green), phosphohistone H3 (red), and Hoechst 33342 (blue). Vehicle-treated cells have highly organized microtubules and low percentage of mitotic cells. Colchicine **1** and the (*E*)-*N*-benzylidene-3,4,5-trimethoxybenzohydrazides **6** and **12** caused a heterogeneous response of tubulin disorganization, increased number of phosphohistone H3-positive cells, chromatin condensation and nuclear fragmentation. Images shown are representative fields from a single experiment repeated three times with similar results.

**Figure 5.** Cell cycle arrest and apoptosis induction by compound **12**. Jurkat cells were treated for 18h with 125 nM compound **12** or DMSO and analyzed by flow cytometry for (A) cell cycle analysis, with propidium iodide staining, and (B) Apoptosis, with Annexin V/propidium iodide double staining.

**Figure 6.** Inhibition of breast tumor MDA-MB-231 cells migration by colchicine **1** (blue) and (*E*)-*N'*-benzylidene-3,4,5-trimethoxybenzohydrazides **6** (black) and **12** (red). **Upper panel:** Photographs of wound healing assay at 0 and 22 h, comparing the wound closure by colchicine **1** and compounds **6** and **12** at 1  $\mu$ M. **Lower panel:** Wound healing assay for inhibition of cell migration caused by **6** (black) and **12** (red) in three different concentrations. Data are the mean  $\pm$  SEM of triplicate wells from a single experiment repeated three times with similar results.

**Figure 7.** Selective cytotoxicity of compound **12**. Human T-cell leukemia (Jurkat) and phytohemagglutinin/IL2-stimulated T-lymphocytes from a healthy donor (PBMC) were cultured for 48h with increasing concentrations of compound **12**. Survival was assessed by the MTT reduction assay. The results are representative of two independent experiments.

**Figure 8.** *In vivo* anti-leukemia activity of compound **12**. NOD/SCID mice were injected with patient-derived xenograft ALL. Treatment started when human CD45+ cells accounted for more than 0.5% of peripheral blood cells in half the animals. Vincristine (0.15 mg/kg), compound **12** (1 mg/kg) or saline (control) were given once a week, intraperitoneally. **(A)** Percentage of leukemia cells (hCD45+) in the peripheral blood of mice over a 4-week treatment period. Each line correspond to one animal. One of the animals in the control group died before completion of the experiment and was therefore excluded from analysis. **(B)** ALL infiltration in bone marrow and secondary organs at the end of the experiment. Bars correspond to the mean  $\pm$  SEM. same individual animal.

**Table 1.** B- and T-cell precursor ALL cell lines' survival rates after 48 h of treatment with 0.1  $\mu$ M of colchicine (**1**), chalcones (**4** and **5**) or the 3,4,5-trimethoxy-hydrazones (**6-36**). (Mean  $\pm$  standard deviation).

Compound	Survival (%)		Compound	Survival (%)	
	BCP-ALL	T-ALL		BCP-ALL	T-ALL
<b>1</b>	14 $\pm$ 1	11 $\pm$ 1	<b>20</b>	88 $\pm$ 12	100 $\pm$ 4
<b>4</b>	102 $\pm$ 3	94 $\pm$ 16	<b>21</b>	37 $\pm$ 1	17 $\pm$ 0
<b>5</b>	106 $\pm$ 6	84 $\pm$ 11	<b>22</b>	88 $\pm$ 5	115 $\pm$ 14
<b>6</b>	92 $\pm$ 5	88 $\pm$ 1	<b>23</b>	97 $\pm$ 5	119 $\pm$ 12
<b>7</b>	45 $\pm$ 1	30 $\pm$ 3	<b>24</b>	94 $\pm$ 1	121 $\pm$ 13
<b>8</b>	98 $\pm$ 5	96 $\pm$ 7	<b>25</b>	100 $\pm$ 6	86 $\pm$ 8
<b>9</b>	99 $\pm$ 8	102 $\pm$ 8	<b>26</b>	102 $\pm$ 9	100 $\pm$ 18
<b>10</b>	103 $\pm$ 2	103 $\pm$ 6	<b>27</b>	97 $\pm$ 2	94 $\pm$ 1
<b>11</b>	99 $\pm$ 5	101 $\pm$ 9	<b>28</b>	96 $\pm$ 3	81 $\pm$ 3
<b>12</b>	39 $\pm$ 1	30 $\pm$ 2	<b>29</b>	95 $\pm$ 3	86 $\pm$ 1
<b>13</b>	109 $\pm$ 7	98 $\pm$ 1	<b>30</b>	89 $\pm$ 5	78 $\pm$ 8
<b>14</b>	60 $\pm$ 15	33 $\pm$ 3	<b>31</b>	90 $\pm$ 15	79 $\pm$ 3
<b>15</b>	43 $\pm$ 2	30 $\pm$ 0	<b>32</b>	91 $\pm$ 3	91 $\pm$ 3
<b>16</b>	68 $\pm$ 4	34 $\pm$ 1	<b>33</b>	94 $\pm$ 11	63 $\pm$ 2
<b>17</b>	106 $\pm$ 1	122 $\pm$ 13	<b>34</b>	98 $\pm$ 8	98 $\pm$ 8
<b>18</b>	101 $\pm$ 1	121 $\pm$ 16	<b>35</b>	85 $\pm$ 3	39 $\pm$ 6
<b>19</b>	94 $\pm$ 2	83 $\pm$ 8	<b>36</b>	78 $\pm$ 4	38 $\pm$ 5

BCP-ALL, B-cell precursor ALL (REH cell line); T-ALL, T-cell precursor ALL (Jurkat cell line).

**Table 2.** IC<sub>50</sub> values of the most potent designed compounds against leukemia cell lines.

Compound	IC <sub>50</sub> (μM) ± 95% CI	
	BCP-ALL	T-ALL
Colchicine (1)	0.012 ± 0.001	0.011 ± 0.002
4	0.79 ± 0.31	0.59 ± 0.30
5	1.07 ± 0.22	1.24 ± 0.29
7	0.039 ± 0.008	0.036 ± 0.005
12	0.015 ± 0.002	0.016 ± 0.002
13	0.387 ± 0.09	0.390 ± 0.09
14	0.39 ± 0.06	0.20 ± 0.01
15	0.21 ± 0.1	0.16 ± 0.03
16	0.31 ± 0.07	0.19 ± 0.02
21	0.068 ± 0.011	0.070 ± 0.013
35	4.73 ± 3.31	2.57 ± 0.16
36	1.76 ± 0.45	0.60 ± 0.07

BCP-ALL, B-cell precursor ALL (REH cell line); T-ALL, T-cell precursor ALL (Jurkat cell line); CI, confidence interval

**Table 3.** IC<sub>50</sub> values of the derivatives or analogs of compound **12** against leukemia cell lines.

Compound	IC <sub>50</sub> (μM) ± 95% CI	
	BCP-ALL	T-ALL
<b>37</b>	>100	>100
<b>38</b>	>100	>100
<b>39</b>	>100	>100
<b>40</b>	>100	>100
<b>41</b>	>100	>100
<b>42</b>	>100	>100
<b>43</b>	>100	>100
<b>44</b>	>100	>100
<b>45</b>	>100	>100
<b>46</b>	>100	>100
<b>47</b>	>100	>100
<b>48</b>	>100	>100
<b>49</b>	nd	Nd
<b>50</b>	96.27 ± 9.63	>100
<b>51</b>	7.26 ± 1.27	2.36 ± 0.56
<b>52</b>	>100	>100
<b>53</b>	27.10 ± 6.02	26.06 ± 3.63
<b>54</b>	20.84 ± 3.49	13.79 ± 4.52
<b>55</b>	>100	>100
<b>56</b>	21.37 ± 2.82	29.34 ± 5.07
<b>57</b>	84.80 ± 3.50	>100
<b>58</b>	57.49 ± 6.86	93.50 ± 6.6
<b>59</b>	27.39 ± 7.73	18.21 ± 4.08
<b>60</b>	>100	>100
<b>61</b>	13.97 ± 5.18	8.50 ± 1.14

nd = not determined (insoluble in the experimental conditions); CI, confidence interval.

**Table 4.** Inhibition of in vitro MT polymerization and high-content analysis of mitotic arrest in HeLa cells treated with *N*-acylhydrazones.

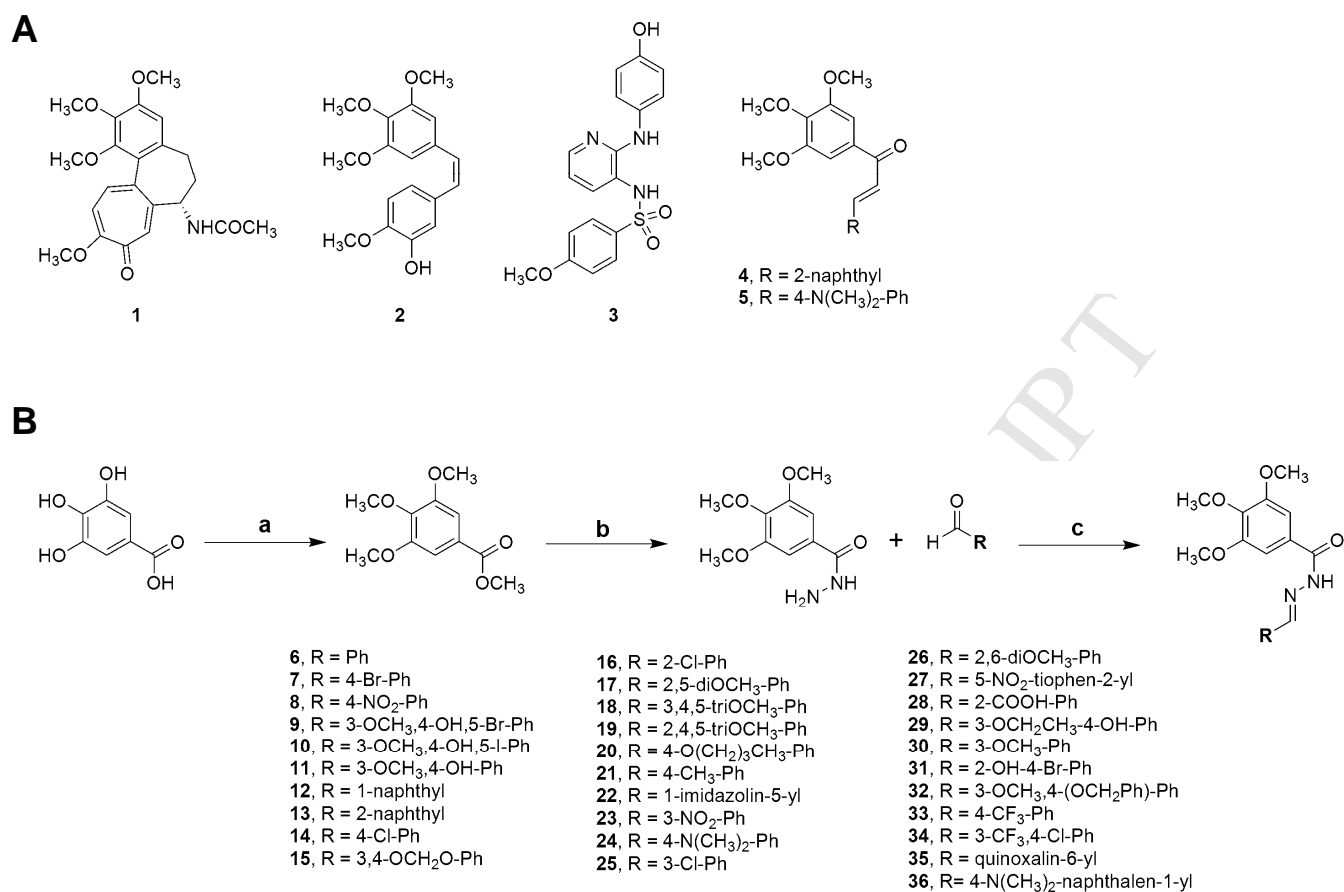
Compound	Inhibition of tubulin assembly IC <sub>50</sub> (μM)	Cell density IC <sub>50</sub> (nM)	MDEC (nM)		
			Nuclear condensation	Tubulin intensity	Mitotic index
<b>1</b>	2.3	34.1 ± 1.4	11.6 ± 0.3	3.7 ± 1.1	14.4 ± 0.4
<b>4</b>	2.2*	684 ± 139*	317 ± 23*	283 ± 52*	397 ± 24*
<b>5</b>	2.8*	357 ± 35*	217 ± 67*	139 ± 13*	200 ± 15*
<b>6</b>	1.8	304.8 ± 18.1	89.1 ± 10.4	93.3 ± 8.4	137.2 ± 31.5
<b>7</b>	0.8	113.5 ± 19.4	73.9 ± 11.1	19.9 ± 11.3	98.3 ± 6.2
<b>8</b>	1.5	380.2 ± 52.3	148.7 ± 17.2	199.5 ± 29.6	241.1 ± 35.6
<b>10</b>	5.7	2,770 ± 356	1037 ± 60	801.8 ± 121.6	1367 ± 41
<b>12</b>	0.7	36.2 ± 3.5	15.9 ± 2.4	11.8 ± 2.3	17.8 ± 3.7
<b>13</b>	0.9	168.3 ± 43.6	68.8 ± 18.5	50.7 ± 13.4	96.9 ± 23.2
<b>15</b>	1.2	211.0 ± 17.5	80.8 ± 12.8	50.9 ± 11.9	78.9 ± 12.3
<b>16</b>	1.1	121.1 ± 27.0	50.4 ± 8.4	45.4 ± 12.2	52.9 ± 8.7
<b>18</b>	> 10	> 50,000	> 50,000	> 50,000	> 50,000
<b>20</b>	> 10	> 50,000	> 50,000	> 50,000	> 50,000
<b>21</b>	0.5	48.3 ± 1.1	24.8 ± 2.9	19.9 ± 2.2	28.1 ± 1.3
<b>22</b>	> 10	> 50,000	> 50,000	> 50,000	> 50,000

\* Already shown [10]; MDEC, Minimum Detectable Effective Concentration

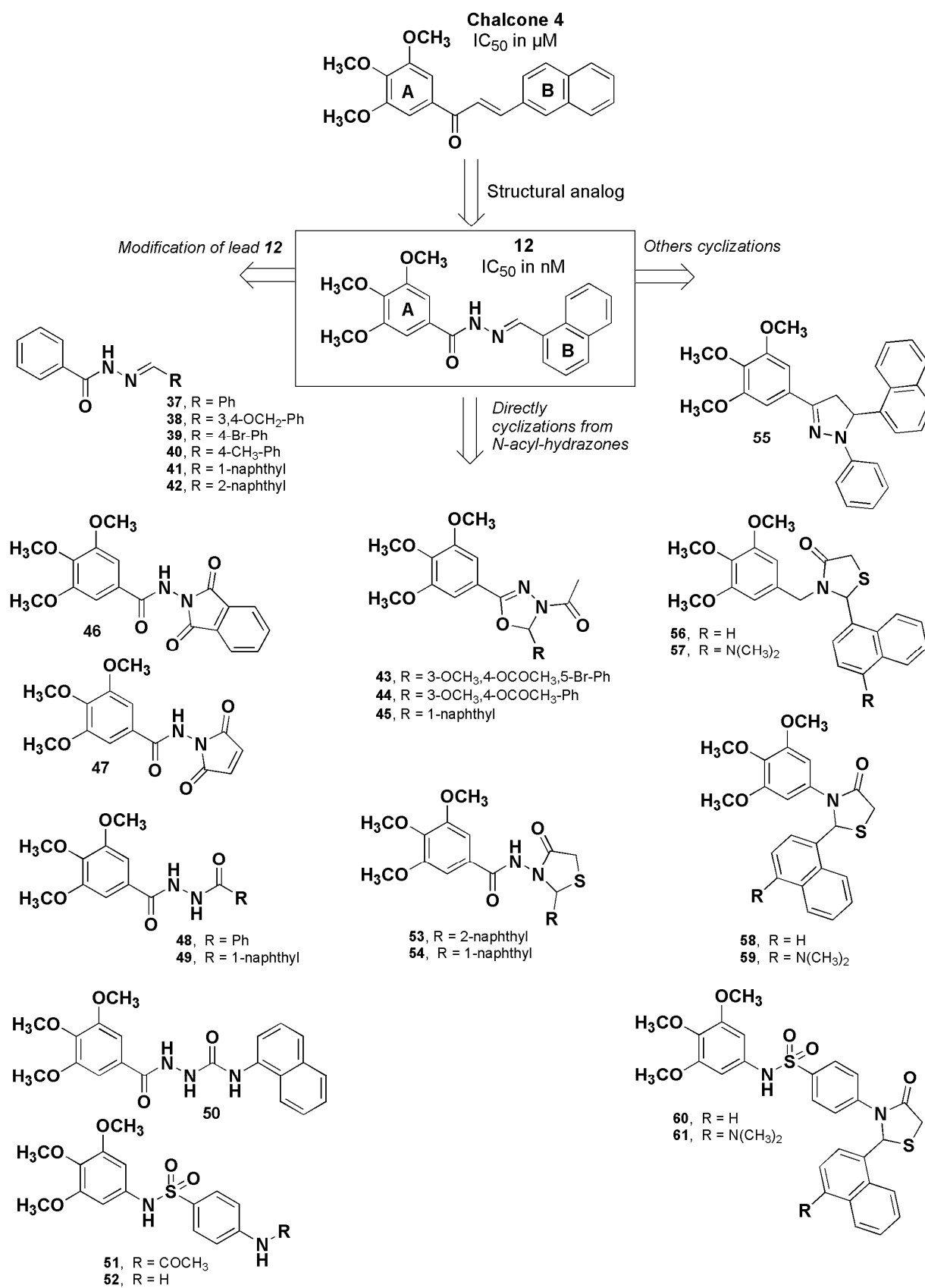
**Table 5.** Effect of selected compounds on the migration of MDA-MB-231 breast cancer cell line.

<b>Compound</b>	<b>Wound healing (% inhibition at 1 <math>\mu</math>M) <sup>a</sup></b>	<b>Transwell migration assay IC<sub>50</sub> (nM) <sup>b</sup></b>
<b>colchicine (1)</b>	70 $\pm$ 5	250 $\pm$ 78
<b>6</b>	60 $\pm$ 9	530 $\pm$ 73
<b>12</b>	80 $\pm$ 4	168 $\pm$ 57

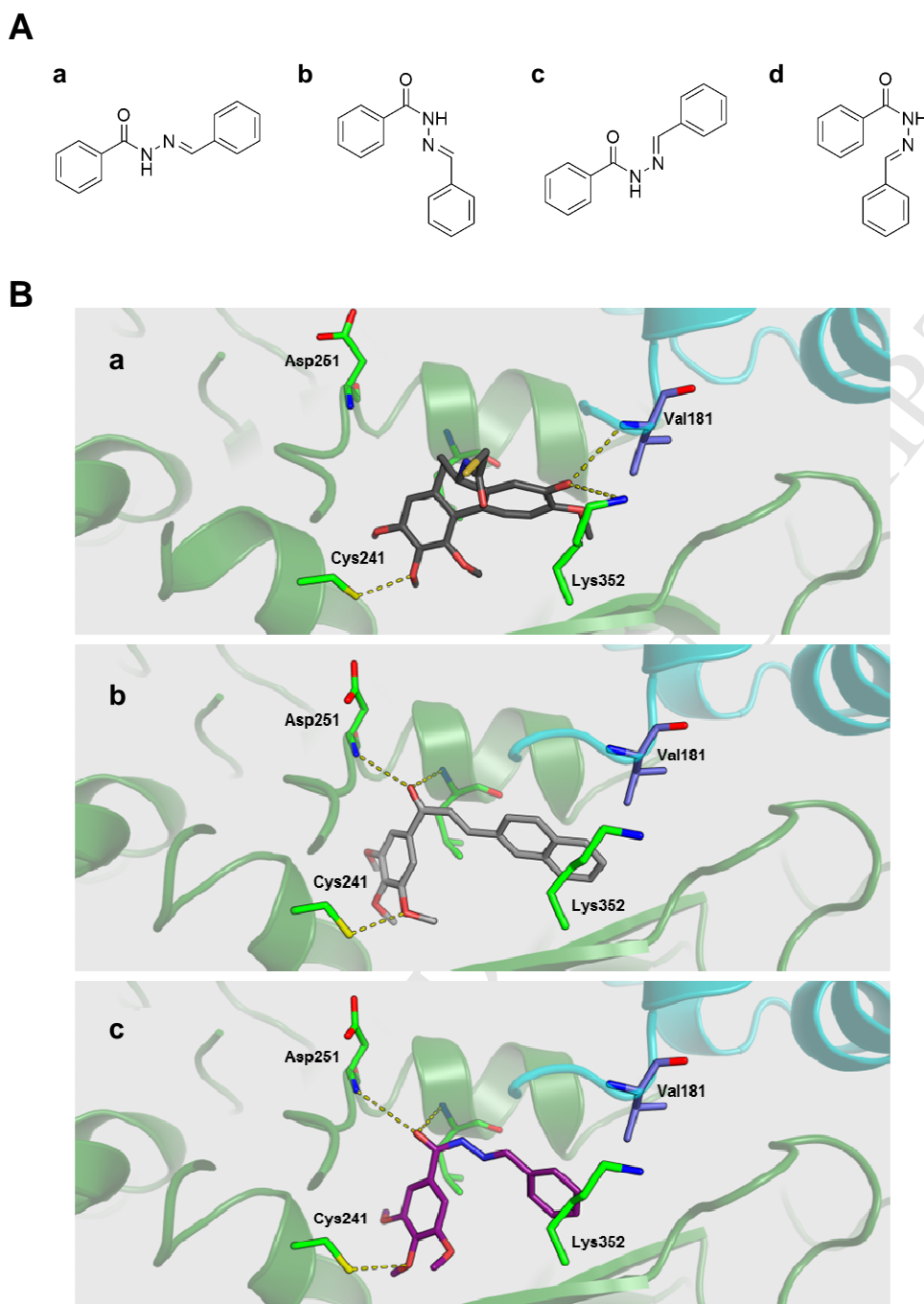
<sup>a</sup>Mean  $\pm$  SD of three independent experiments. <sup>b</sup>Mean  $\pm$  range of two independent experiments. Pictures of the transwell migration assays are shown in Supplementary Figure 2.



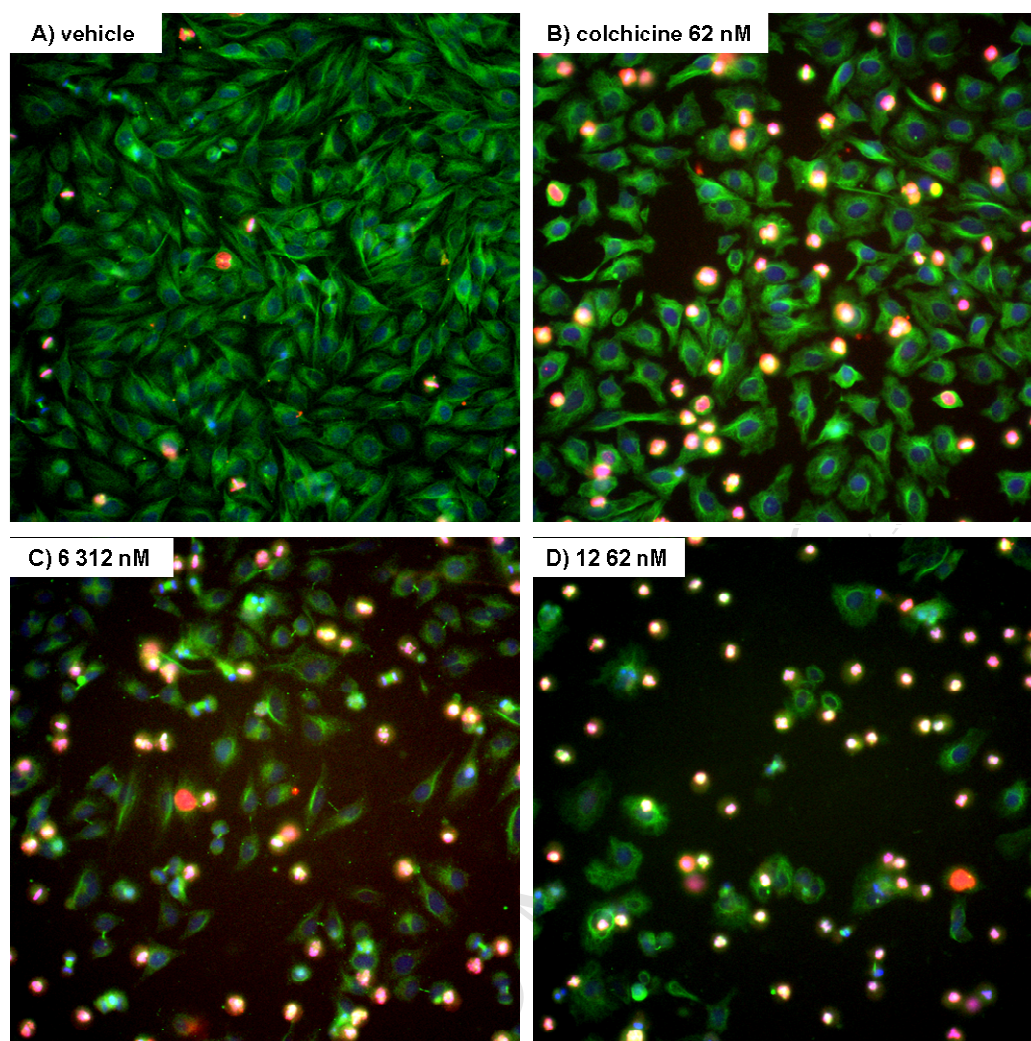
**Figure 1.** (A) Representative microtubule-interacting agents that binds to the colchicine site on tubulin. Ph, phenyl (B) Synthesized 3,4,5-trimethoxy-acylhydrazones (6-36). Reagents and conditions: (a) (CH<sub>3</sub>)<sub>2</sub>SO<sub>4</sub>, K<sub>2</sub>CO<sub>3</sub>, TBAI, acetone, reflux, 12 h; (b) N<sub>2</sub>H<sub>4</sub>·H<sub>2</sub>O, methanol, reflux, 5 h; (c) methanol, reflux, 2 h.



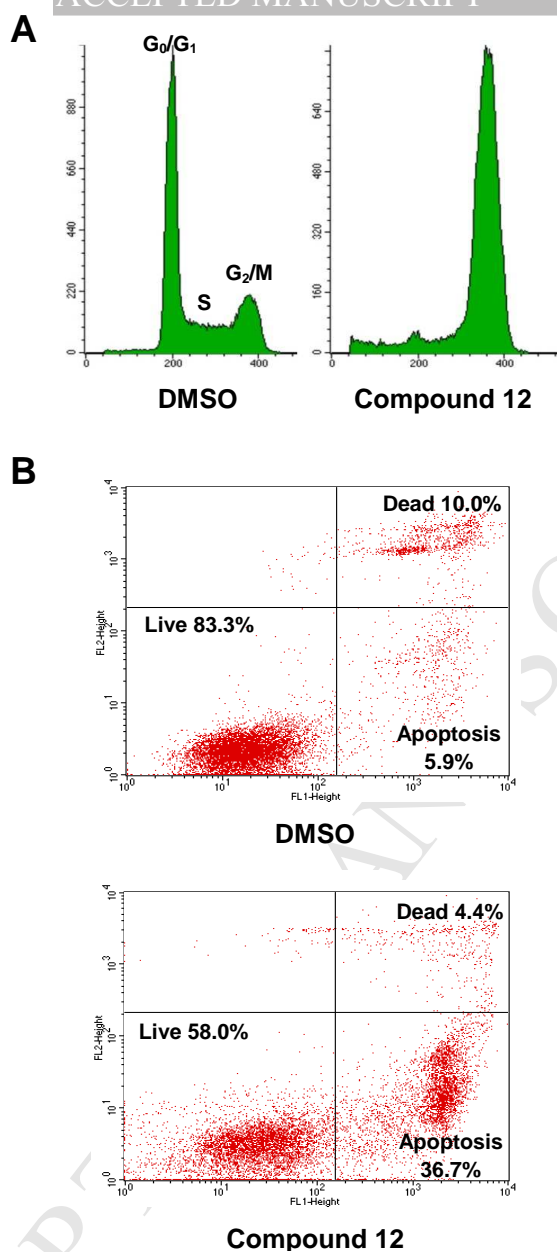
**Figure 2.** Derivatives and analogs from compound **12** designed and synthesized in this work.



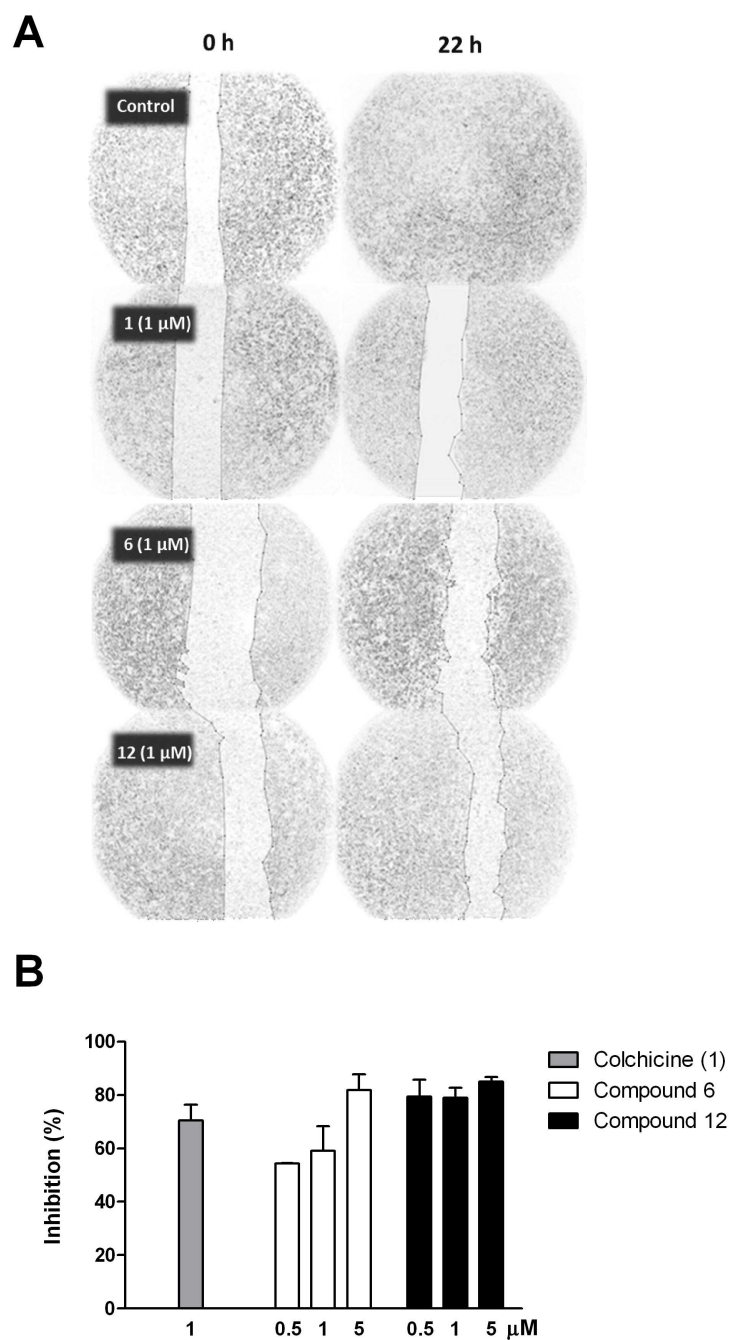
**Figure 3.** (A) Conformational states of *N*-acylhydrazone backbone (a-d). (B) Crystallographic position of DAMA-colchicine (dark gray) into the tubulin binding cavity (a); Docking pose of chalcone **4** (light gray) into the tubulin binding cavity (b); Docking pose of B-conformation of *N*-acylhydrazone **6** (violet) into the tubulin binding cavity (c). Tubulin PDB file 1SA0.



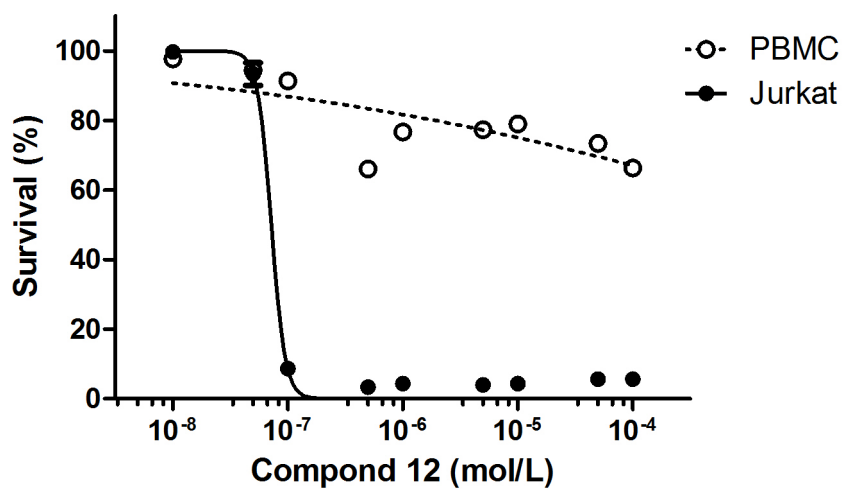
**Figure 4.** Immunofluorescence staining for markers of mitotic arrest in HeLa cells. HeLa cells were treated with (A) vehicle (dimethyl sulfoxide, DMSO 0.1%), (B) colchicine **1** (62 nM), (C) the general backbone of the series **6** (312 nM), or (D) the most potent derivative **12** (62 nM), followed by simultaneous immunostaining of  $\alpha$ -tubulin (green), phosphohistone H3 (red), and Hoechst 33342 (blue). Vehicle-treated cells have highly organized microtubules and low percentage of mitotic cells. Colchicine **1** and the (*E*)-*N'*-benzylidene-3,4,5-trimethoxybenzohydrazides **6** and **12** caused a heterogeneous response of tubulin disorganization, increased number of phosphohistone H3-positive cells, chromatin condensation and nuclear fragmentation. Images shown are representative fields from a single experiment repeated three times with similar results.



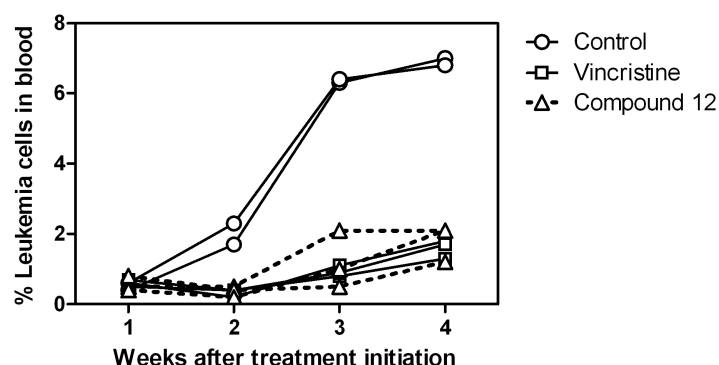
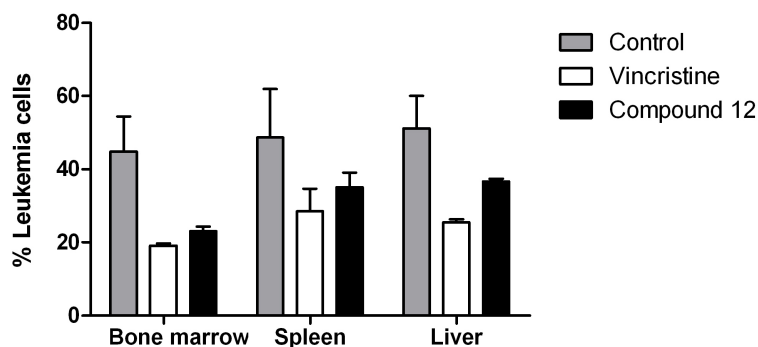
**Figure 5.** Cell cycle arrest and apoptosis induction by compound 12. Jurkat cells were treated for 18h with 125 nM compound 12 or DMSO and analyzed by flow cytometry for (A) cell cycle analysis, with propidium iodide staining, and (B) Apoptosis, with Annexin V/propidium iodide double staining.



**Figure 6.** Inhibition of breast tumor MDA-MB-231 cells migration by colchicine **1** (blue) and (*E*)-*N'*-benzylidene-3,4,5-trimethoxybenzohydrazides **6** (black) and **12** (red). **Upper panel:** Photographs of wound healing assay at 0 and 22 h, comparing the wound closure by colchicine **1** and compounds **6** and **12** at 1  $\mu$ M. **Lower panel:** Wound healing assay for inhibition of cell migration caused by **6** (black) and **12** (red) in three different concentrations. Data are the mean  $\pm$  SEM of triplicate wells from a single experiment repeated three times with similar results.

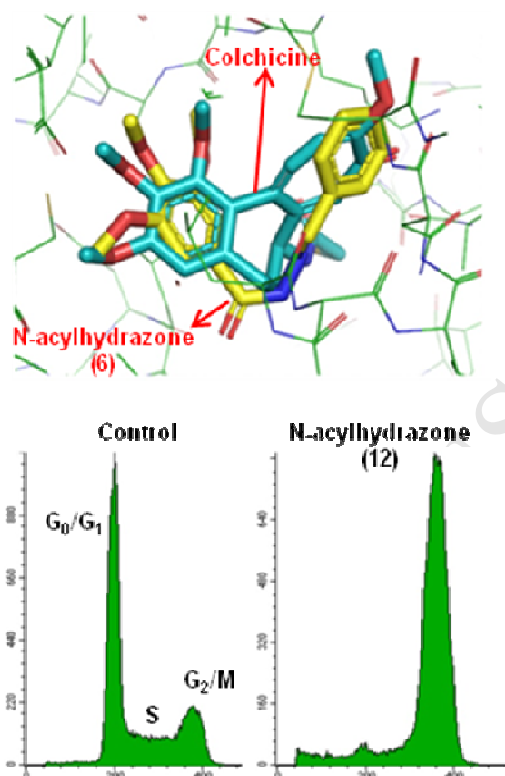


**Figure 7.** Selective cytotoxicity of compound **12**. Human T-cell leukemia (Jurkat) and phytohemagglutinin/IL2-stimulated T-lymphocytes from a healthy donor (PBMC) were cultured for 48h with increasing concentrations of compound **12**. Survival was assessed by the MTT reduction assay. The results are representative of two independent experiments.

**A****B**

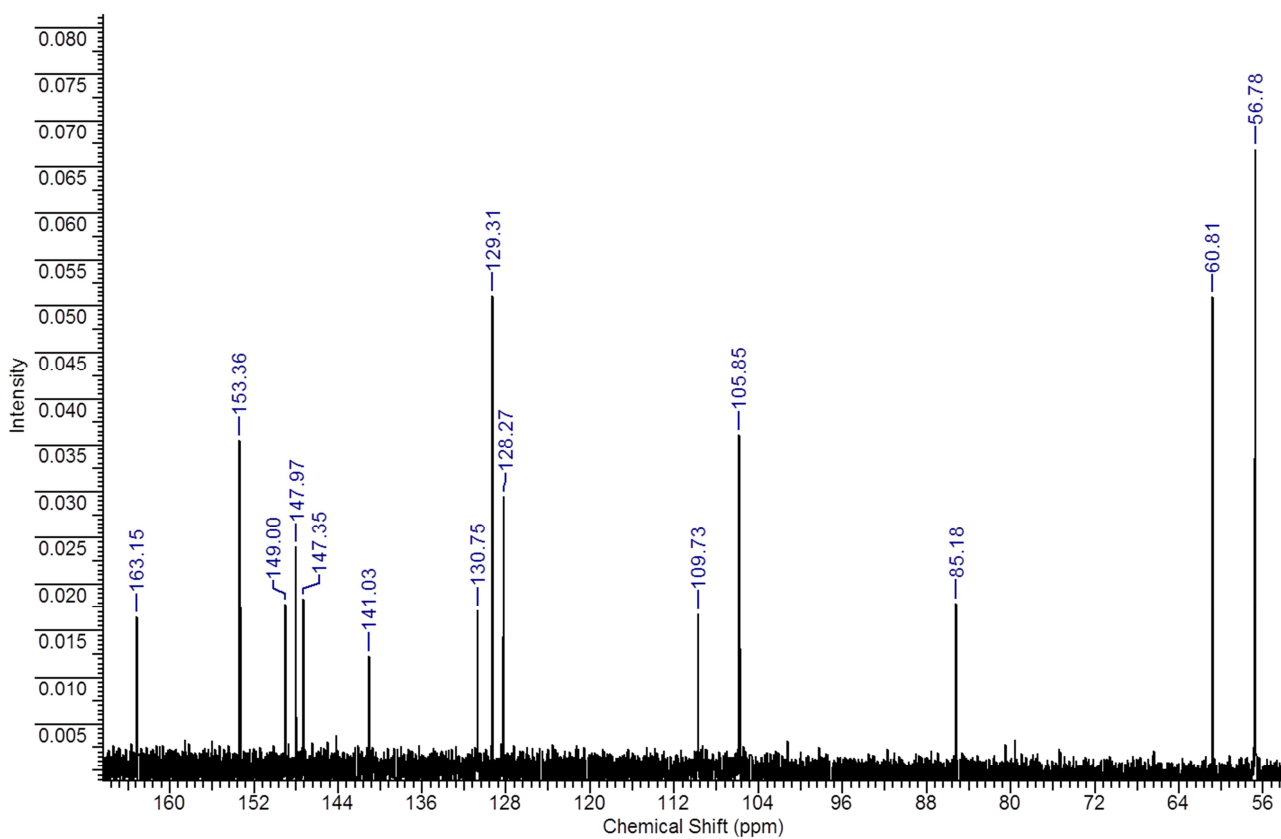
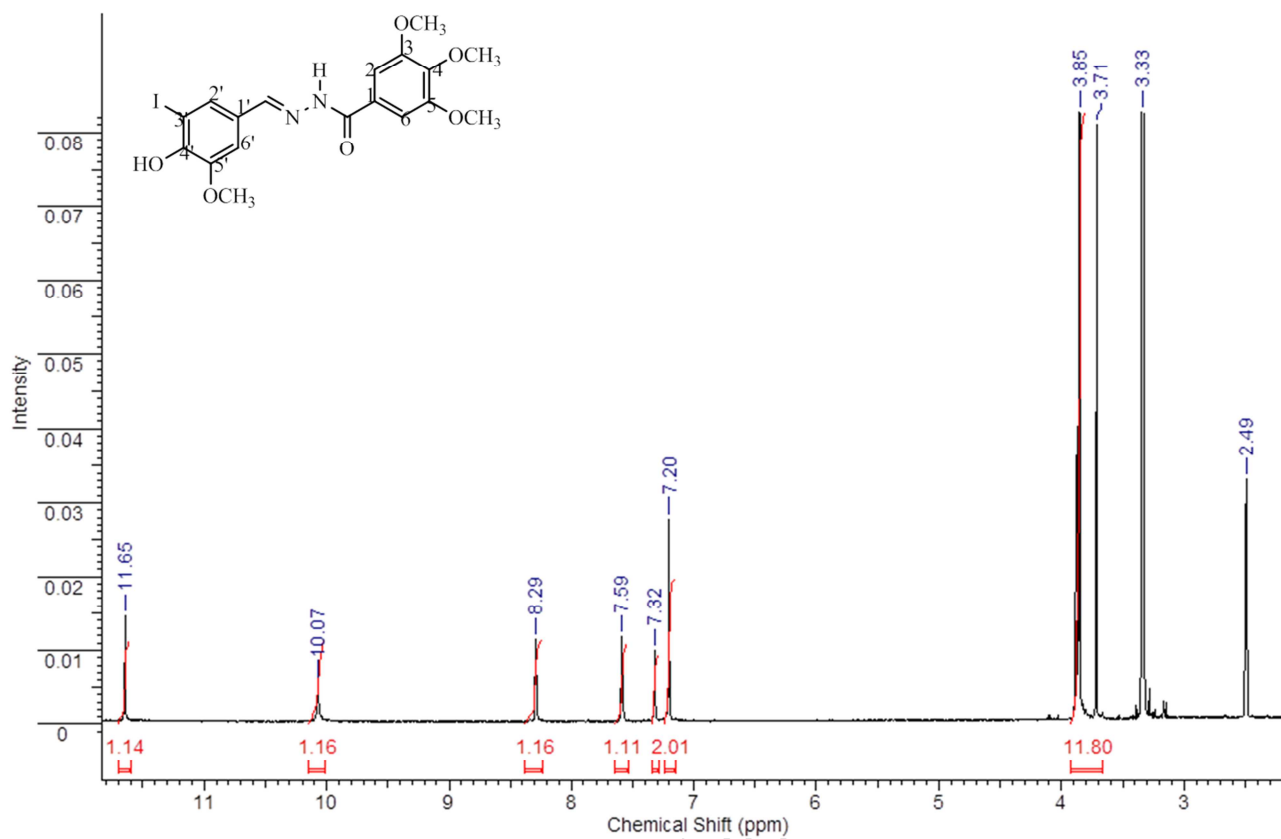
**Figure 8.** *In vivo* anti-leukemia activity of compound **12**. NOD/SCID mice were injected with patient-derived xenograft ALL. Treatment started when human CD45+ cells accounted for more than 0.5% of peripheral blood cells in half the animals. Vincristine (0.15 mg/kg), compound **12** (1 mg/kg) or saline (control) were given once a week, intraperitoneally. **(A)** Percentage of leukemia cells (hCD45+) in the peripheral blood of mice over a 4-week treatment period. Each line correspond to one animal. One of the animals in the control group died before completion of the experiment and was therefore excluded from analysis. **(B)** ALL infiltration in bone marrow and secondary organs at the end of the experiment. Bars correspond to the mean  $\pm$  SEM. same individual animal.

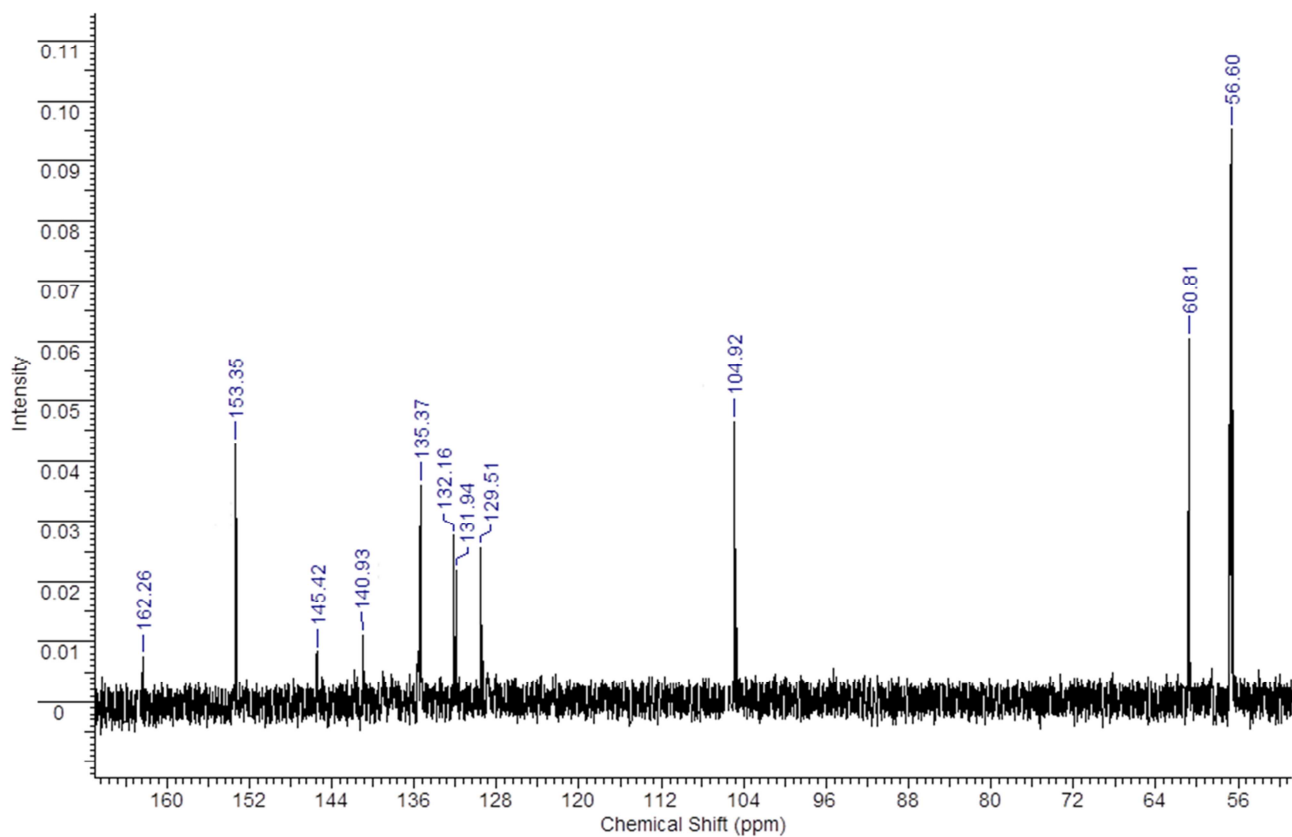
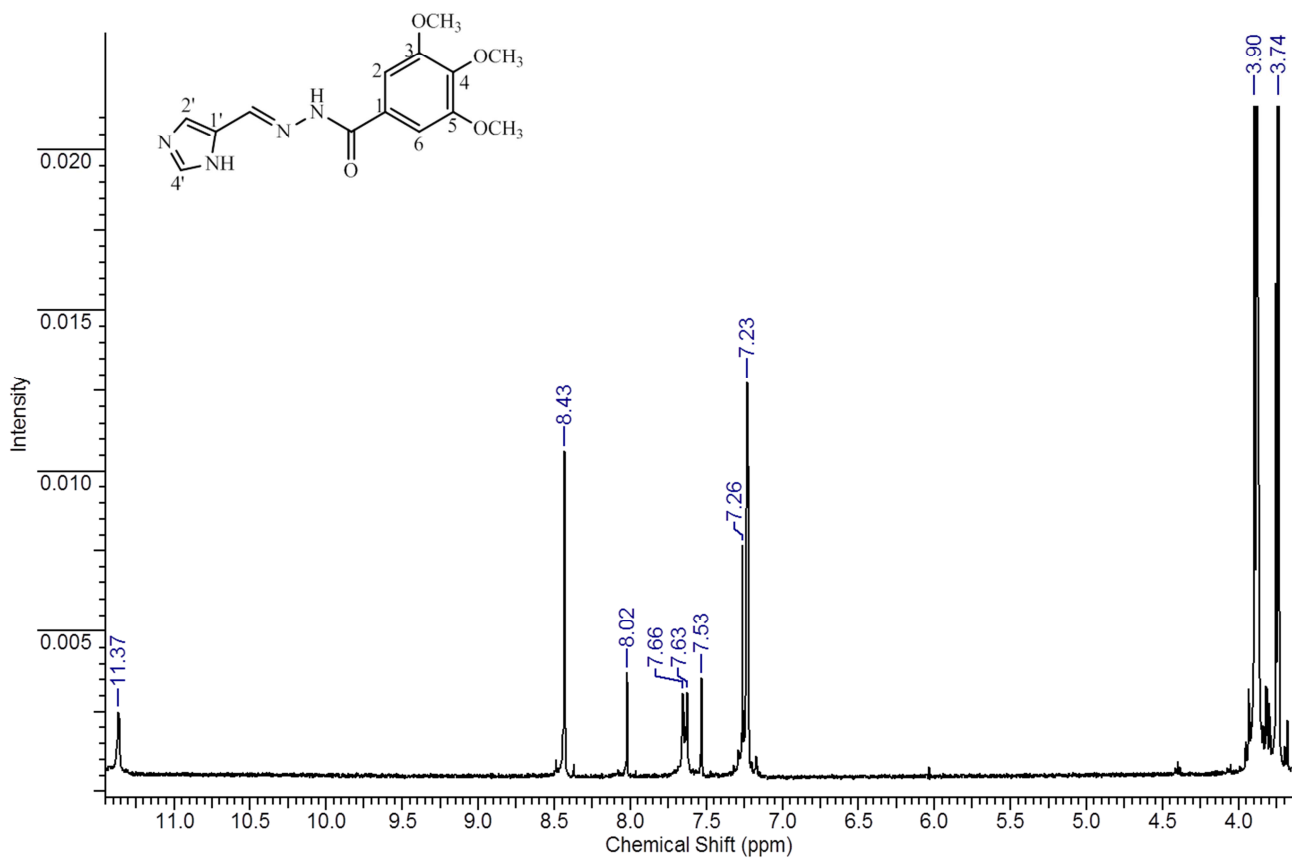
## Table of Contents graphic

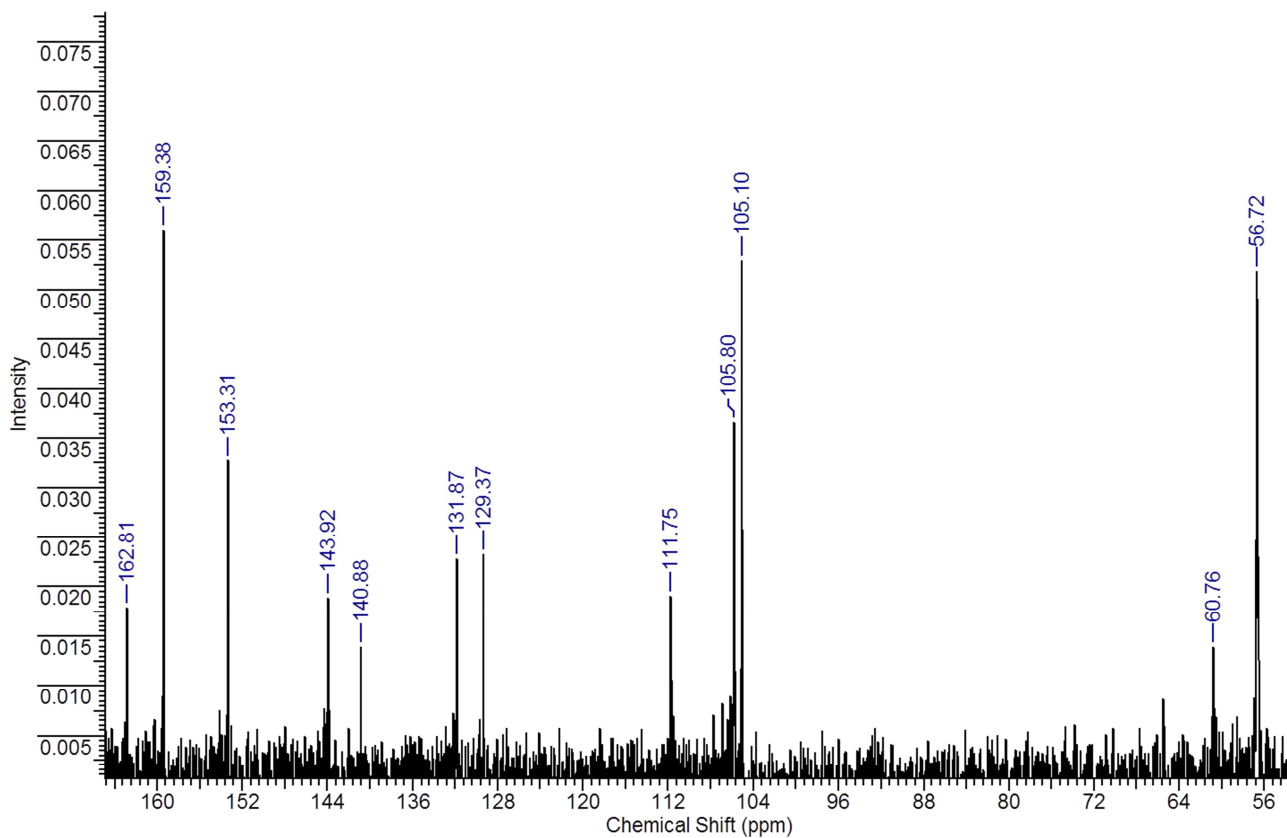
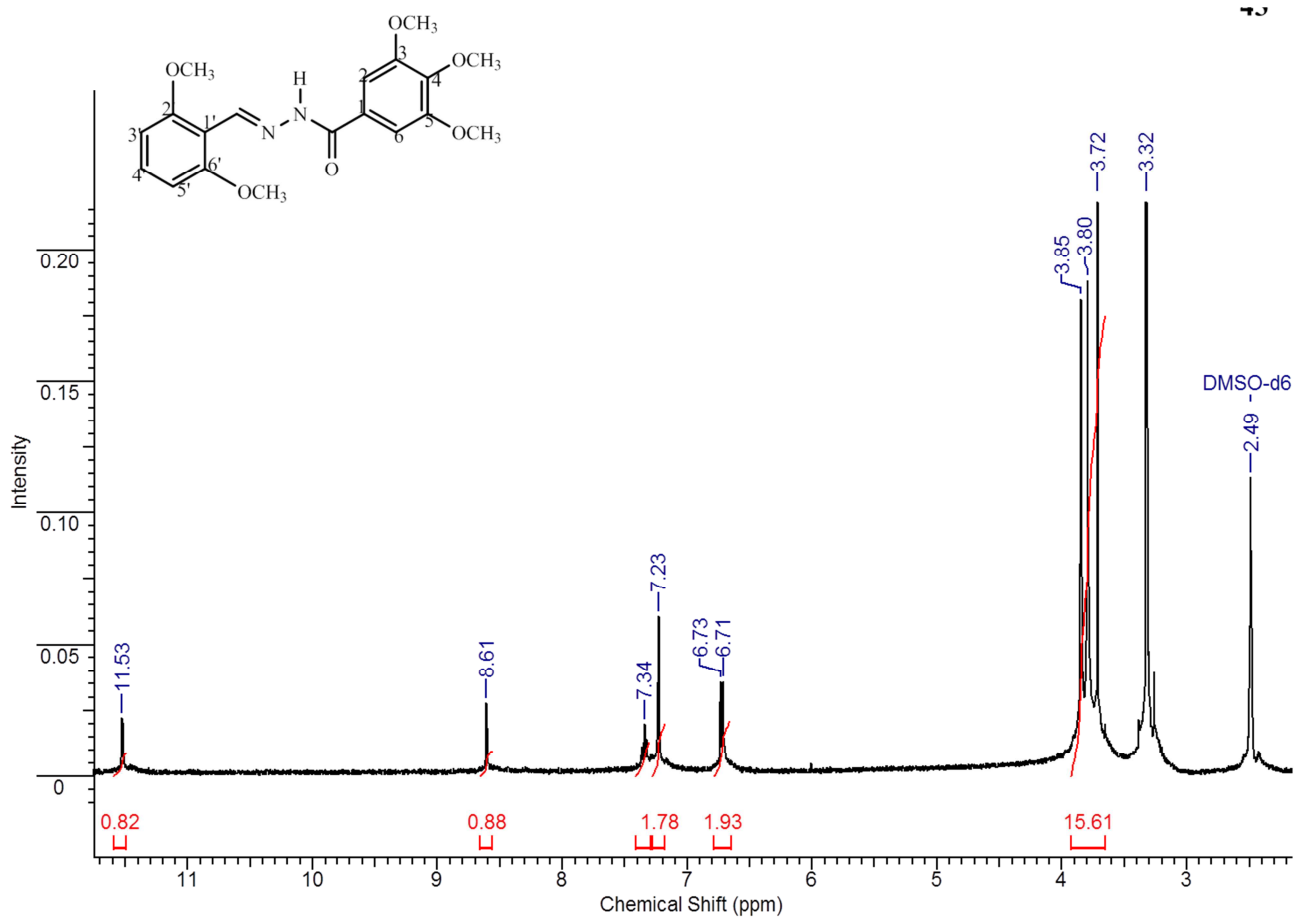


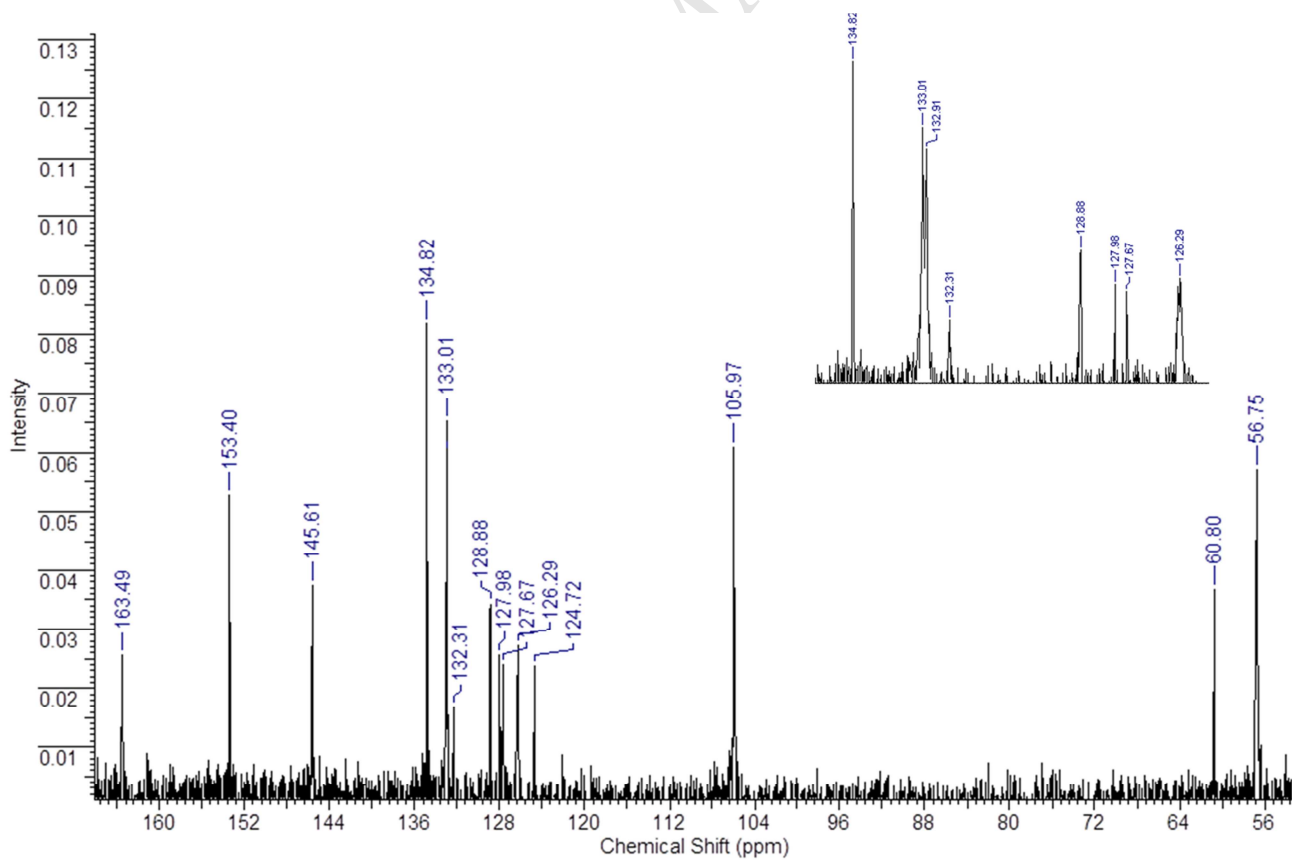
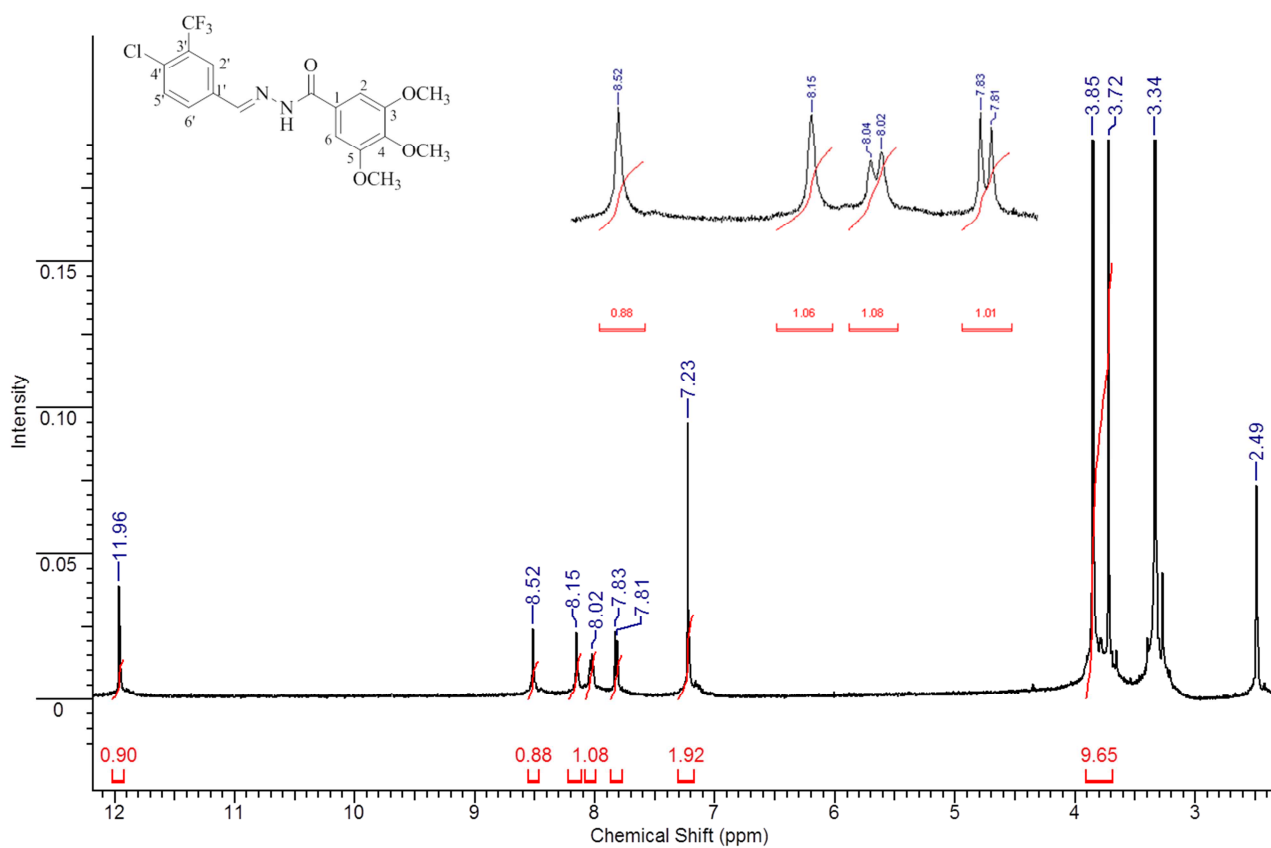
**Highlights**

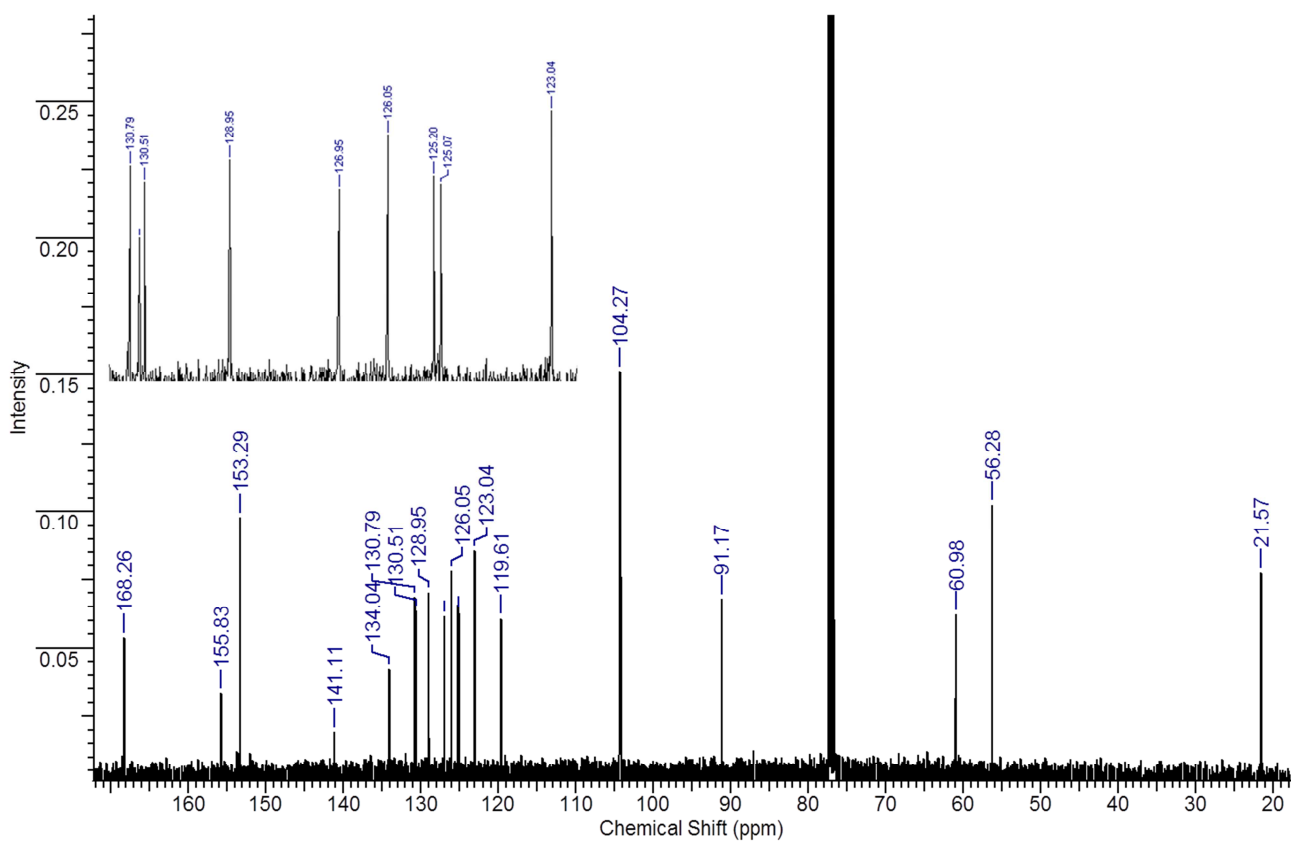
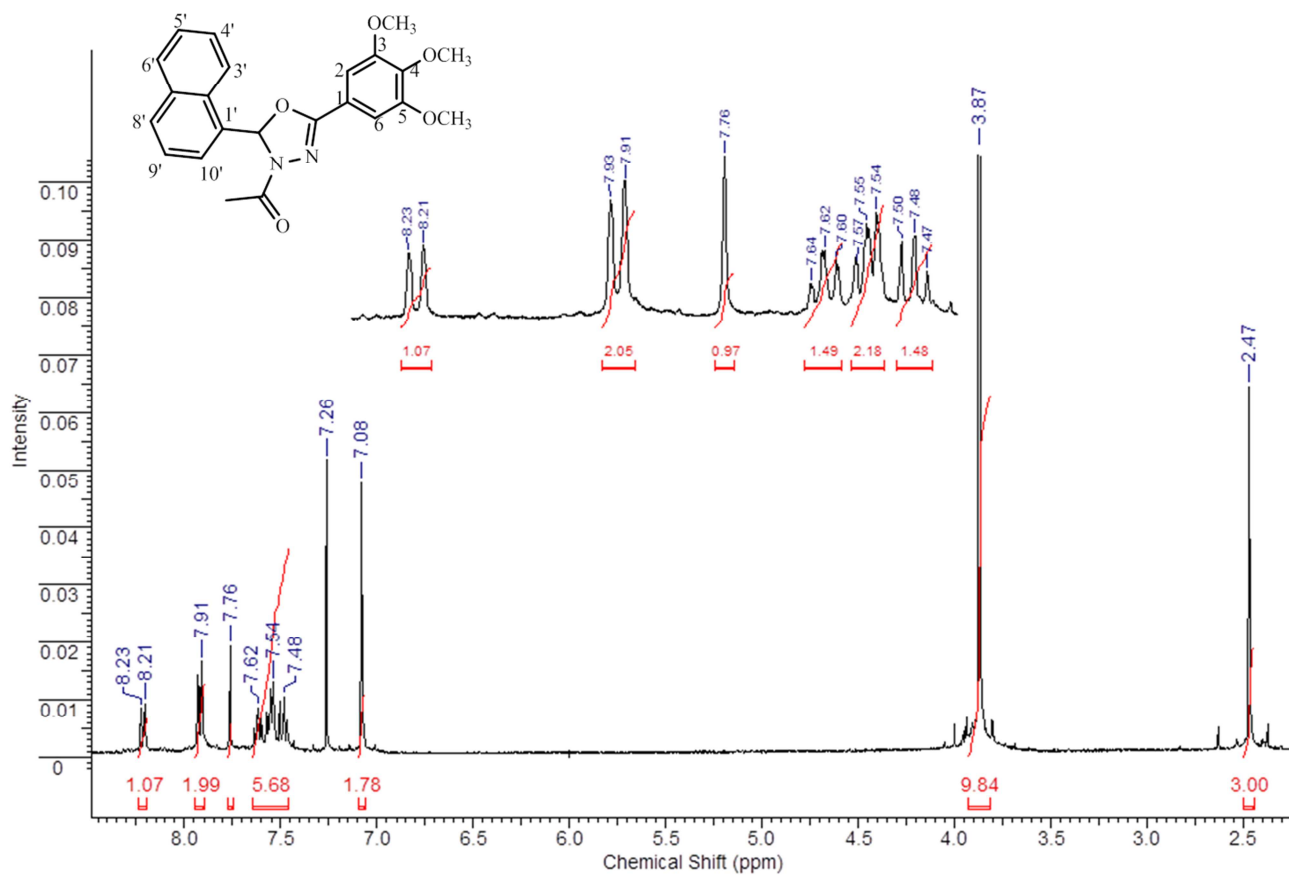
- Cytotoxicity and inhibition of cell migration;
- *in vivo* activity against acute lymphoblastic leukemia;
- Tubulin-interacting agents and interfere with MT polymerization;
- Selective toxicity against leukemia cells in comparison with stimulated normal lymphocytes.

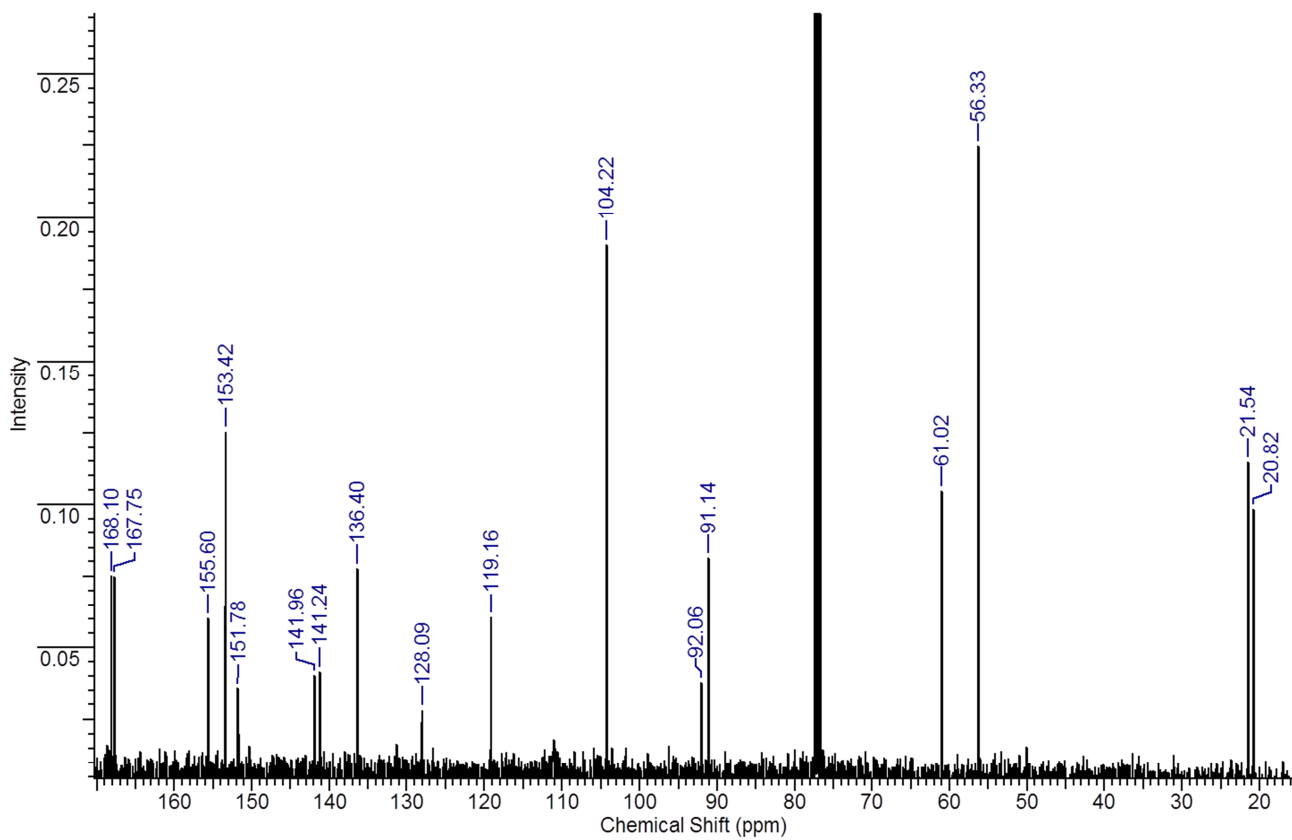
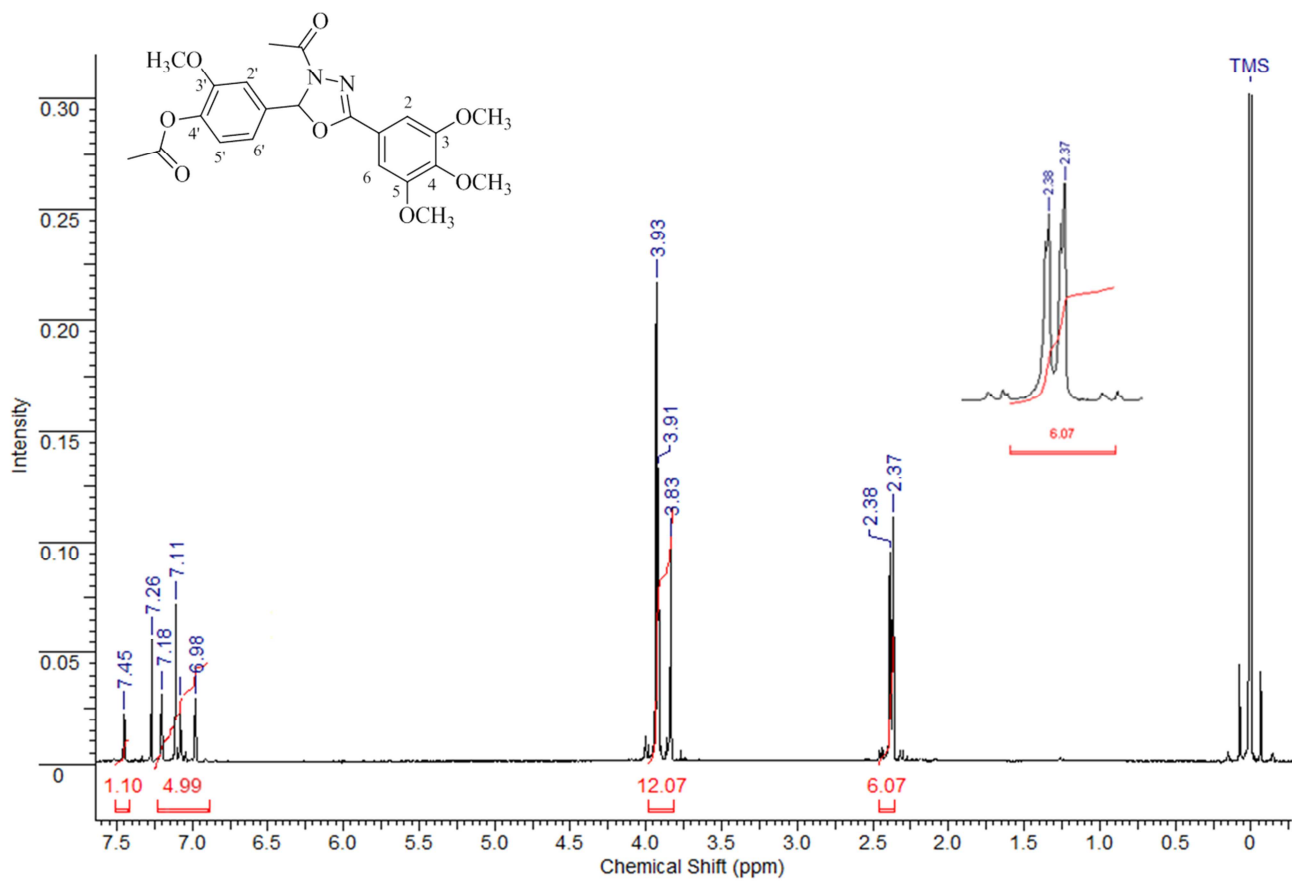


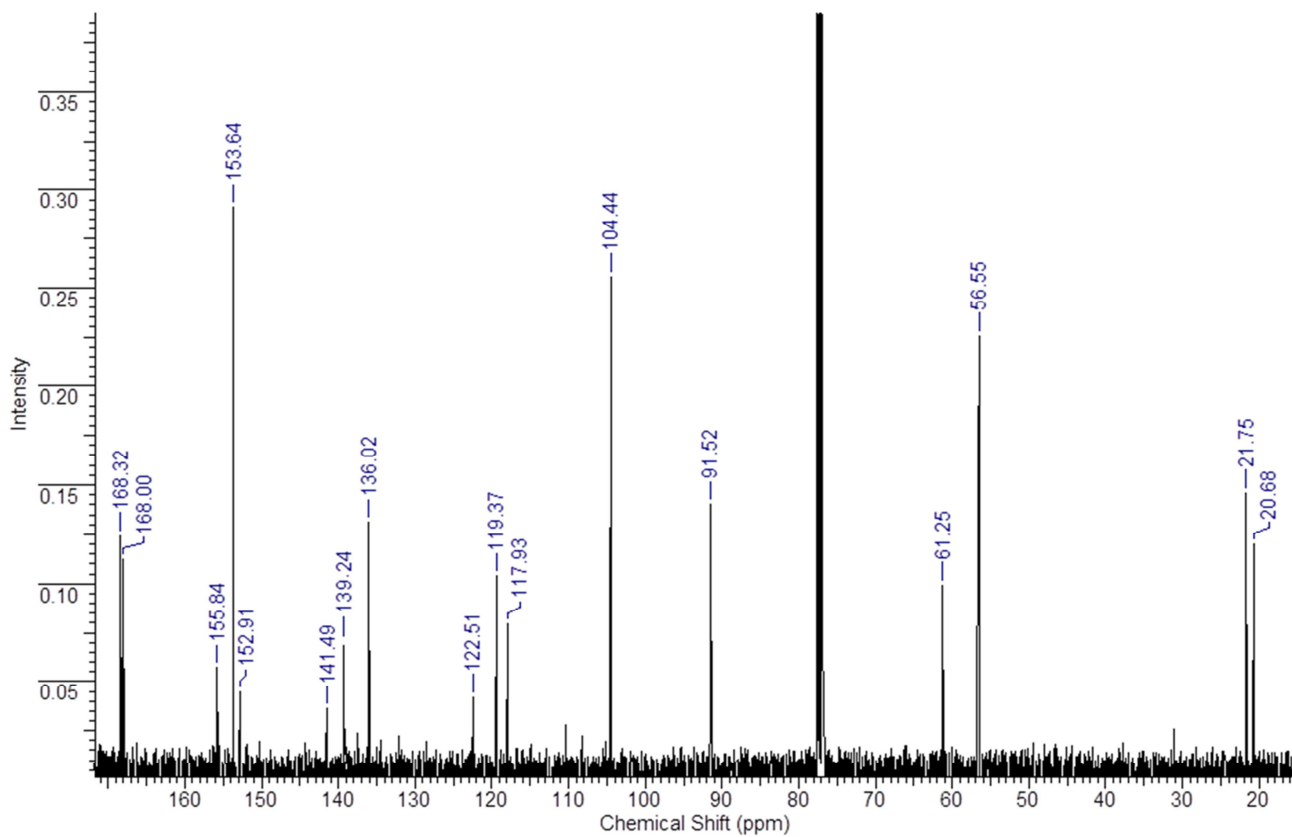
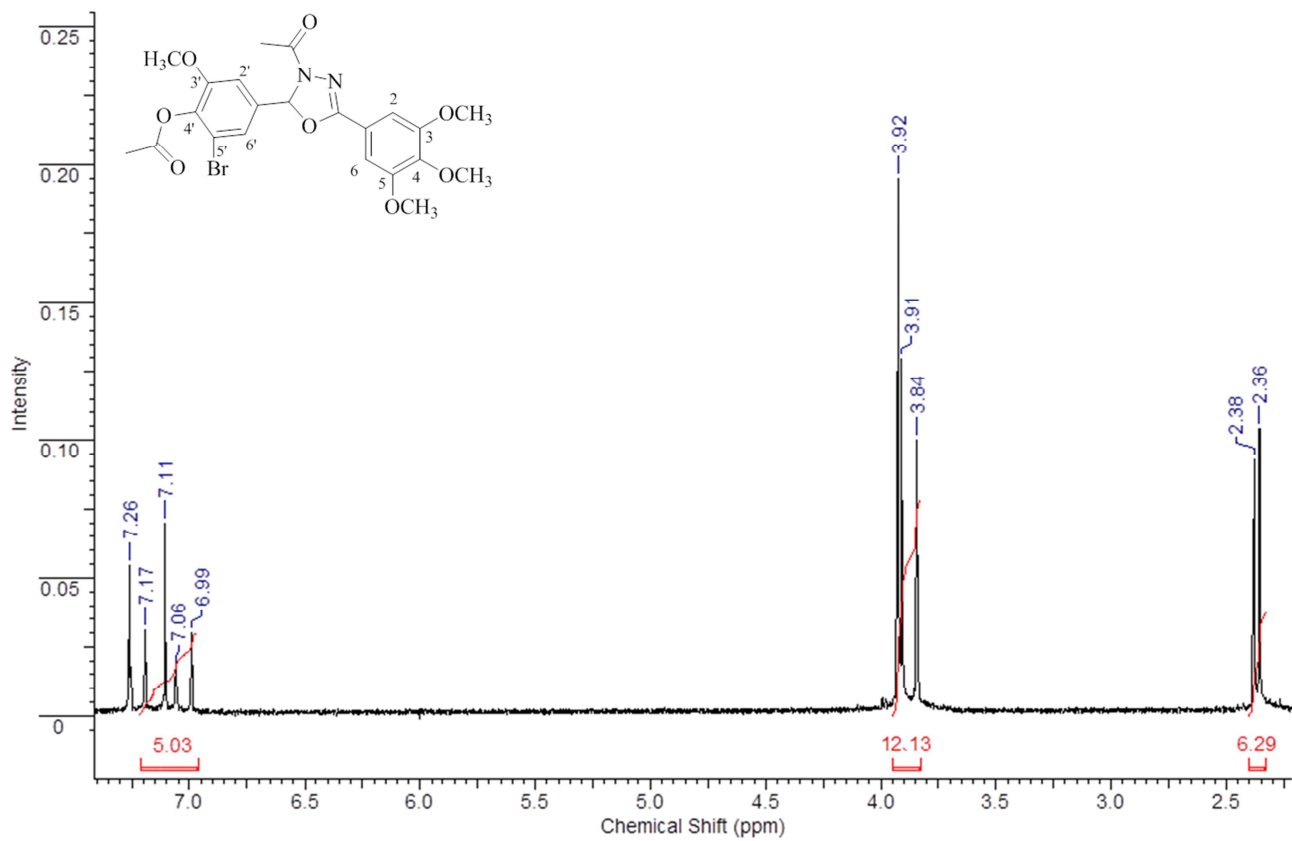


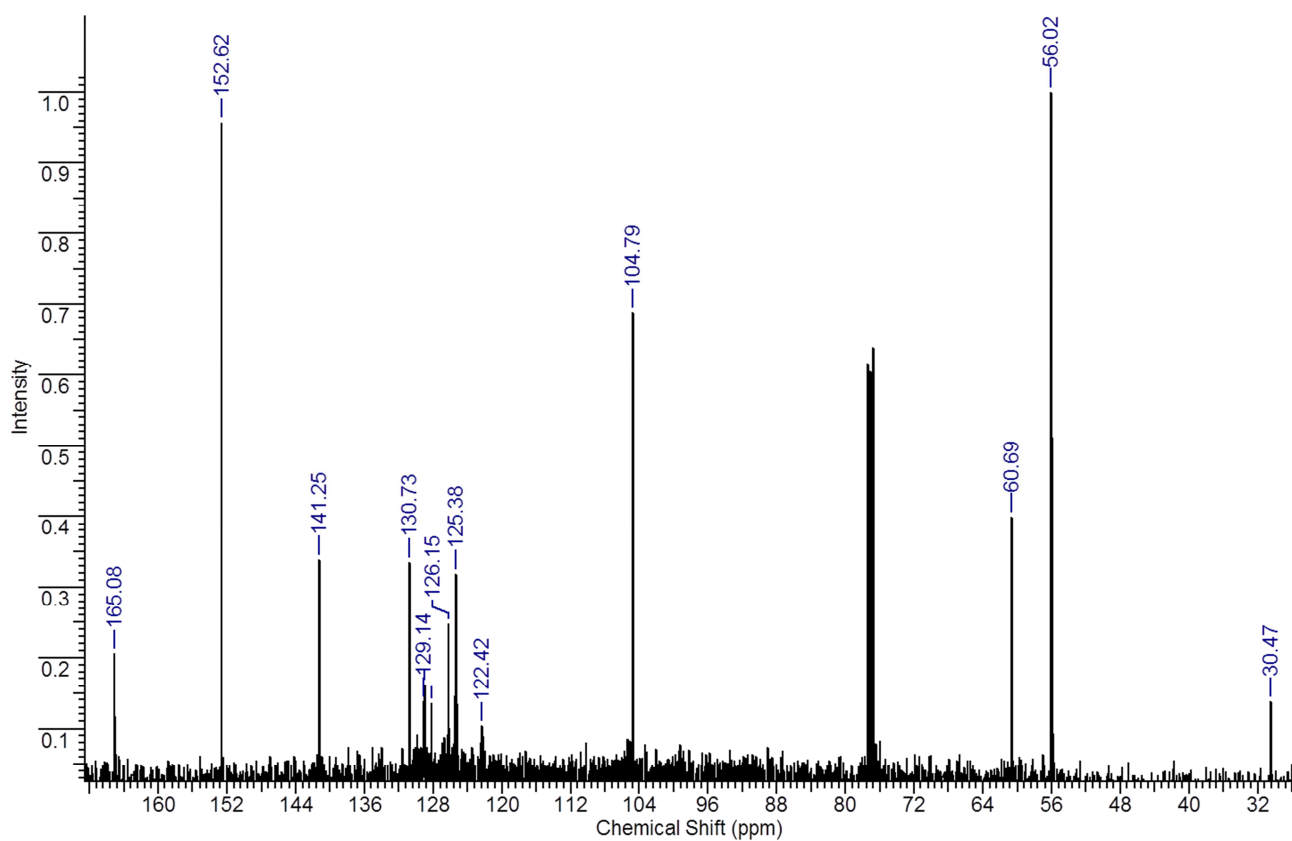
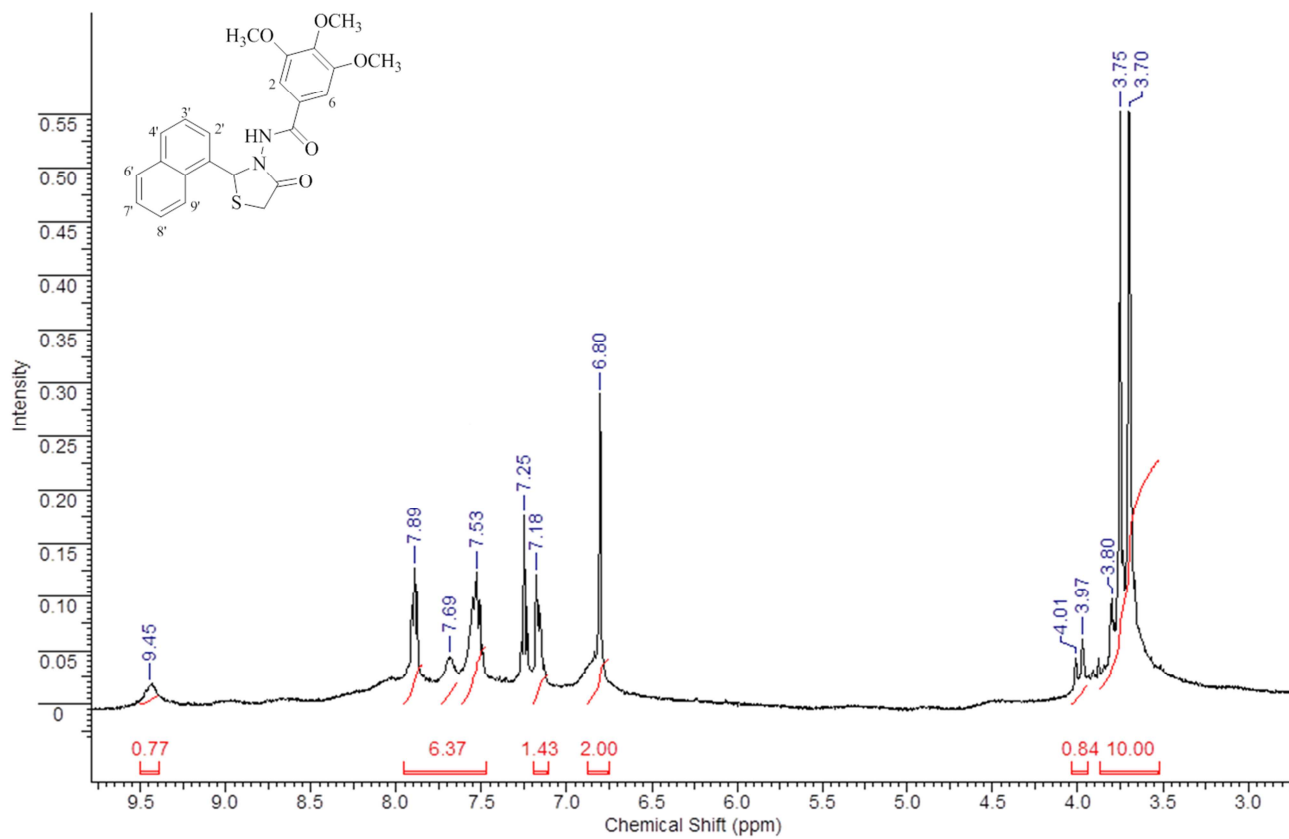


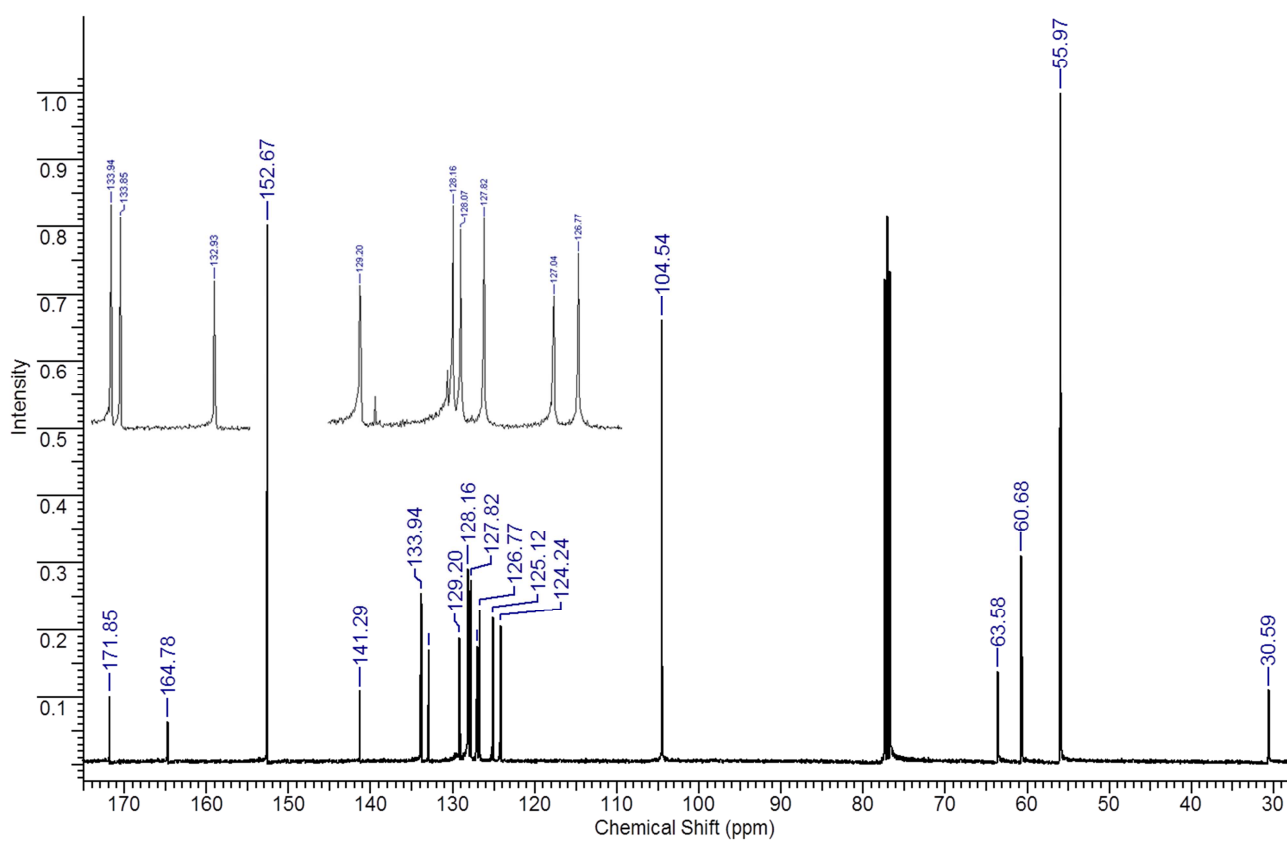
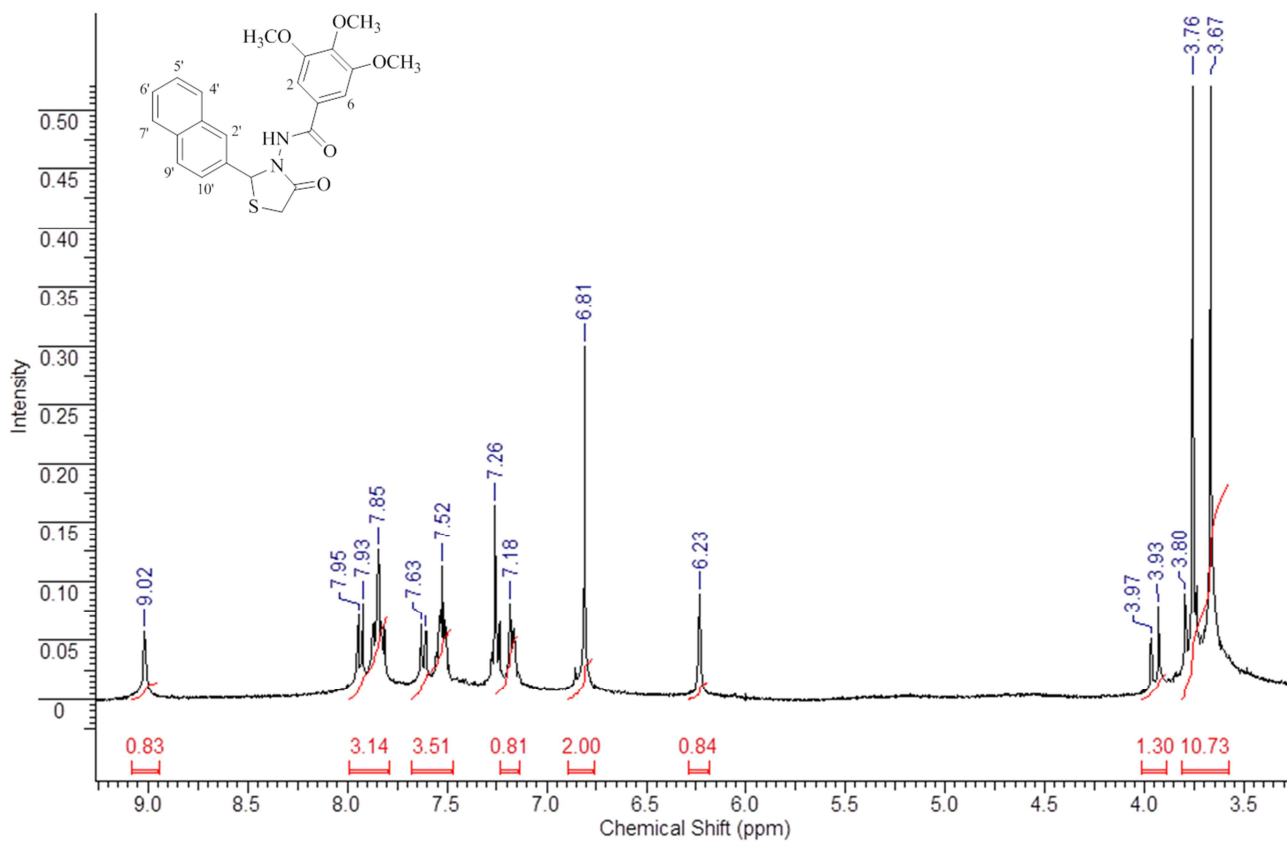


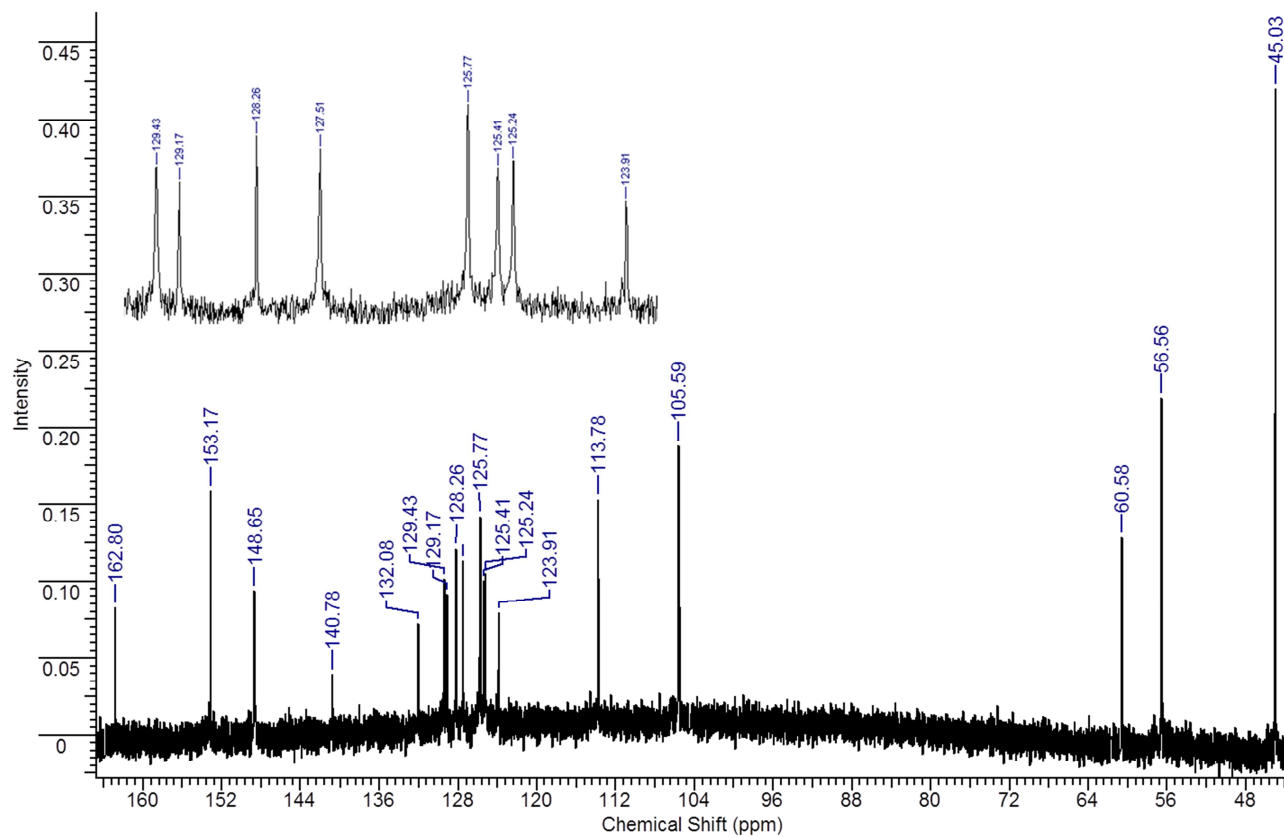
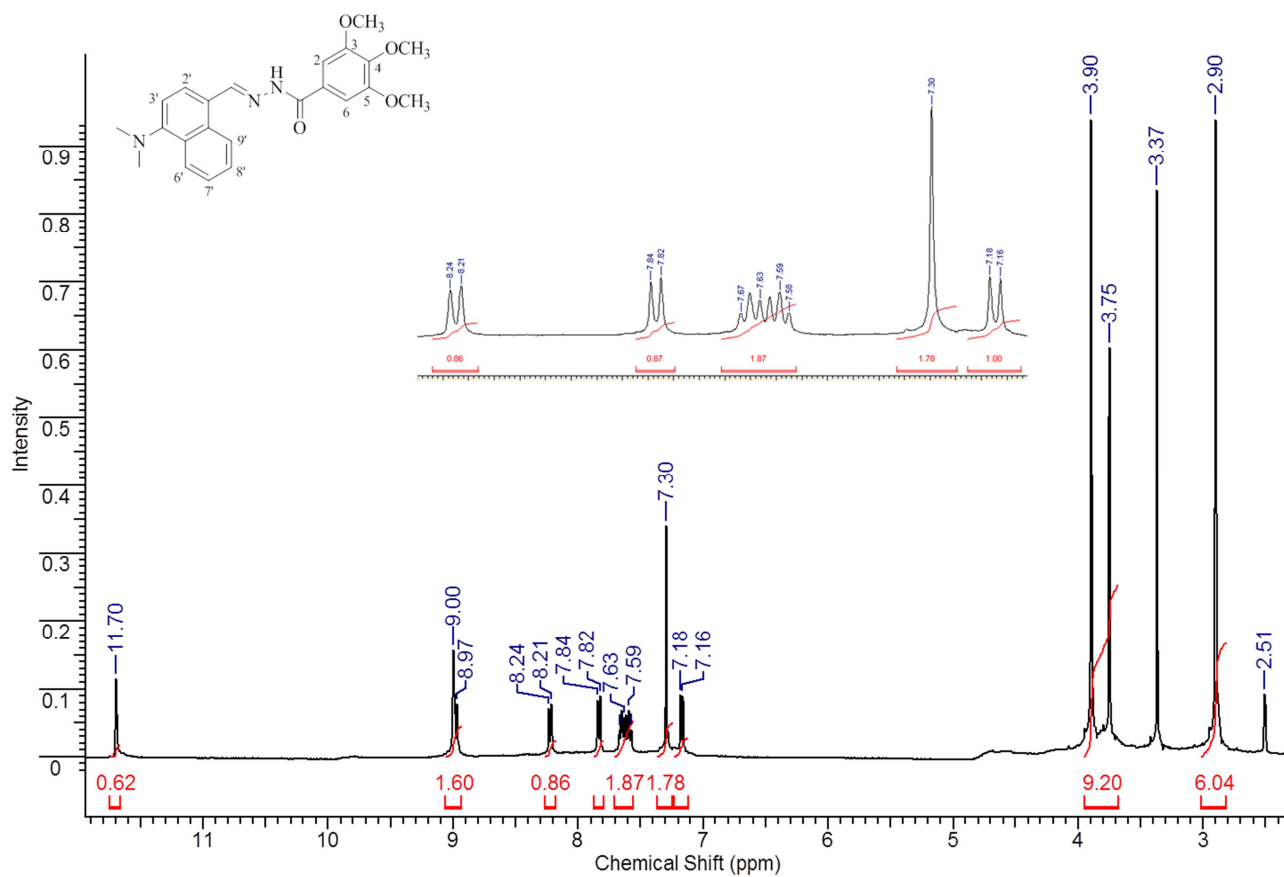


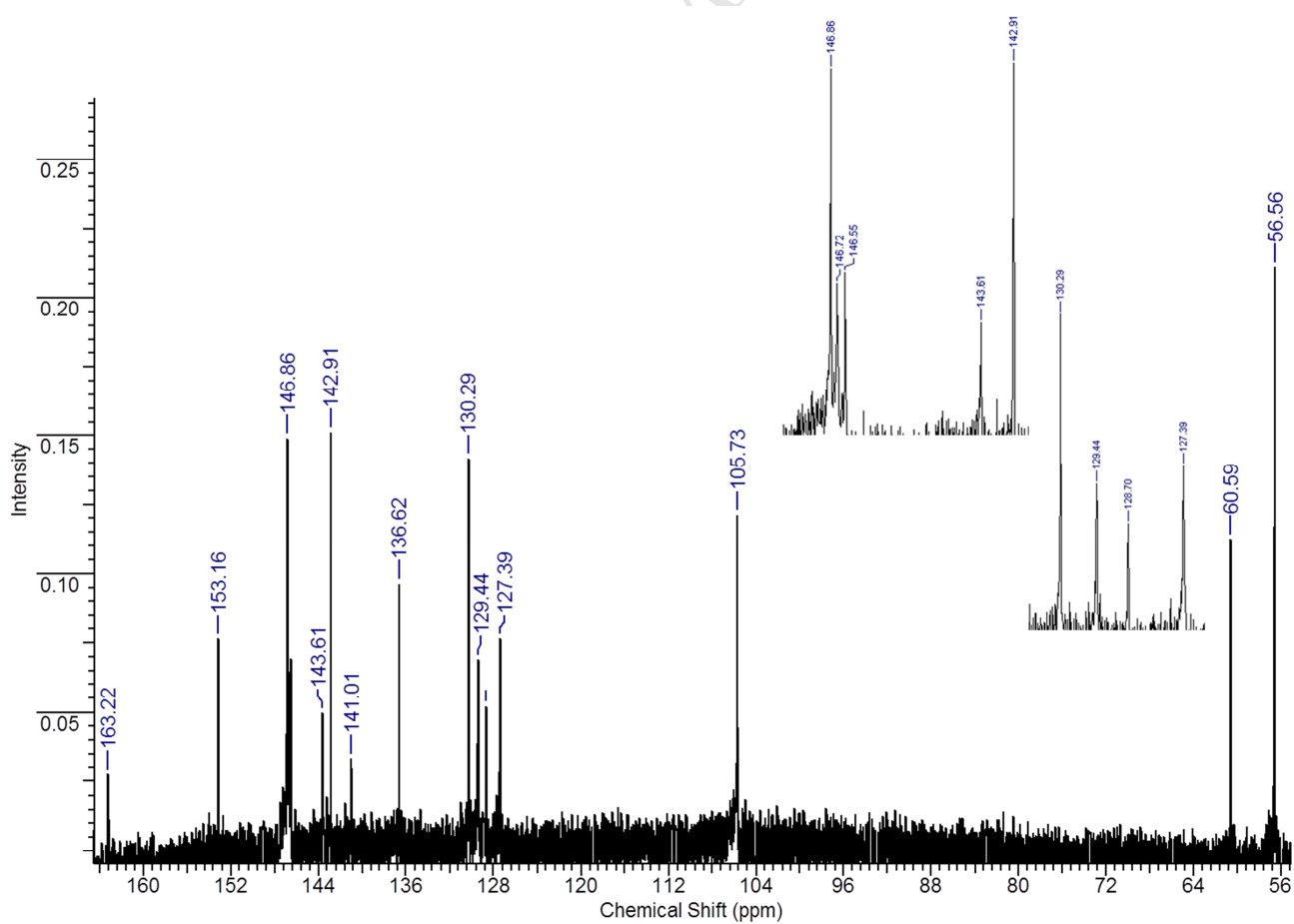
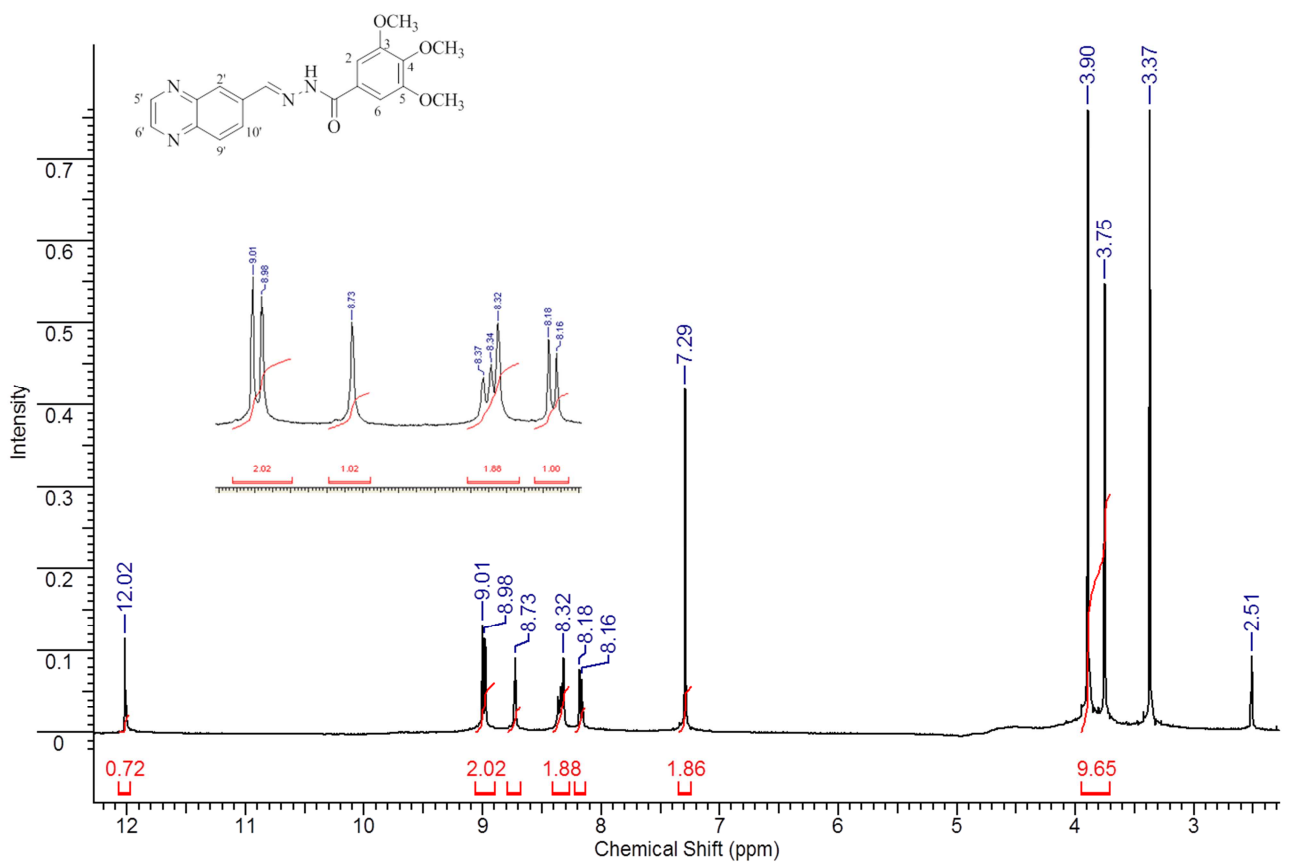


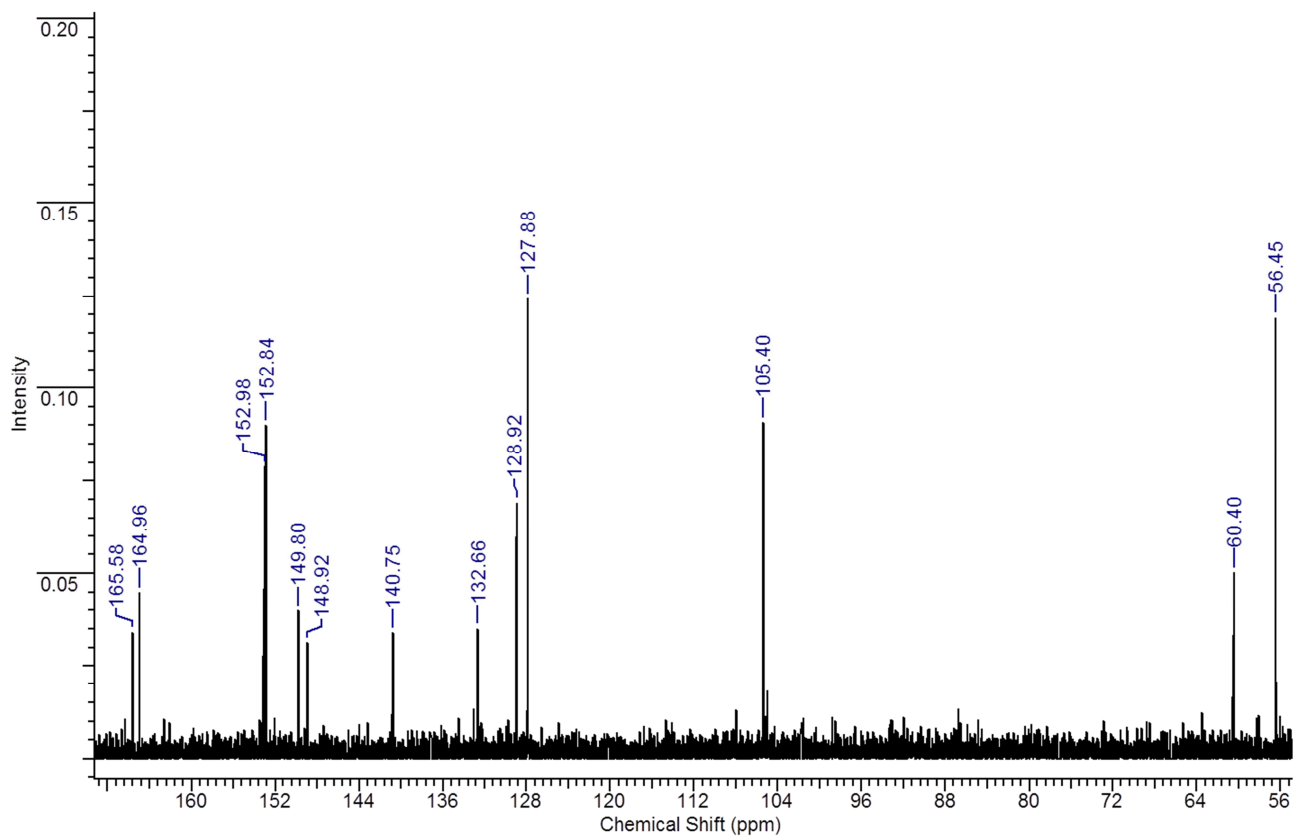
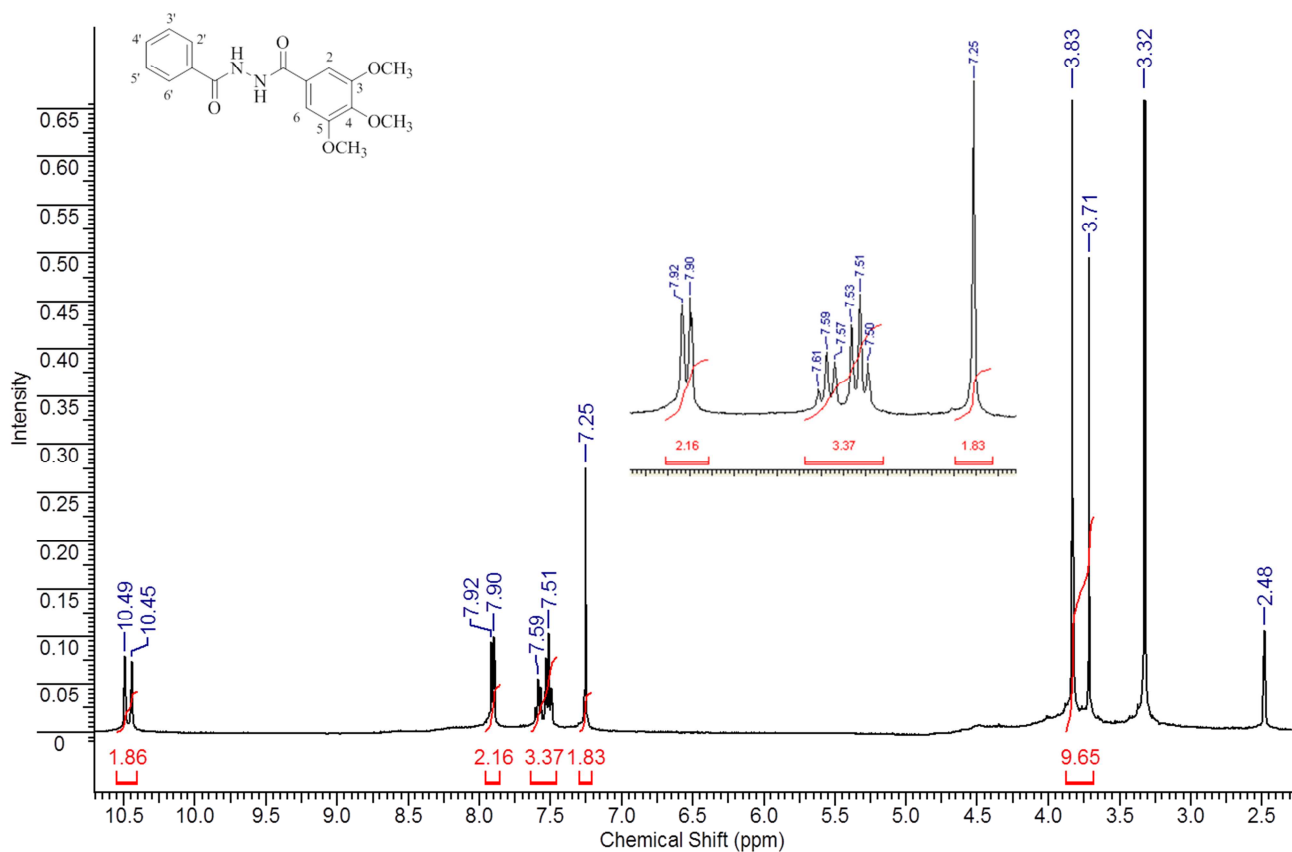


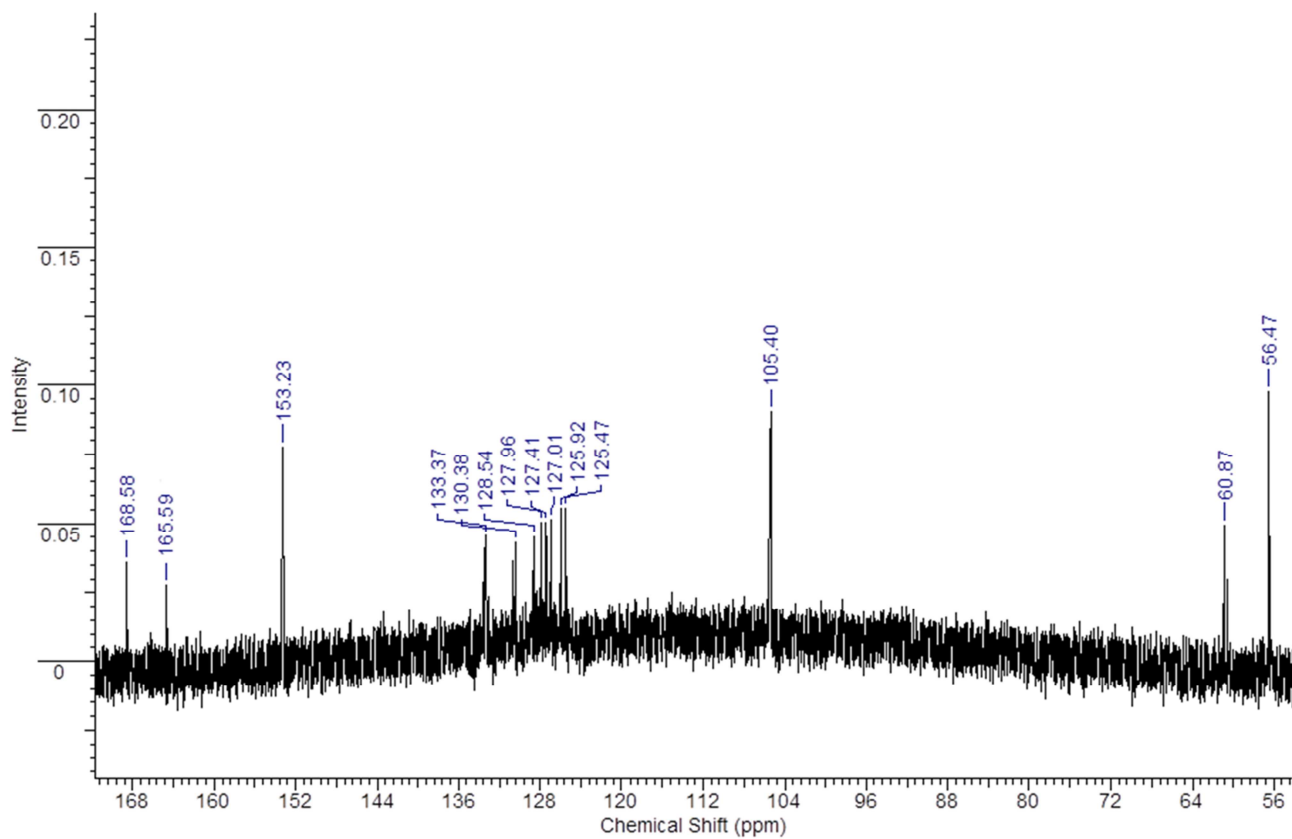
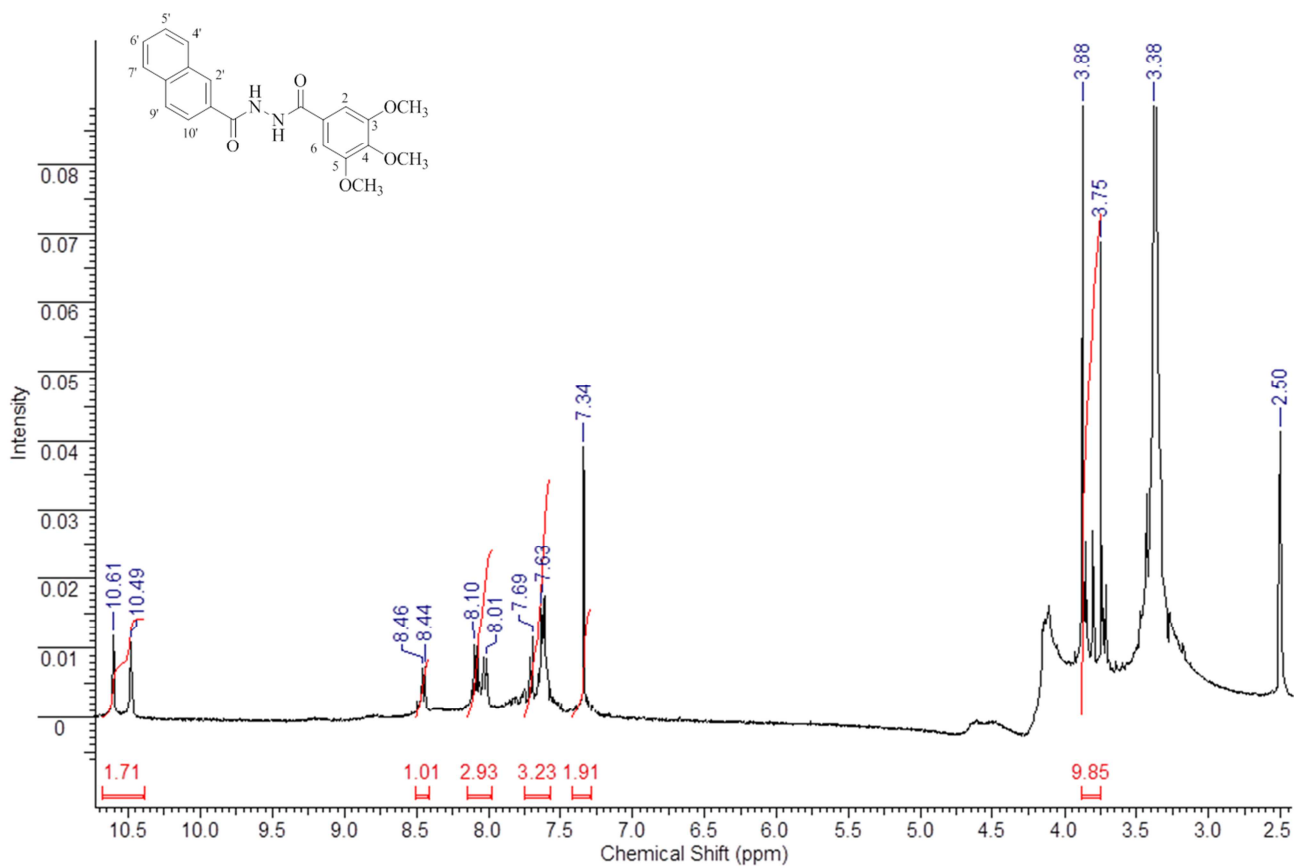


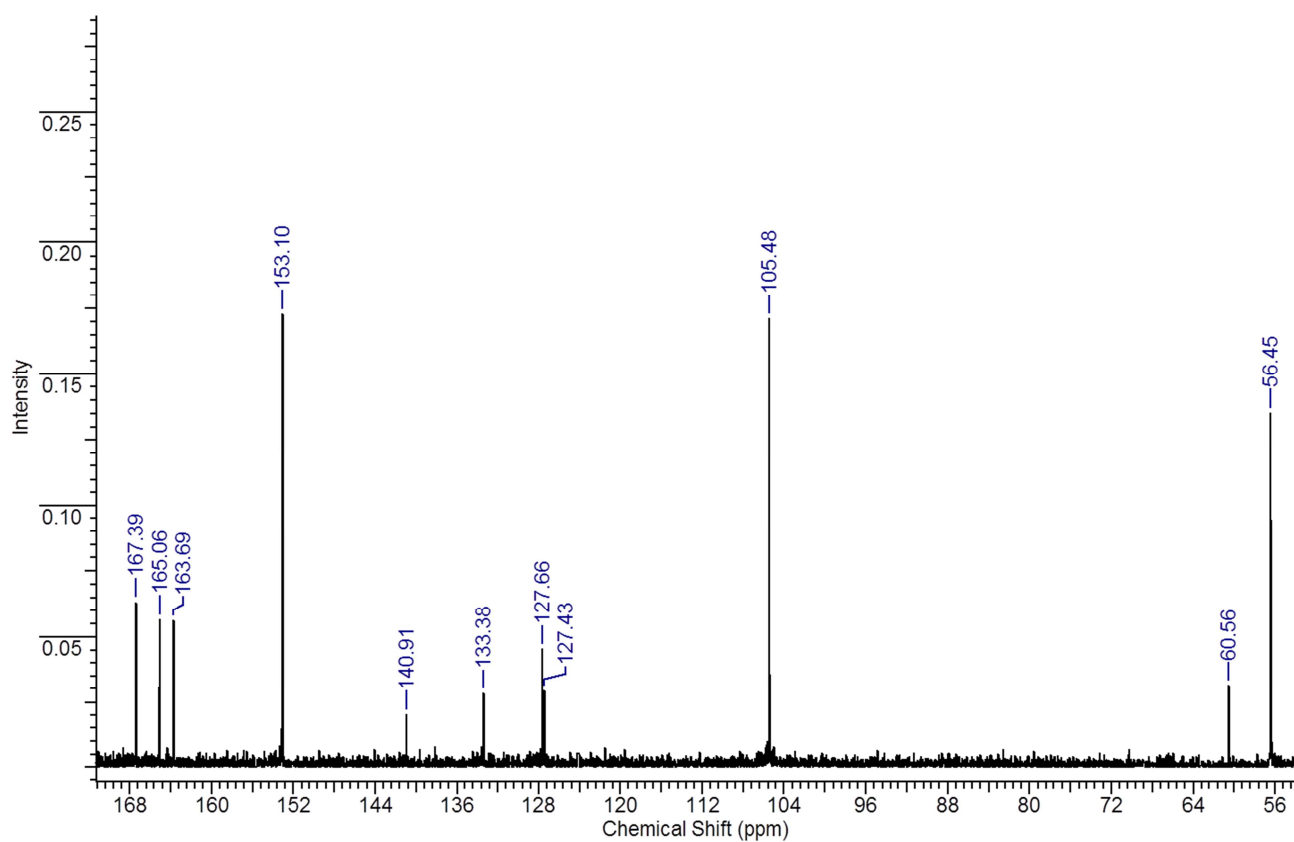
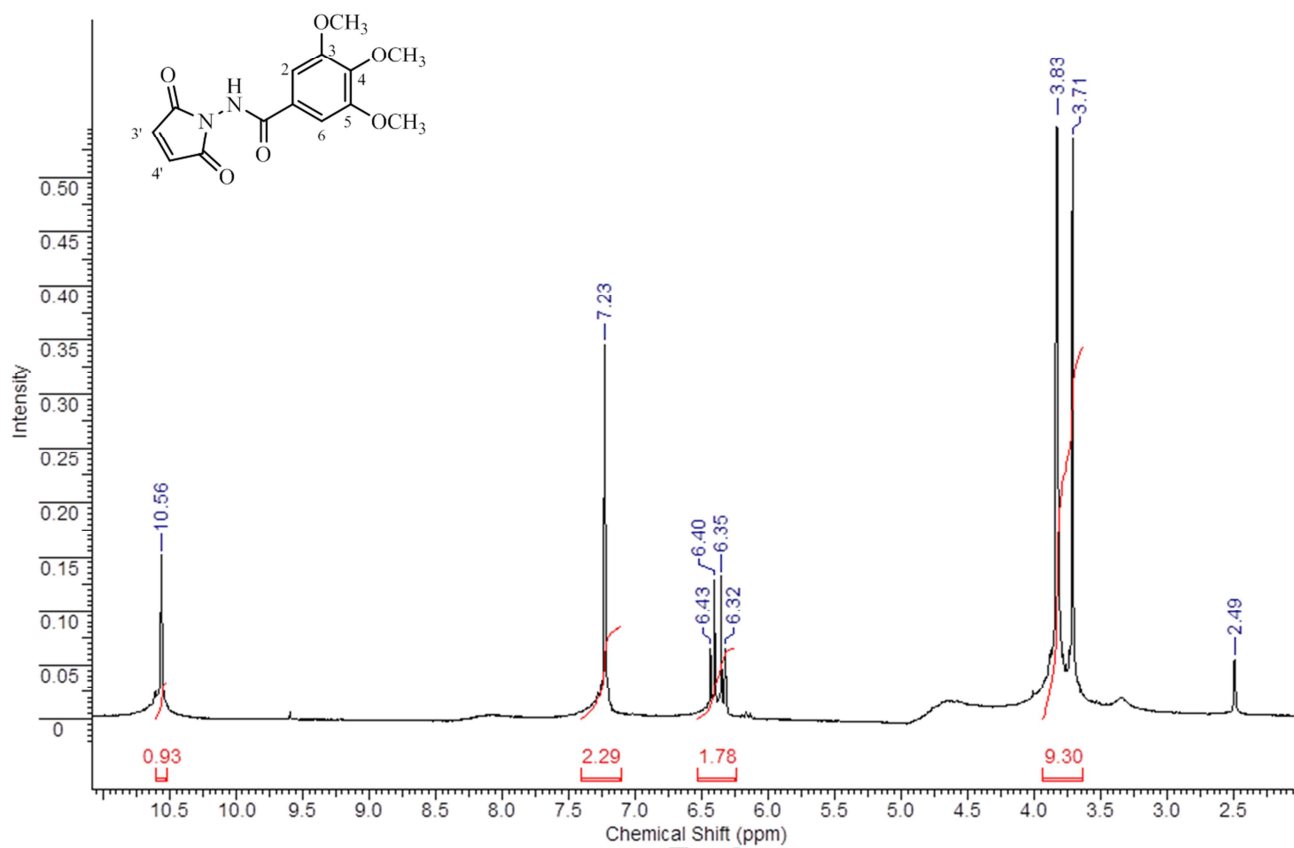


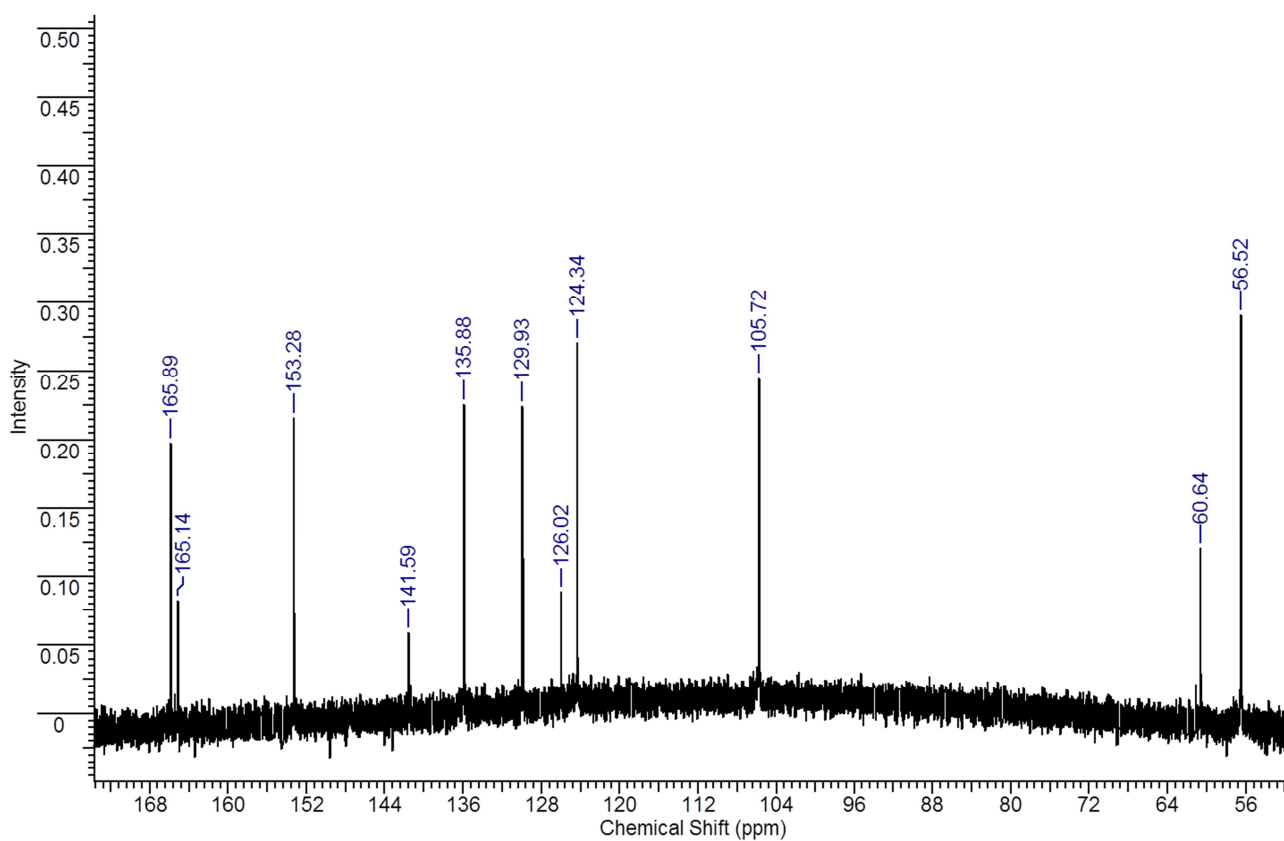
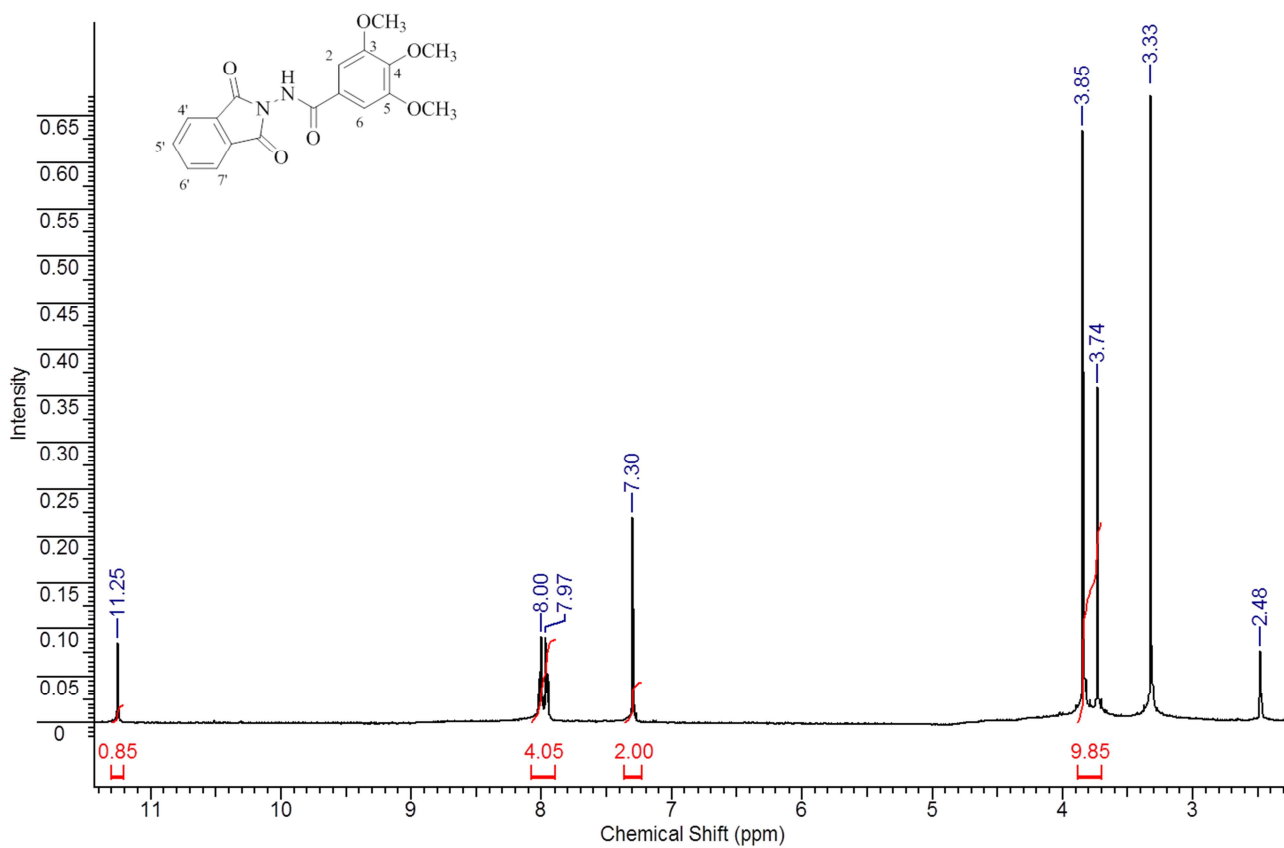


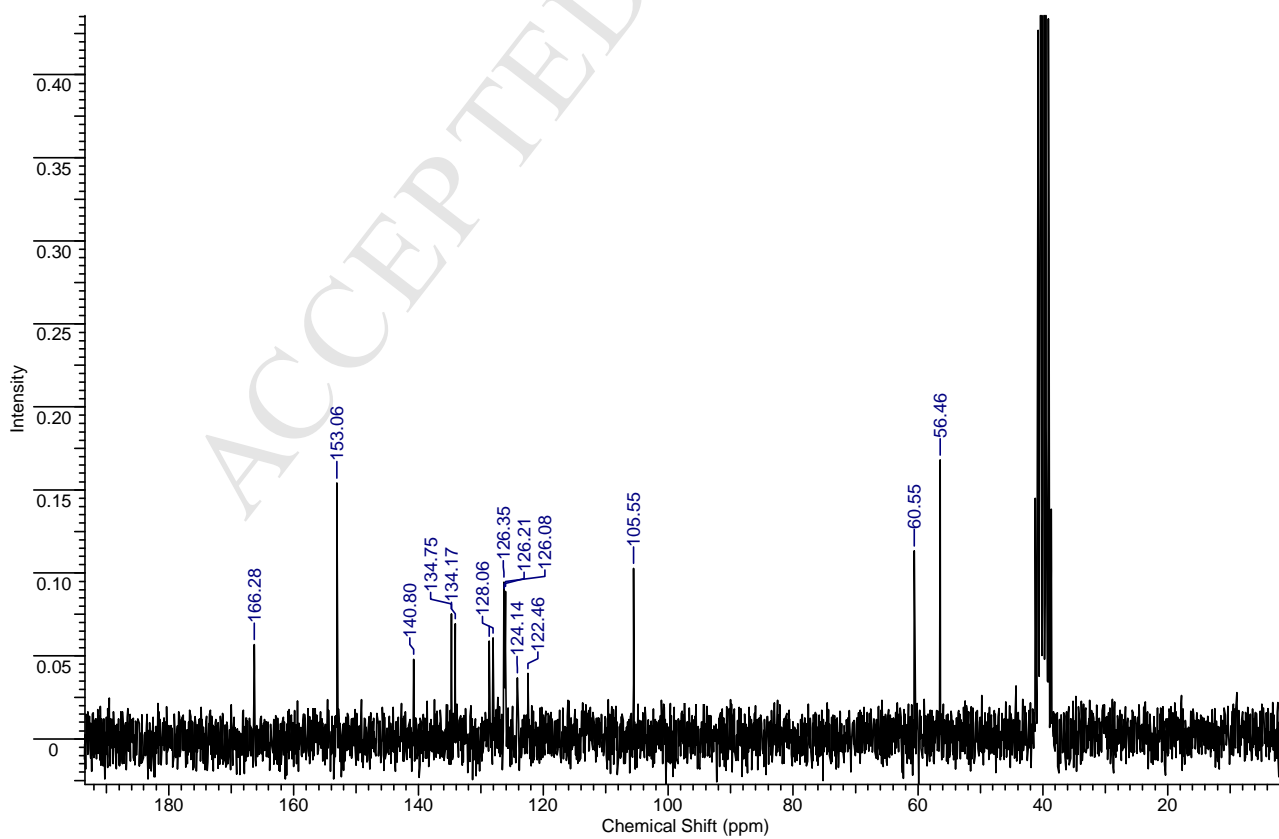
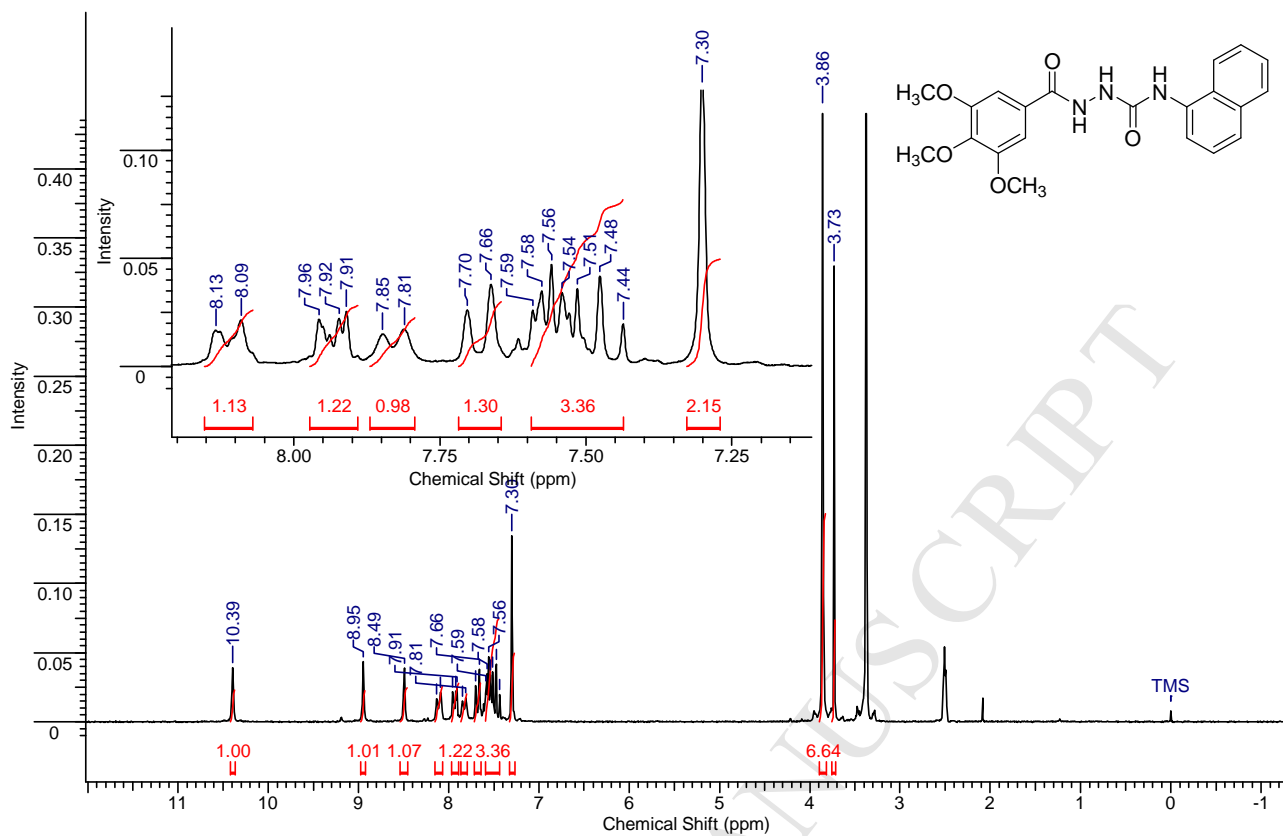


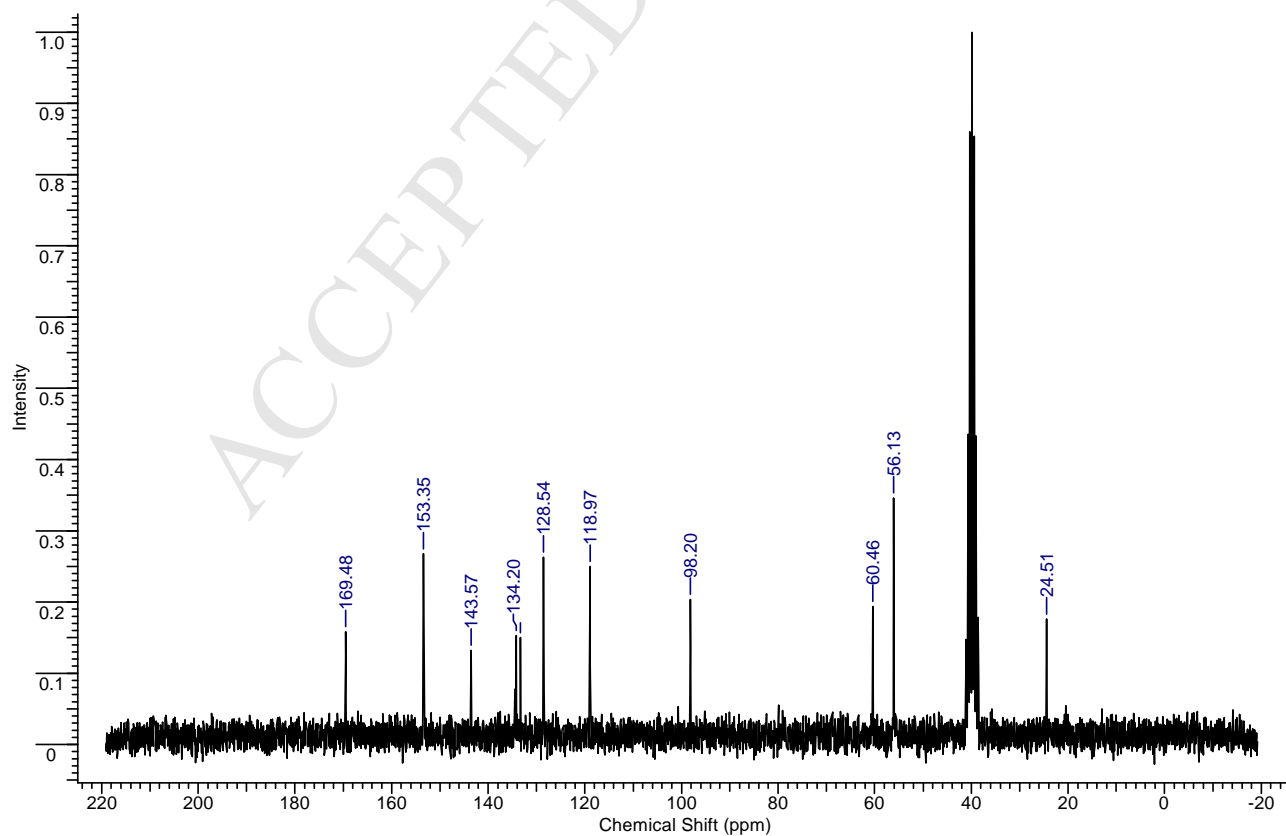
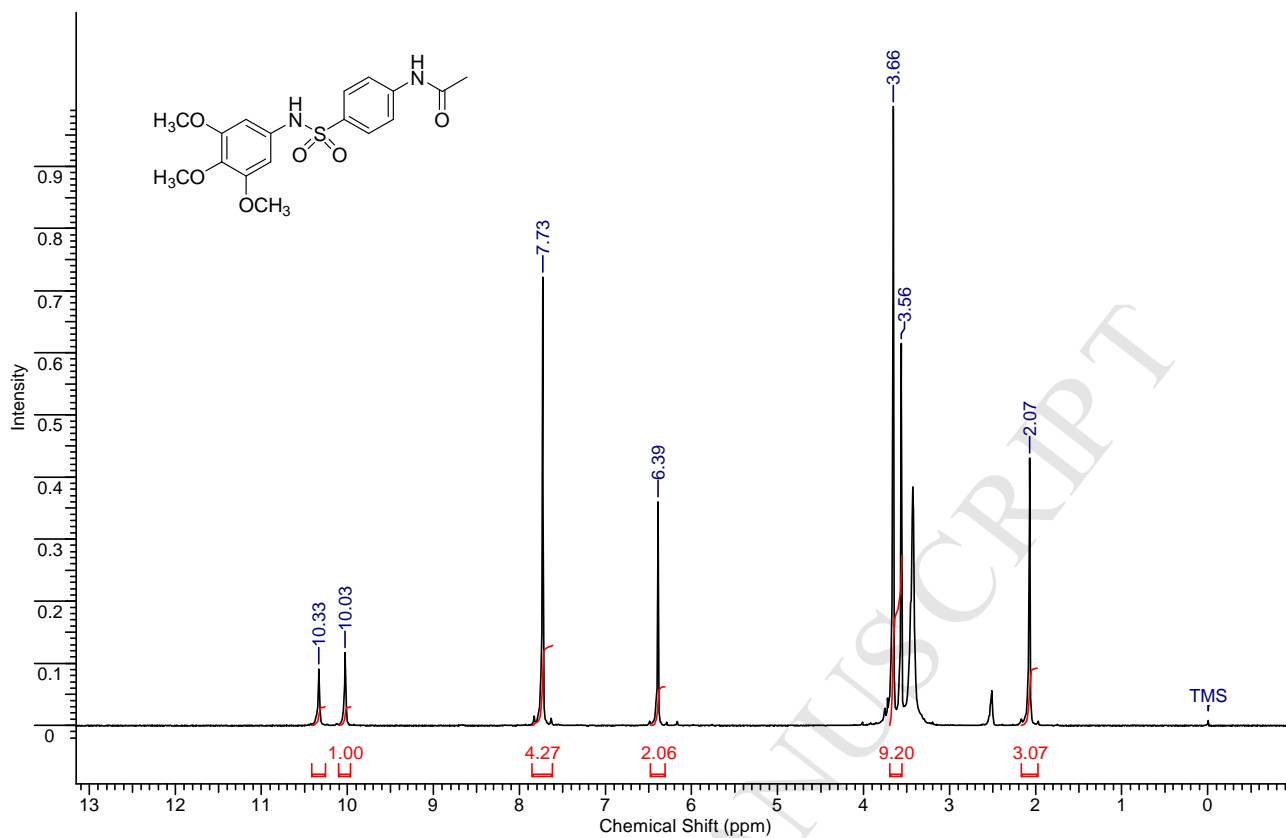


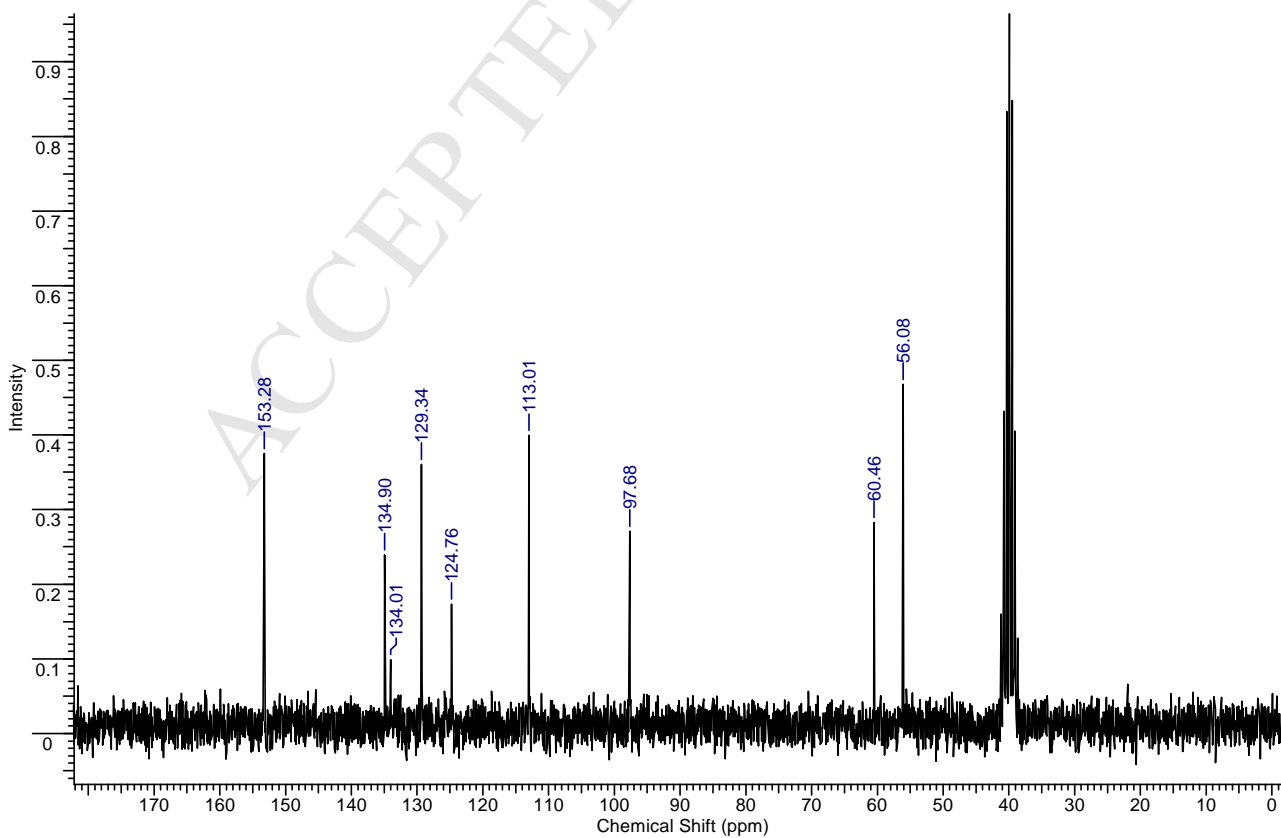
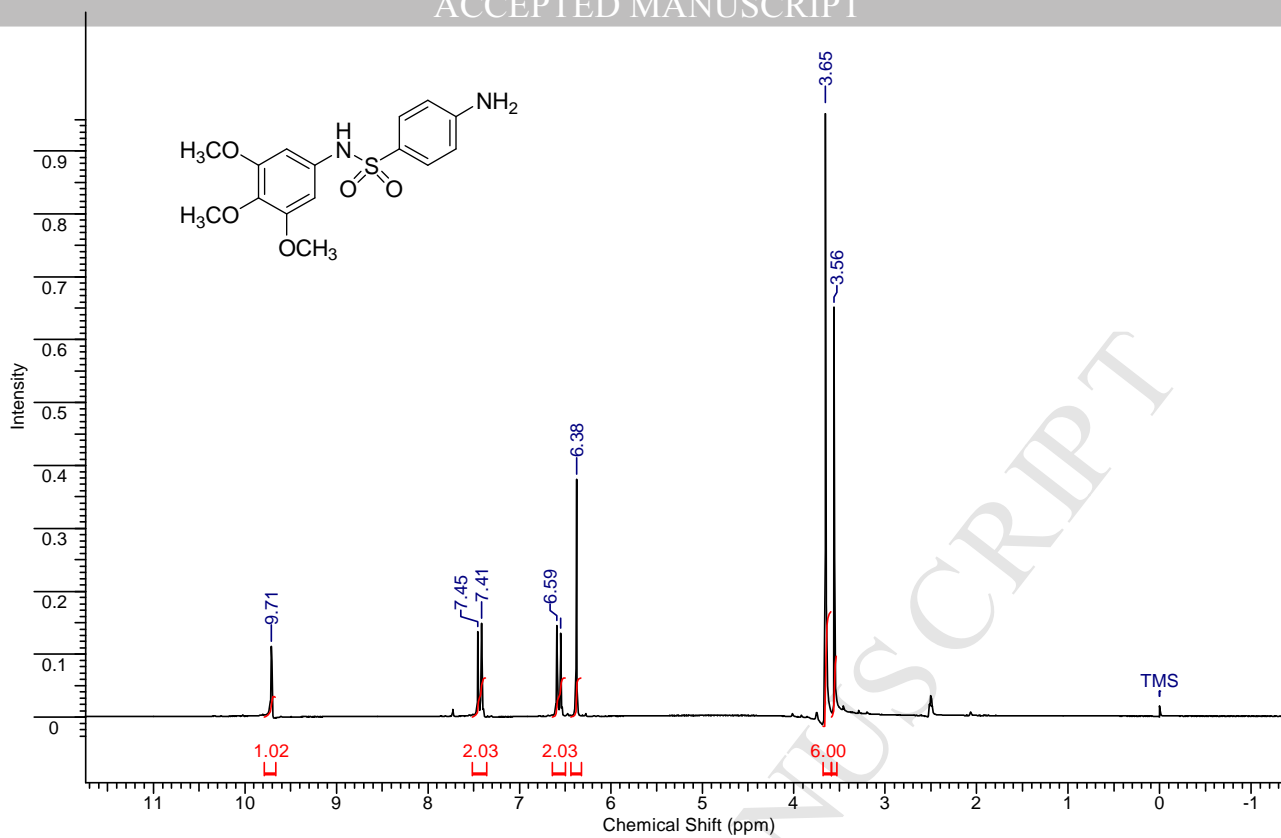


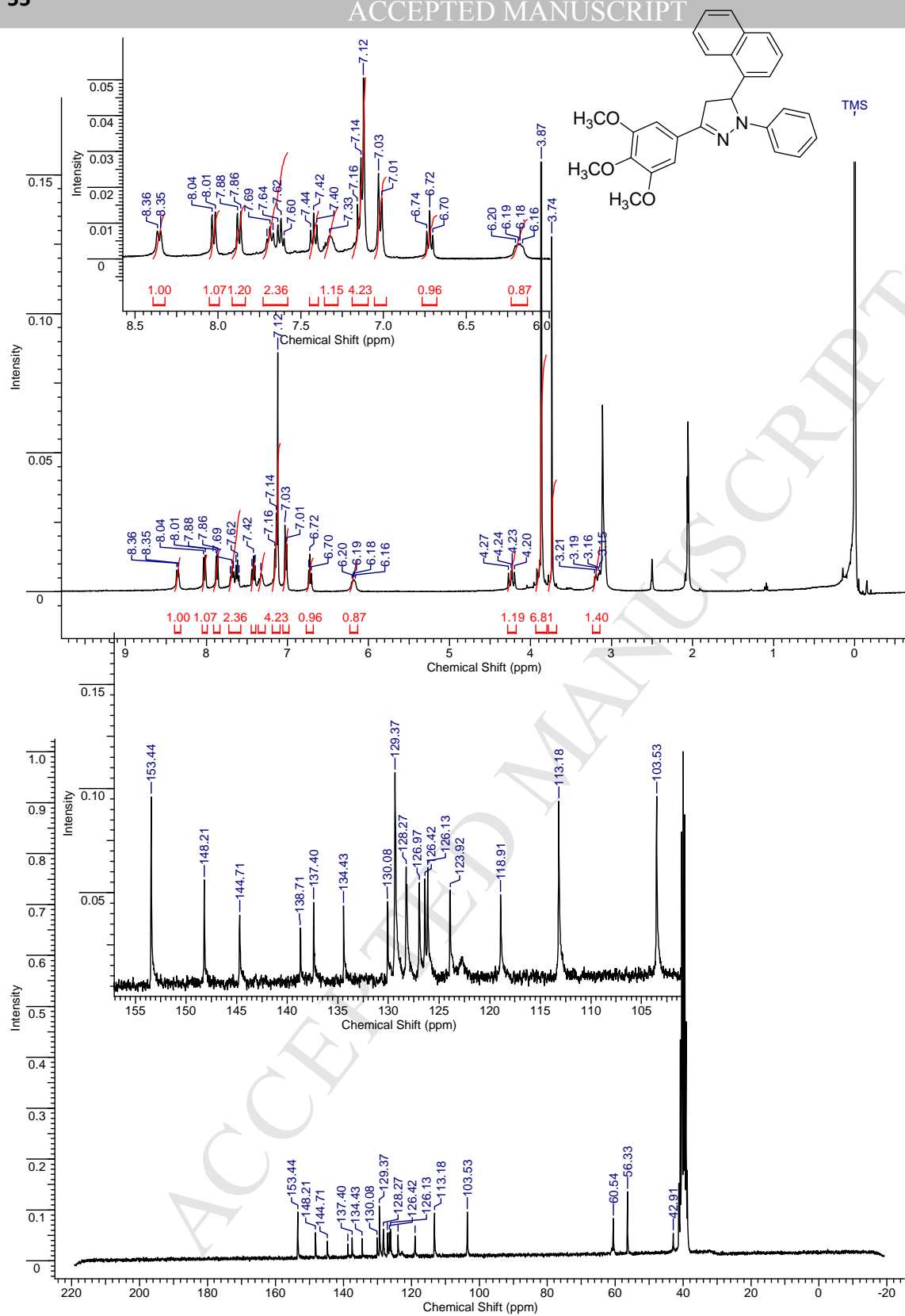


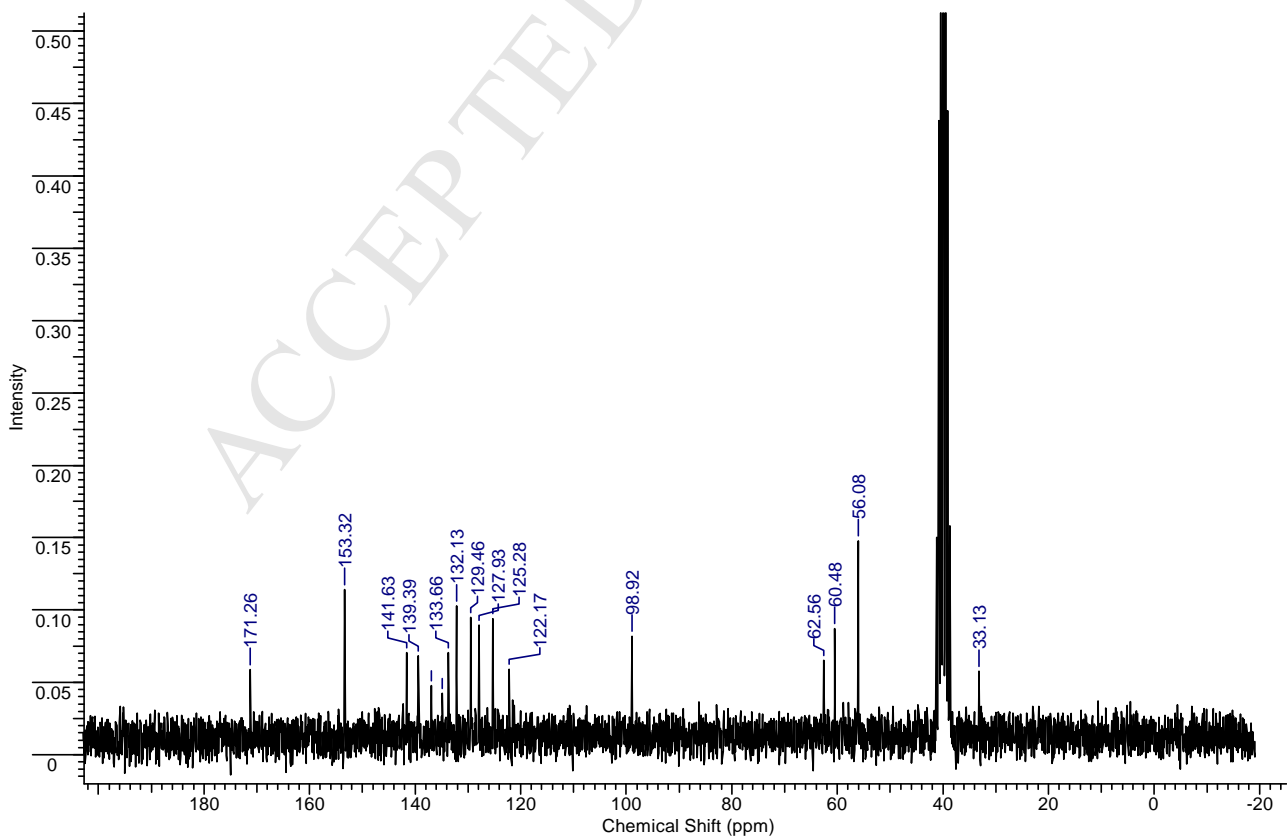
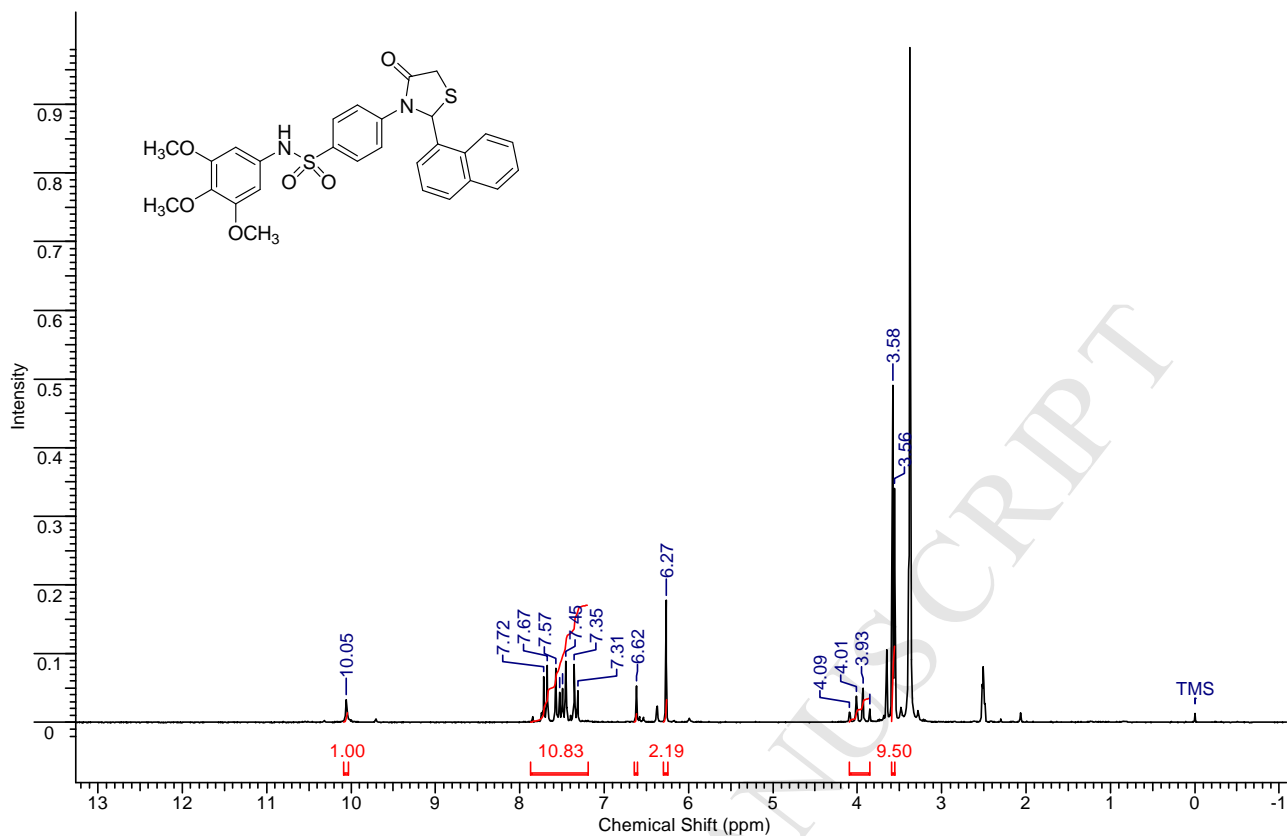


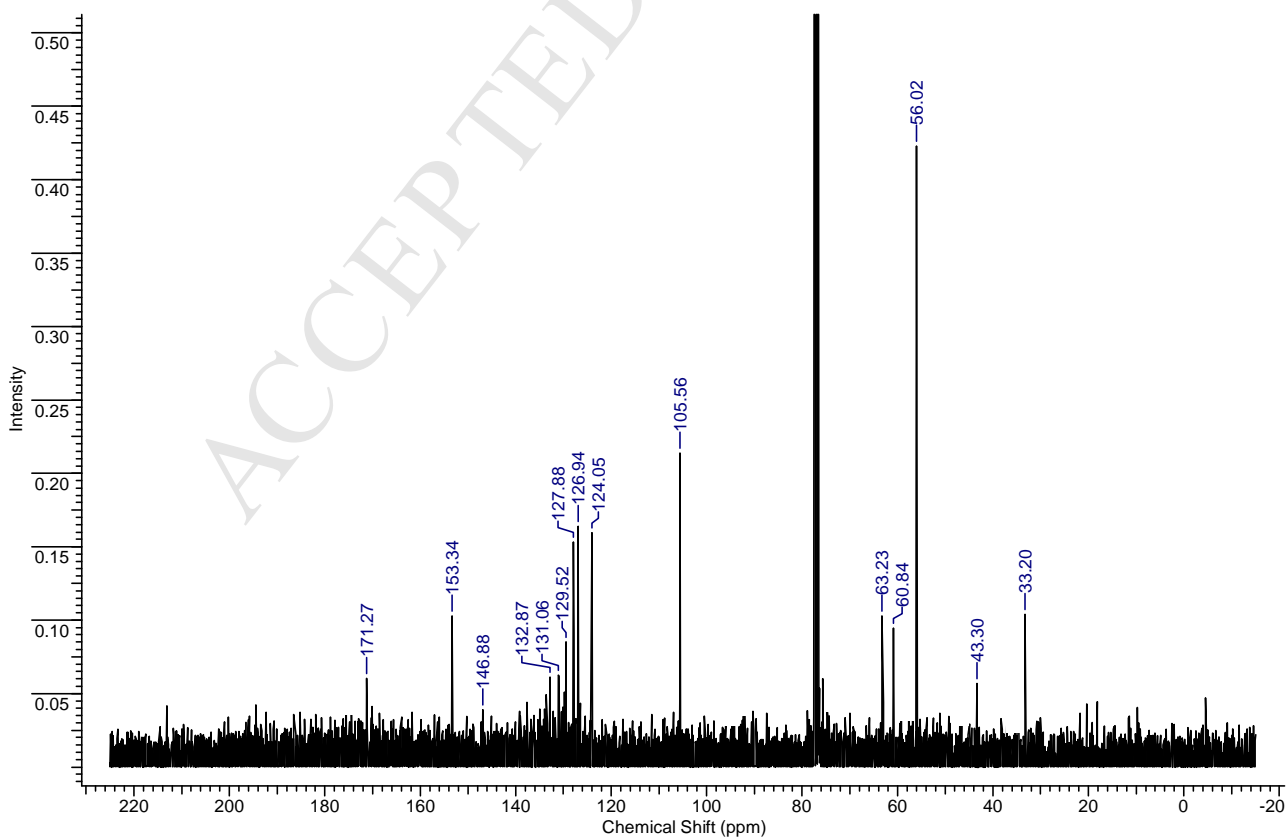
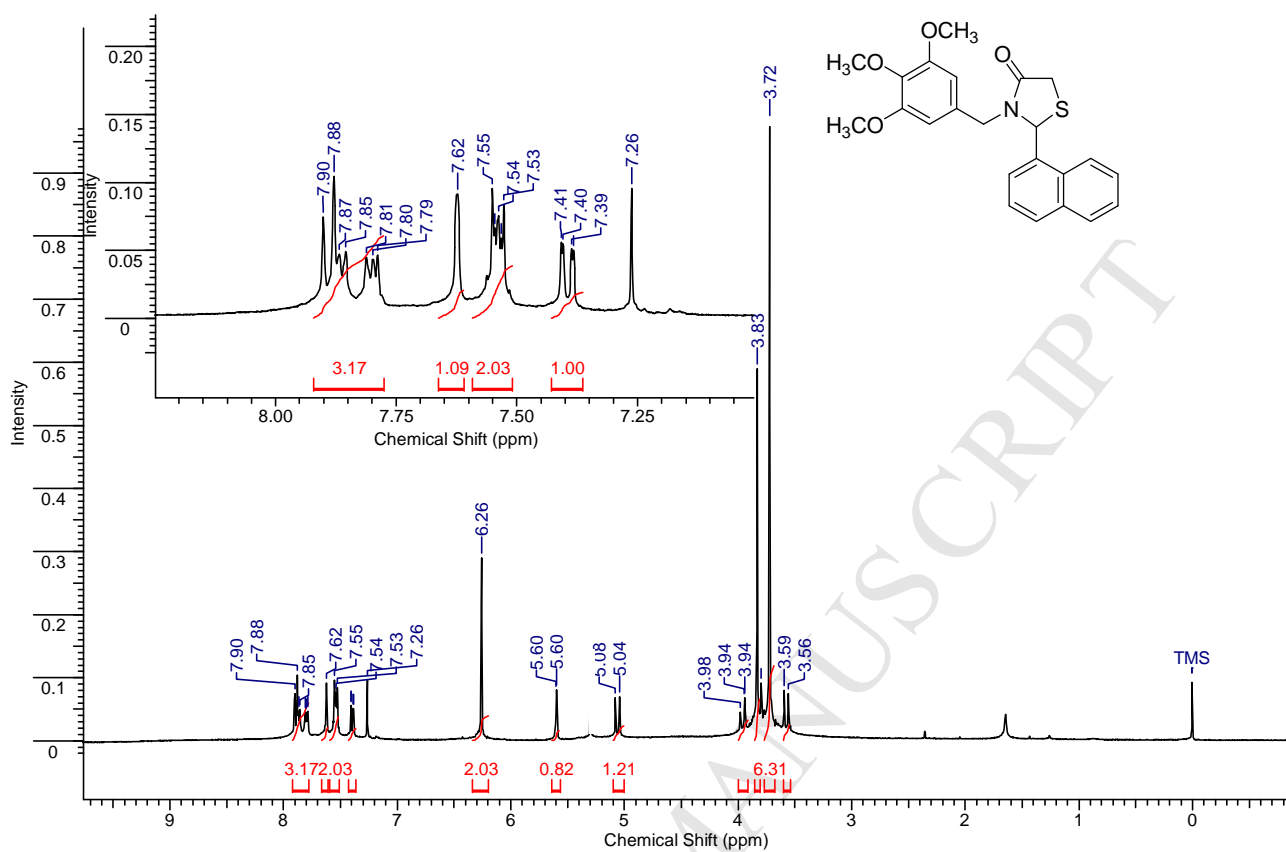


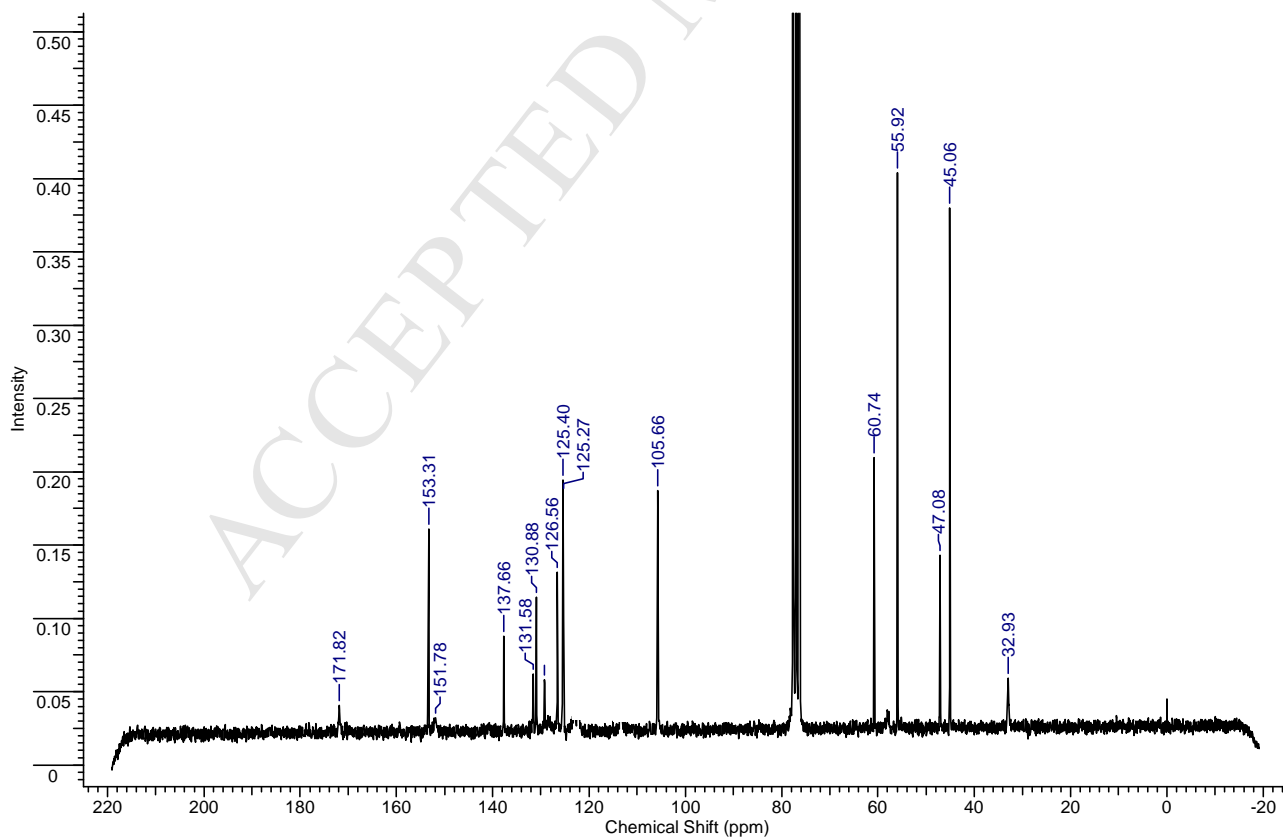
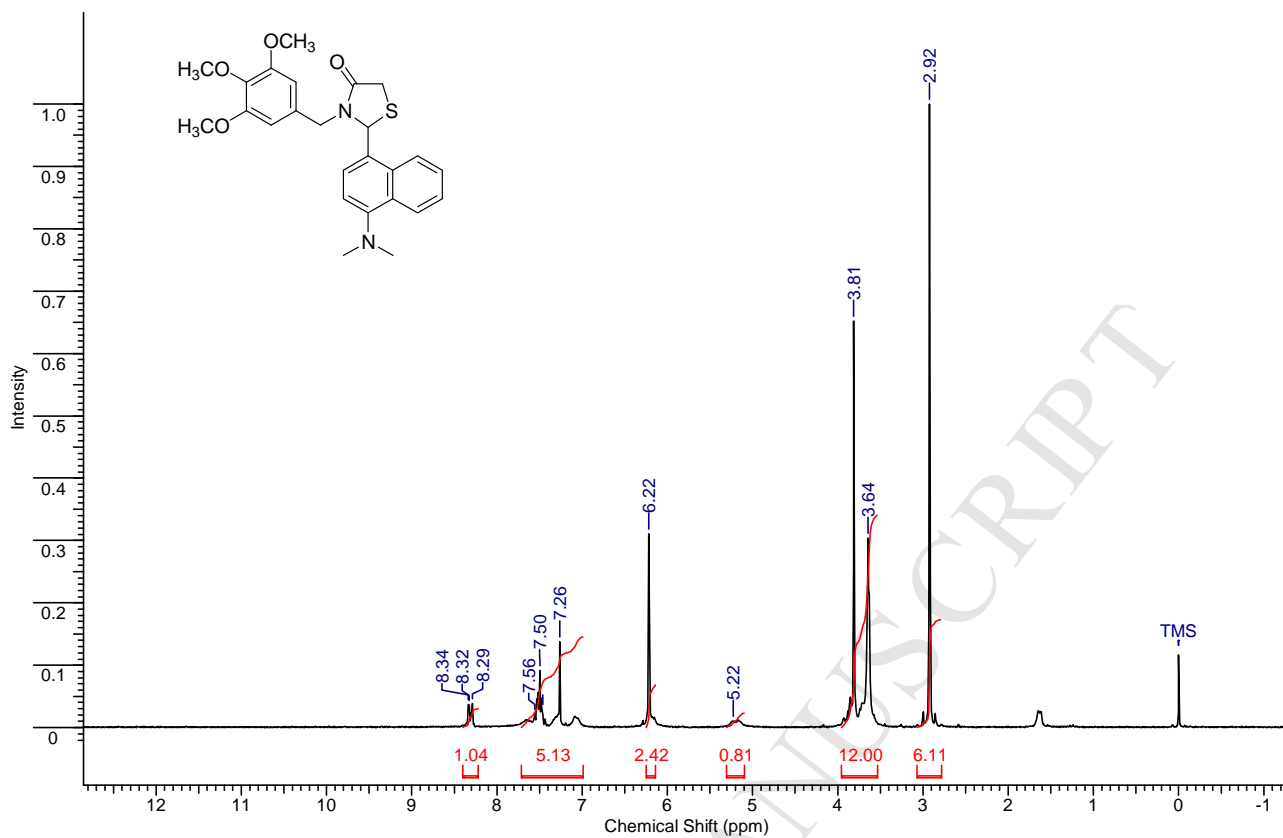


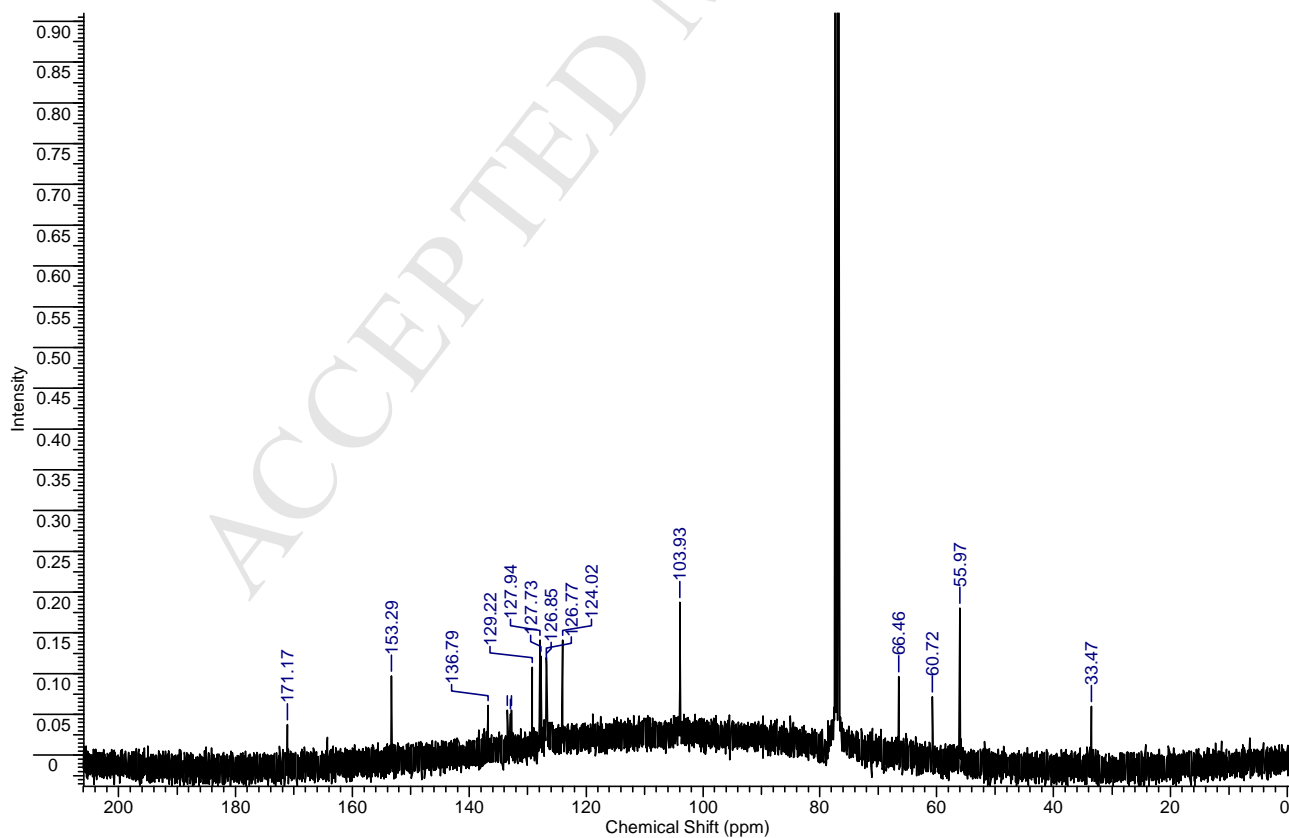
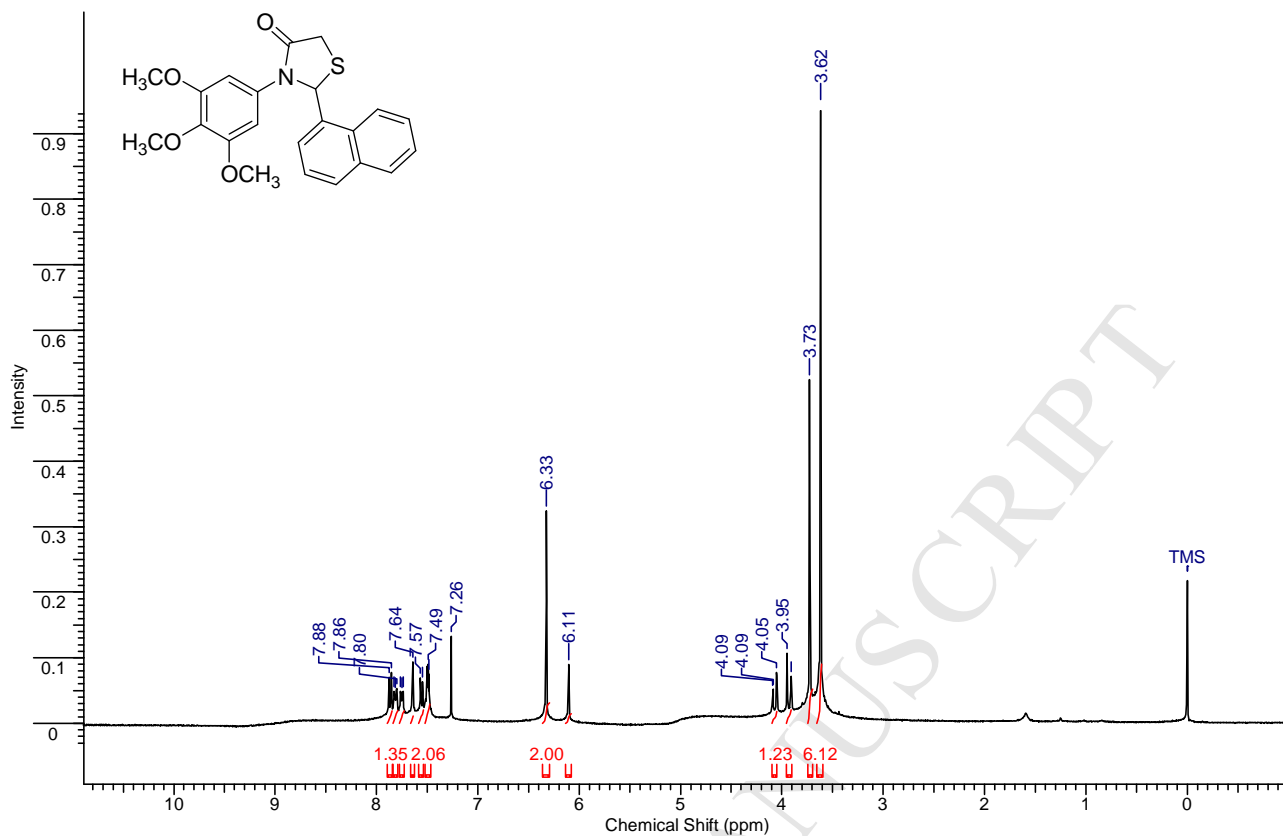


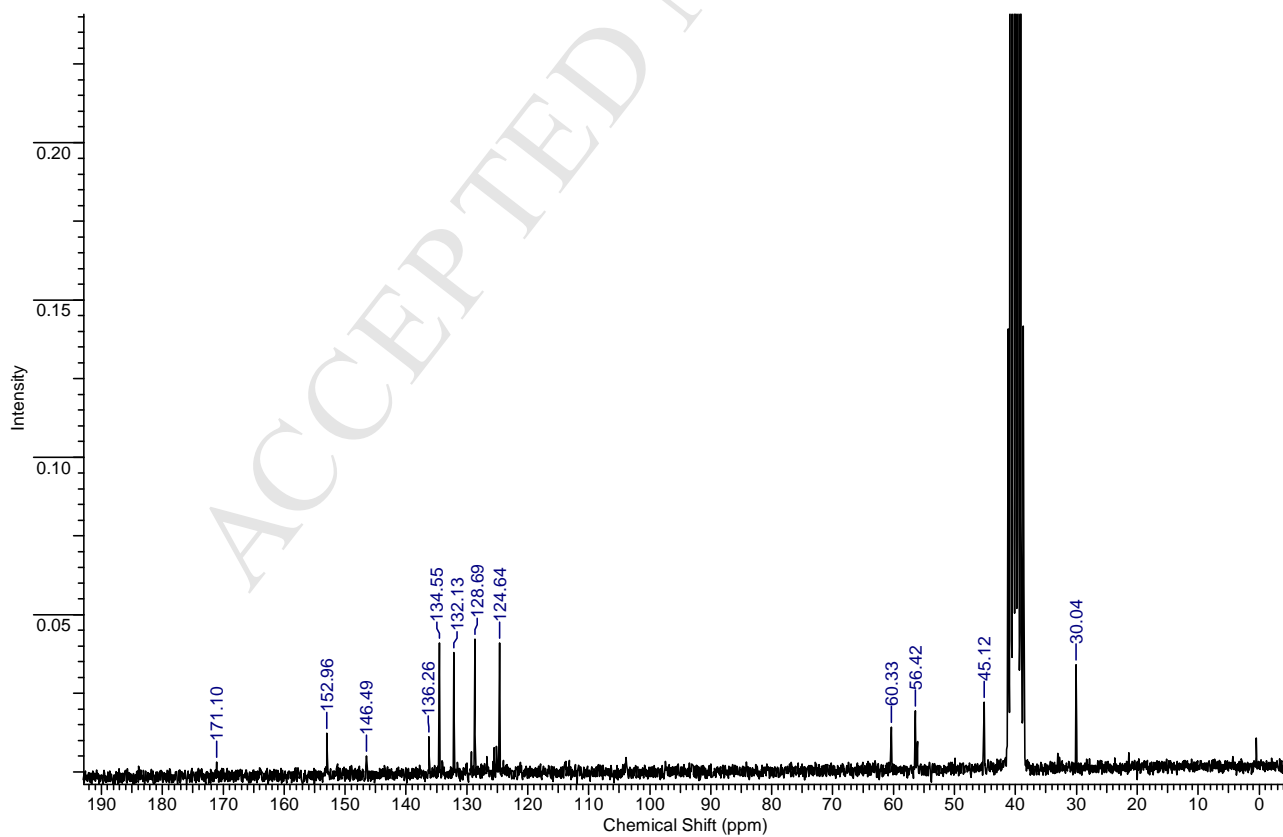
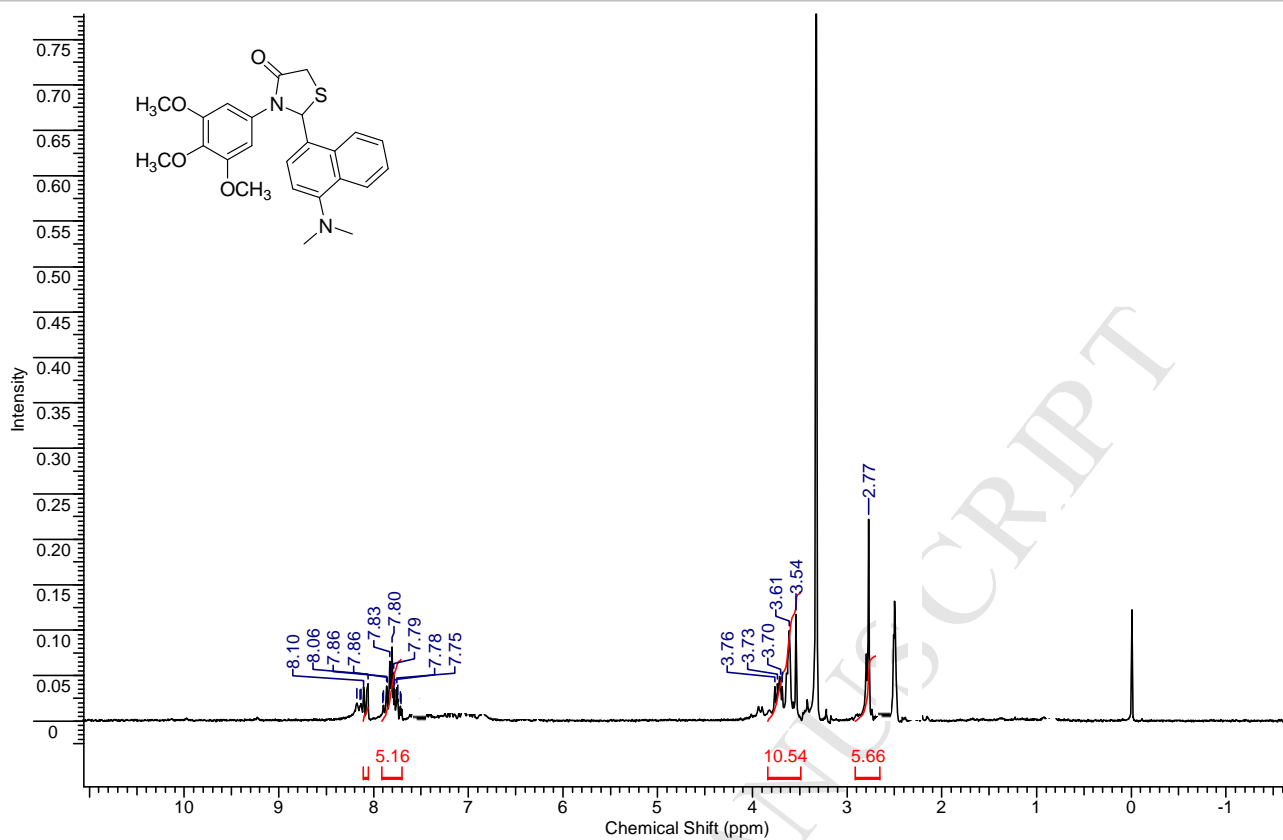












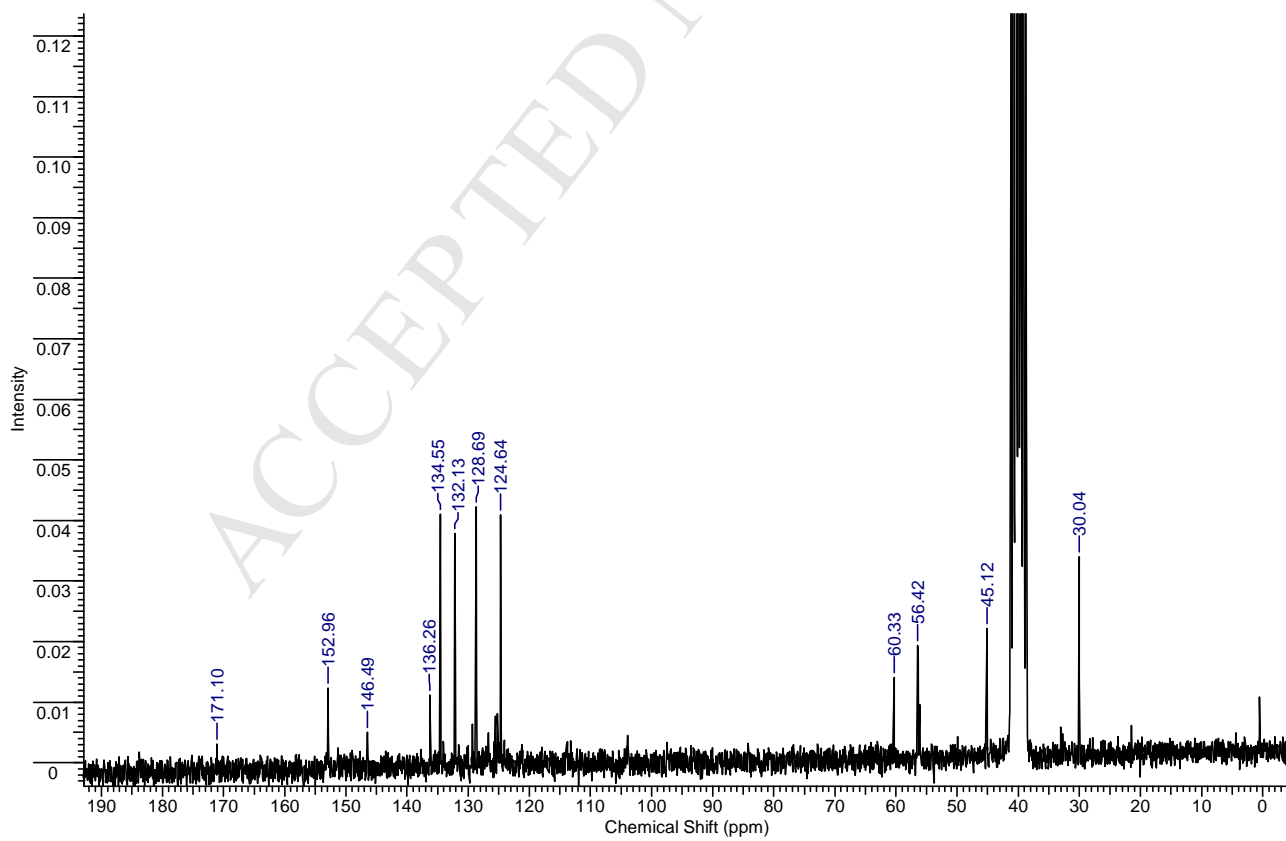
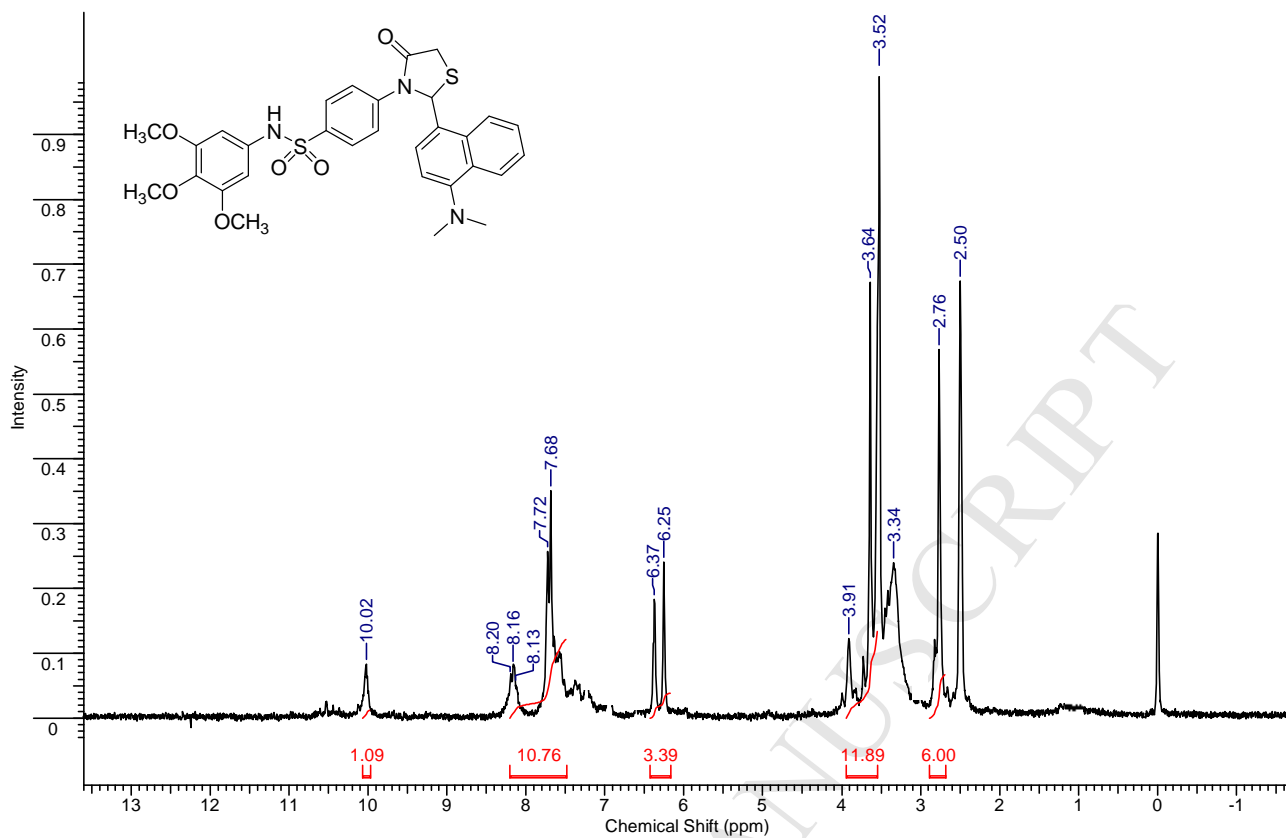


**Table S1.** Survival rates (%) of B-cell precursor (BCP-) and T-cell ALL (T-ALL) cell lines after 48 h of treatment with 1, 0.1 and 0.01  $\mu\text{M}$  of colchicine (**1**), chalcones (**4** and **5**) or the designed compounds (**6-61**). (Mean  $\pm$  standard deviation).

Compound	BCP-ALL			T-ALL		
	1 $\mu\text{M}$	0.1 $\mu\text{M}$	0.01 $\mu\text{M}$	1 $\mu\text{M}$	0.1 $\mu\text{M}$	0.01 $\mu\text{M}$
<b>1</b>	6 $\pm$ 1	14 $\pm$ 1	66 $\pm$ 4	5 $\pm$ 1	11 $\pm$ 1	57 $\pm$ 1
<b>4</b>	36 $\pm$ 5	102 $\pm$ 3	95 $\pm$ 6	25 $\pm$ 1	94 $\pm$ 16	97 $\pm$ 9
<b>5</b>	28 $\pm$ 10	106 $\pm$ 6	100 $\pm$ 10	18 $\pm$ 1	84 $\pm$ 11	88 $\pm$ 12
<b>6</b>	33 $\pm$ 3	92 $\pm$ 5	87 $\pm$ 3	22 $\pm$ 2	88 $\pm$ 1	92 $\pm$ 9
<b>7</b>	34 $\pm$ 8	45 $\pm$ 1	70 $\pm$ 1	23 $\pm$ 1	30 $\pm$ 3	69 $\pm$ 7
<b>8</b>	43 $\pm$ 2	98 $\pm$ 5	104 $\pm$ 7	33 $\pm$ 2	96 $\pm$ 7	99 $\pm$ 4
<b>9</b>	97 $\pm$ 6	99 $\pm$ 8	94 $\pm$ 5	105 $\pm$ 8	102 $\pm$ 8	96 $\pm$ 7
<b>10</b>	99 $\pm$ 5	103 $\pm$ 2	101 $\pm$ 9	110 $\pm$ 9	103 $\pm$ 6	101 $\pm$ 15
<b>11</b>	100 $\pm$ 5	99 $\pm$ 5	106 $\pm$ 5	92 $\pm$ 4	101 $\pm$ 9	95 $\pm$ 7
<b>12</b>	31 $\pm$ 1	39 $\pm$ 1	76 $\pm$ 5	26 $\pm$ 2	30 $\pm$ 2	107 $\pm$ 8
<b>13</b>	14 $\pm$ 1	109 $\pm$ 7	101 $\pm$ 2	13 $\pm$ 1	98 $\pm$ 1	88 $\pm$ 5
<b>14</b>	45 $\pm$ 2	60 $\pm$ 15	101 $\pm$ 8	30 $\pm$ 1	33 $\pm$ 3	95 $\pm$ 4
<b>15</b>	60 $\pm$ 2	43 $\pm$ 2	97 $\pm$ 1	32 $\pm$ 0	30 $\pm$ 0	86 $\pm$ 13
<b>16</b>	42 $\pm$ 3	68 $\pm$ 4	103 $\pm$ 2	26 $\pm$ 2	34 $\pm$ 1	118 $\pm$ 15
<b>17</b>	98 $\pm$ 3	106 $\pm$ 1	108 $\pm$ 4	110 $\pm$ 16	122 $\pm$ 13	94 $\pm$ 24
<b>18</b>	88 $\pm$ 4	101 $\pm$ 1	101 $\pm$ 1	113 $\pm$ 9	121 $\pm$ 16	111 $\pm$ 12
<b>19</b>	98 $\pm$ 6	94 $\pm$ 2	88 $\pm$ 12	96 $\pm$ 4	83 $\pm$ 8	96 $\pm$ 5
<b>20</b>	102 $\pm$ 13	88 $\pm$ 12	107 $\pm$ 9	87 $\pm$ 17	100 $\pm$ 4	95 $\pm$ 8
<b>21</b>	35 $\pm$ 1	37 $\pm$ 1	85 $\pm$ 11	18 $\pm$ 0	17 $\pm$ 0	58 $\pm$ 3
<b>22</b>	109 $\pm$ 3	88 $\pm$ 5	100 $\pm$ 6	119 $\pm$ 12	115 $\pm$ 14	109 $\pm$ 13
<b>23</b>	95 $\pm$ 2	97 $\pm$ 5	104 $\pm$ 0	117 $\pm$ 8	119 $\pm$ 12	116 $\pm$ 10
<b>24</b>	45 $\pm$ 2	94 $\pm$ 1	99 $\pm$ 4	29 $\pm$ 9	121 $\pm$ 13	109 $\pm$ 16
<b>25</b>	42 $\pm$ 1	100 $\pm$ 6	99 $\pm$ 2	21 $\pm$ 0	86 $\pm$ 8	88 $\pm$ 5
<b>26</b>	89 $\pm$ 11	102 $\pm$ 9	106 $\pm$ 1	98 $\pm$ 18	100 $\pm$ 18	96 $\pm$ 1
<b>27</b>	59 $\pm$ 6	97 $\pm$ 2	97 $\pm$ 2	31 $\pm$ 5	94 $\pm$ 1	100 $\pm$ 2
<b>28</b>	113 $\pm$ 1	96 $\pm$ 3	90 $\pm$ 10	91 $\pm$ 23	81 $\pm$ 3	104 $\pm$ 7
<b>29</b>	85 $\pm$ 8	95 $\pm$ 3	98 $\pm$ 0	91 $\pm$ 14	86 $\pm$ 1	94 $\pm$ 7
<b>30</b>	62 $\pm$ 5	89 $\pm$ 5	95 $\pm$ 7	20 $\pm$ 3	78 $\pm$ 8	82 $\pm$ 8

<b>31</b>	71 ± 2	90 ± 15	102 ± 2	36 ± 12	79 ± 3	71 ± 12
<b>32</b>	70 ± 1	91 ± 3	90 ± 11	76 ± 8	91 ± 3	85 ± 0
<b>33</b>	37 ± 2	94 ± 11	99 ± 11	24 ± 1	63 ± 2	94 ± 2
<b>34</b>	100 ± 6	98 ± 8	99 ± 6	104 ± 6	98 ± 8	102 ± 11
<b>35</b>	91 ± 7	92 ± 6	100 ± 3	88 ± 1	100 ± 5	102 ± 3
<b>36</b>	54 ± 4	95 ± 6	99 ± 3	15 ± 1	100 ± 3	100 ± 3
<b>37</b>	88 ± 1	105 ± 1	105 ± 1	100 ± 6	121 ± 9	121 ± 9
<b>38</b>	101 ± 5	102 ± 1	102 ± 1	94 ± 6	111 ± 11	111 ± 11
<b>39</b>	115 ± 24	124 ± 4	104 ± 14	107 ± 10	111 ± 9	103 ± 11
<b>40</b>	97 ± 14	114 ± 6	120 ± 3	95 ± 8	110 ± 13	107 ± 7
<b>41</b>	116 ± 1	123 ± 19	120 ± 7	101 ± 6	106 ± 8	102 ± 3
<b>42</b>	105 ± 11	104 ± 13	106 ± 9	95 ± 7	99 ± 5	95 ± 4
<b>43</b>	92 ± 7	103 ± 4	93 ± 9	100 ± 7	93 ± 2	96 ± 1
<b>44</b>	88 ± 7	99 ± 8	99 ± 8	104 ± 6	108 ± 12	106 ± 5
<b>45</b>	99 ± 1	94 ± 8	98 ± 9	95 ± 4	97 ± 7	94 ± 2
<b>46</b>	93 ± 8	86 ± 15	96 ± 1	84 ± 5	93 ± 9	94 ± 3
<b>47</b>	96 ± 4	91 ± 3	99 ± 5	90 ± 8	95 ± 11	107 ± 2
<b>48</b>	99 ± 7	104 ± 4	105 ± 7	87 ± 8	90 ± 1	88 ± 5
<b>49</b>	102 ± 3	101 ± 5	105 ± 4	105 ± 14	93 ± 6	93 ± 8
<b>50</b>	109 ± 4	nd	nd	115 ± 2	nd	nd
<b>51</b>	90 ± 4	92 ± 4	98 ± 5	88 ± 6	91 ± 5	93 ± 13
<b>52</b>	93 ± 7	91 ± 11	nd	96 ± 4	101 ± 6	nd
<b>53</b>	95 ± 1	102 ± 3	105 ± 11	94 ± 4	93 ± 3	94 ± 6
<b>54</b>	95 ± 5	98 ± 4	90 ± 4	89 ± 4	92 ± 8	91 ± 9
<b>55</b>	97 ± 8	99 ± 2	nd	95 ± 5	96 ± 2	nd
<b>56</b>	100 ± 9	105 ± 4	103 ± 2	87 ± 1	91 ± 9	101 ± 11
<b>57</b>	79 ± 3	90 ± 8	88 ± 1	87 ± 6	90 ± 7	96 ± 2
<b>58</b>	99 ± 6	100 ± 5	nd	105 ± 2	96 ± 6	nd
<b>59</b>	88 ± 6	90 ± 6	94 ± 1	94 ± 3	90 ± 5	95 ± 7
<b>60</b>	98 ± 3	103 ± 4	nd	115 ± 10	120 ± 5	nd
<b>61</b>	81 ± 5	85 ± 4	89 ± 3	93 ± 10	86 ± 8	93 ± 4

nd, not determined.

**Table S2.** Acute toxicity test: food and water consumption by animals following compound **12** administration.

<b>Group (mg/Kg, v.o.)</b>	<b>Sex</b>	<b>Food (g/animal/day)</b>	<b>Water (mL/animal/day)</b>
Vehicle	Male	7.64 ± 0.82	6.82 ± 0.95
0.1	Male	7.44 ± 1.02	7.18 ± 0.59
1	Male	7.54 ± 1.31	7.44 ± 0.77
10	Male	7.54 ± 0.98	7.18 ± 0.77
100	Male	7.86 ± 1.05	7.44 ± 1.01
1,000	Male	7.24 ± 1.05	6.62 ± 0.94
Vehicle	Female	5.83 ± 0.49	6.53 ± 0.74
0.1	Female	5.30 ± 0.37	6.09 ± 0.88
1	Female	4.95 ± 0.48	5.62 ± 0.69
10	Female	5.32 ± 0.40	6.62 ± 1.02
100	Female	5.16 ± 0.41	6.09 ± 0.77
1,000	Female	6.08 ± 0.53	6.51 ± 0.76

Values are means (n=6) ± SEM.

**Table S3.** Acute toxicity test: relative weight of organs and glands from female mice, 14 days after compound **12** administration.

Organ / Gland	Compound 12 (mg/Kg, p.o.)					
	Vehicle	0.1	1	10	100	1,000
<b>Spleen</b>	0.46 (0.41 – 0.50)	0.41 (0.36 – 0.47)	0.49 (0.40 – 0.58)	0.47 (0.42 – 0.51)	0.48 (0.39 – 0.57)	0.38 (0.33 – 0.44)
<b>Kidney</b>	0.532 (0.50 – 0.55)	0.53 (0.48 – 0.58)	0.53 (0.49 – 0.57)	0.49 (0.42 – 0.57)	0.55 (0.51 – 0.59)	0.52 (0.47 – 0.57)
<b>Heart</b>	0.36 (0.35 – 0.38)	0.35 (0.34 – 0.37)	0.35 (0.32 – 0.38)	0.33 (0.30 – 0.37)	0.34 (0.32 – 0.36)	0.34 (0.32 – 0.37)
<b>Lungs</b>	0.65 (0.44 – 0.86)	0.77 (0.60 – 0.94)	0.59 (0.54 – 0.64)	0.79 (0.34 – 1.25)	0.64 (0.46 – 0.81)	0.76 (0.63 – 0.89)
<b>Liver</b>	4.22 (3.77 – 4.67)	4.38 (3.85 – 4.91)	4.60 (4.04 – 5.16)	4.48 (3.76 – 5.19)	3.79 (3.46 – 4.12)	3.90 (3.54 – 4.25)
<b>Mesenteric lymph node</b>	0.12 (0.07 – 0.16)	0.11 (0.08 – 0.14)	0.13 (0.05 – 0.22)	0.12 (0.07 – 0.17)	0.11 (0.09 – 0.14)	0.10 (0.08 – 0.12)
<b>Adrenal gland</b>	0.02 (0.01 – 0.02)	0.01 (0.01 – 0.02)	0.01 (0.01 – 0.02)	0.01 (0.01 – 0.02)	0.01 (0.01 – 0.02)	0.01 (0.01 – 0.02)
<b>Thymus</b>	0.26 (0.21 – 0.32)	0.28 (0.21 – 0.36)	0.27 (0.22 – 0.33)	0.25 (0.16 – 0.35)	0.29 (0.20 – 0.39)	0.25 (0.14 – 0.35)
<b>Stomach</b>	0.67 (0.62 – 0.72)	0.81 (0.75 – 0.86)	0.71 (0.66 – 0.76)	0.76 (0.62 – 0.91)	0.64 (0.60 – 0.69)	0.69 (0.55 – 0.82)
<b>Brain</b>	0.89 (0.84 – 0.95)	0.96 (0.85 – 1.06)	0.88 (0.75 – 1.02)	0.97 (0.93 – 1.02)	0.95 (0.76 – 1.14)	0.88 (0.79 – 0.97)
<b>Ovary and oviducts</b>	0.40 (0.32 – 0.49)	0.39 (0.26 – 0.51)	0.35 (0.28 – 0.42)	0.36 (0.16 – 0.56)	0.41 (0.31 – 0.51)	0.40 (0.24 – 0.56)
<b>Salivary gland</b>	0.42 (0.30 – 0.54)	0.33 (0.31 – 0.35)	0.31 (0.24 – 0.40)	0.32 (0.22 – 0.42)	0.38 (0.27 – 0.49)	0.31 (0.22 – 0.40)

Values were obtained by the formula [(organ weight/animal weight) x 100] and are expressed in terms of mean (n =6) and 95% confidence interval.

**Table S4.** Acute toxicity test: relative weight of organs from male mice, 14 days after compound **12** administration.

Organ / Gland	Compound 12 (mg/Kg, p.o.)					
	Vehicle	0.1	1	10	100	1,000
<b>Spleen</b>	0.27 (0.25 – 0.29)	0.34 (0.29 – 0.39)	0.38 (0.22 – 0.54)	0.38 (0.33 – 0.43)	0.3 (0.30 – 0.46)	0.38 (0.27 – 0.49)
<b>Kidney</b>	0.51 (0.42 – 0.60)	0.54 (0.46 – 0.62)	0.60 (0.54 – 0.66)	0.57 (0.52 – 0.63)	0.58 (0.48 – 0.68)	0.60 (0.54 – 0.67)
<b>Heart</b>	0.33 (0.27 – 0.39)	0.33 (0.30 – 0.37)	0.35 (0.33 – 0.38)	0.33 (0.29 – 0.37)	0.36 (0.31 – 0.42)	0.37 (0.31 – 0.43)
<b>Lungs</b>	0.48 (0.38 – 0.58)	0.55 (0.43 – 0.67)	0.53 (0.43 – 0.62)	0.57 (0.43 – 0.71)	0.58 (0.48 – 0.69)	0.57 (0.33 – 0.82)
<b>Liver</b>	4.16 (3.89 – 4.43)	4.23 (3.94 – 4.52)	4.24 (3.77 – 4.72)	3.85 (2.84 – 4.85)	4.93 (3.62 – 6.24)	4.16 (3.89 – 4.43)
<b>Mesenteric lymph node</b>	0.11 (0.08 – 0.14)	0.11 (0.09 – 0.13)	0.14 (0.09 – 0.13)	0.12 (0.09 – 0.16)	0.12 (0.04 – 0.20)	0.07 (0.03 – 0.11)
<b>Adrenal gland</b>	0.008 (0.005 – 0.010)	0.007 (0.005 – 0.010)	0.006 (0.004 – 0.009)	0.006 (0.004 – 0.008)	0.007 (0.004 – 0.011)	0.006 (0.004 – 0.008)
<b>Thymus</b>	0.17 (0.09 – 0.24)	0.24 (0.19 – 0.26)	0.23 (0.19 – 0.29)	0.24 (0.17 – 0.30)	0.23 (0.17 – 0.27)	0.26 (0.13 – 0.38)
<b>Stomach</b>	0.75 (0.59 – 0.92)	0.60 (0.50 – 0.70)	0.68 (0.62 – 0.75)	0.69 (0.59 – 0.79)	0.67 (0.58 – 0.76)	0.72 (0.65 – 0.77)
<b>Brain</b>	0.71 (0.58 – 0.84)	0.71 (0.65 – 0.76)	0.75 (0.67 – 0.84)	0.75 (0.69 – 0.81)	0.80 (0.72 – 0.88)	0.71 (0.65 – 0.77)
<b>Testicles</b>	0.38 (0.45 – 0.70)	0.37 (0.32 – 0.42)	0.43 (0.38 – 0.49)	0.42 (0.32 – 0.52)	0.41 (0.36 – 0.46)	0.40 (0.37 – 0.49)
<b>Salivary gland</b>	0.58 (0.43 – 0.72)	0.60 (0.49 – 0.71)	0.65 (0.52 – 0.78)	0.51 (0.36 – 0.66)	0.58 (0.51 – 0.65)	0.55 (0.42 – 0.68)

Values were obtained by the formula [(organ weight/animal weight) x 100] and are expressed in terms of mean (n =6) and 95% confidence interval.

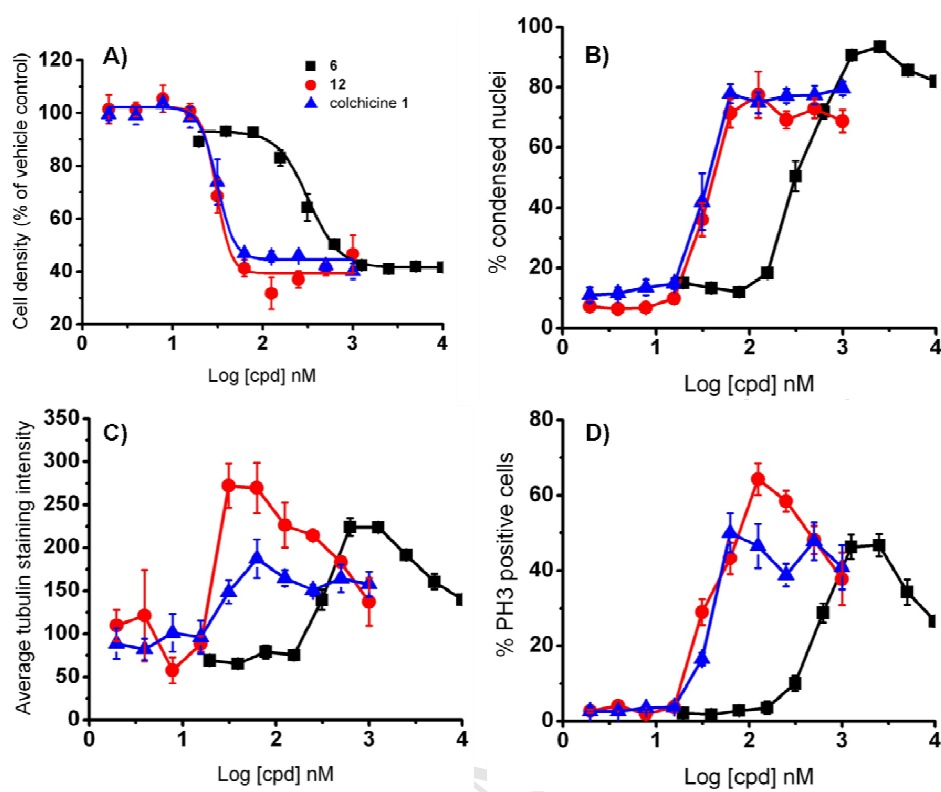


**Figure S1.** High-content analysis of mitotic arrest profiles in cells treated with microtubule perturbing agents. HeLa cells were treated in 384-well plates with 10 point, two-fold dilutions of colchicine and derivatives **6** and **12**, and analyzed by high-content analysis for (A) cell density, (B) chromatin condensation, (C) microtubule density and (D) mitotic index. All agents caused cell loss, enhanced mitotic index and nuclear condensation, and provoked an initial increase in microtubule density that reversed at higher concentrations. (Data: mean  $\pm$  SEM of quadruplicate wells from a single experiment repeated three times with similar results).

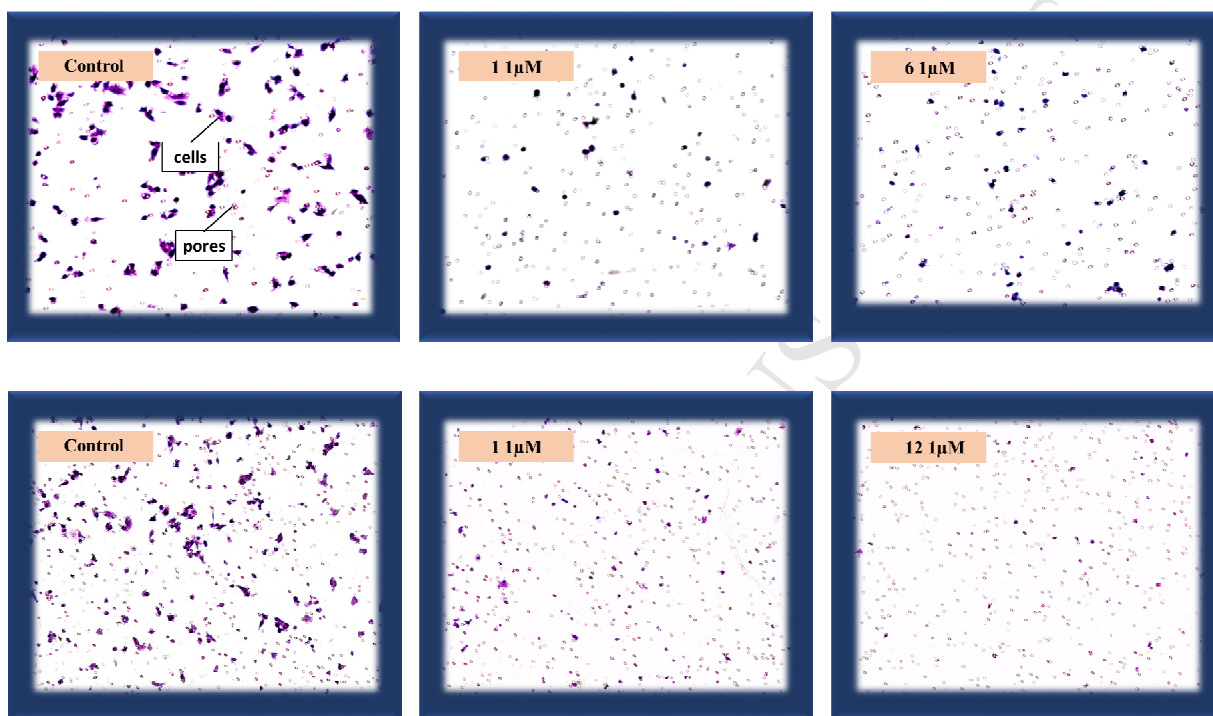


**Figure S2.** Effects of compounds **6** and **12** on MDA-MB-231 cell migration transwell assays. Photographs show cells that migrated through the membrane of the insert after staining with toluidine. Colchicine **1** was used as positive control.

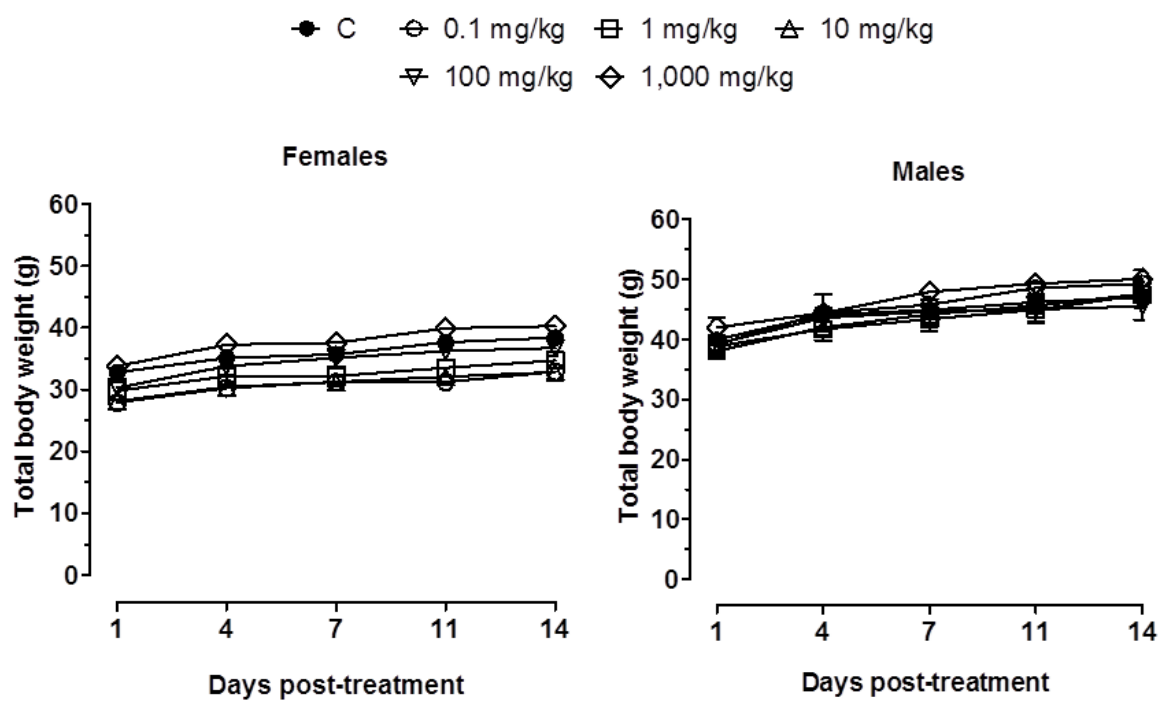


**Figure S3.** Acute toxicity test: weight of animals following compound **12** administration. Mean (n=6)  $\pm$  SEM.